ABSTRACT

Title of Dissertation: OSCILLATIONS OF MICROSCALE COMPOSITE STRUCTURES WITH APPLICATIONS TO MICRORESONATORS

He Li, Doctor of Philosophy, 2006

Directed By: Professor Balakumar Balachandran
Professor Clayton Daniel Mote, Jr.
Department of Mechanical Engineering
University of Maryland, College Park

Free and forced oscillations of piezoelectric microelectromechanical resonators fabricated as clamped-clamped laminate structures are studied in this dissertation. Piezoelectric actuation is used to excite these structures on the input side, and piezoelectric sensing is carried out on the output side. A refined mechanics model is developed for composite beam structures and used for studying the nonlinear transverse vibrations of the microresonators. The model accounts for longitudinal extension due to transverse displacements, distributed actuation, and stepwise axially varying properties. Assuming a buckling induced non-flat equilibrium position, an approximation for the static equilibrium position is determined and the free vibration problem is solved. For weak damping and weak forcing, the method of multiple scales is used to obtain an approximate frequency-response solution. Following this

work, a complete solution for the pre-buckling, critical-buckling, and post-buckling problem for axially elastic beams is developed from the nonlinear model.

The analytical predictions are compared with experimental data and they are found to be in good agreement. The present work provides a means for determining the spatial and temporal response of microresonators and it can be used as a design tool for many microelectromechanical systems (MEMS). The present work provides the first evidence for buckling influenced dynamics in microresonators.

OSCILLATIONS OF MICROSCALE COMPOSITE STRUCTURES WITH APPLICATIONS TO MICRORESONATORS

By

He Li

Dissertation submitted to the Faculty of the Graduate School of the
University of Maryland, College Park, in partial fulfillment
of the requirements for the degree of
Doctor of Philosophy
April 2006

Advisory Committee:

Professor Balakumar Balachandran, Chair/Advisor
Professor Clayton Daniel Mote, Jr., Co-Advisor
Professor Amr Baz
Professor Inderjit Chopra
Associate Professor Donald Lad DeVoe
Associate Professor Bongtae Han

Dedication

To my parents.

Acknowledgements

I would like to express my deep gratitude to my advisor, Professor Balakumar Balachandran, for his insightful instructions, encouragement, and all the patience, support, and enthusiasm he gave me. And I would also like to show my sincere thanks to my co-advisor, Professor Clayton Daniel Mote, Jr., for his invaluable suggestions to my research and his time spent on reviewing my reports. The advice received from my advisor and co-advisor was more than they could have given as an advisor to a student; many of what they said would guide my life beyond school.

I would also like to thank Associate Professor Donald Lad DeVoe and Dr. Sergio Preidikman for their support and instruction during the doctoral study. Professor Amr Baz, Professor Inderjit Chopra, and Associate Professor Bongtae Han are also thanked for their willingness to serve on my advisory committee. I should mention that I benefited from the courses that I had with Professors Baz, Chopra and Han.

Dr. Moustafa Al-Bassyiouni, Mr. Andrew James Dick, Dr. Parshant Kumar, Dr. Lihua Li, Mr. Xinhua Long, and Dr. Miao Yu are also thanked for their help during my doctoral study.

I also gratefully acknowledge the support received for this dissertation work through DARPA Contract No. F3060202C0016 and AFOSR Grant No. F49620-03-10181.

Table of Contents

List of Tables

List of Figures

Chapter 1

1 Introduction and Background

Development of new technologies for affordable, lightweight, small profile, and low power radio frequency (RF) components that do not compromise performance for communication are necessary with the increasing technical requirements of wireless communications, multifunction programmable receivers, frequency hopping radios, reconfigurable antennas, and new radar architectures. In this chapter, a brief introduction to previous work conducted in this area as well as some relevant work in the area of nonlinear oscillations are presented along with the objectives and scope of this dissertation work. The organization of this dissertation is also discussed within this chapter.

1.1. Previous work

1.1.1. Microresonators and Applications

Discrete filter components such as quartz and ceramic surface acoustic wave (SAW) resonators currently make up the bulk of the volume and weight in receivers. Quartz resonators have the advantages of extreme frequency stability, temperature stability, and the high quality factor (Q) value required for many clock operations. The typical frequency range covered by quartz resonators is 1 kHz to 200 kHz. The typical range for ceramic SAW resonators is 50 MHz to 2 GHz. Ceramic resonators tend to have inferior Q values but they are cheaper and smaller, and they have replaced quartz resonators in many filter applications where frequency stability and high Q

specifications have been relaxed. Typically, these resonators are as large as 1 cm^2, which is still large for communication devices like the cell phone.

The fact that ceramic resonators are still on the millimeter scale highlights the need for new microelectromechanical systems (MEMS) RF resonator technology. Micromachining and MEMS fabrication are technologies well suited for improving the performance, size and cost of resonating systems. The first demonstration of micromechanical polysilicon resonators was presented by Howe and Muller in 1984 [1]. Since then, significant progress has been reported for resonators that utilize electrostatic transduction. For example, Nguyen, Wong and Wang [2]-[4] worked on micromachined electromechanical filters (Figure 1.1); Roessig, Howe, and Pisano [5] worked on MEMS accelerometers, Nguyen and Howe [6] worked on microoscillators, and Lin, Howe and Pisano [7], as well as Wang, Nguyen and Lee [3], [8], [9] worked on coupled resonator filters (Figure 1.2). There are also many other studies and applications, where the dynamics of a micromachined structure is used to realize a mechanical transfer function between the drive and sense signals in the electrical domain. These devices have not replaced quartz and ceramic devices primarily because of the following issues: (*i*) the frequency range is not high enough; (*ii*) the need for vacuum conditions to attain a high Q; and (*iii*) impedance values higher than those normally exhibited by macroscopic high-Q resonators [10].

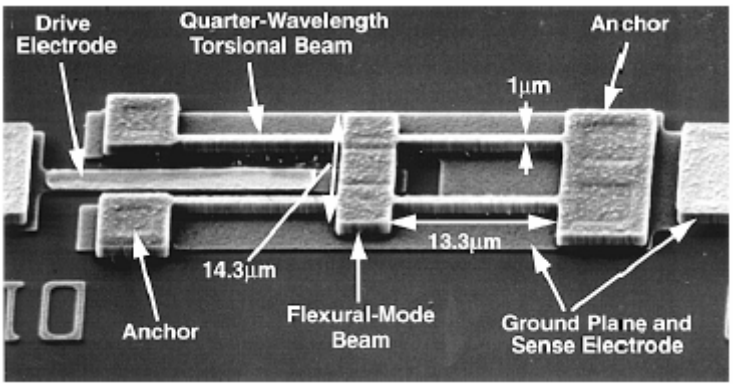

Figure 1.1: Scanning Electron Micrograph (SEM) of a 71.49-MHz free–free beam micromechanical resonator [4].

By using concepts similar to those of the macroscale resonant sensor patented by Weisbord [11], in 1969, Van Mullem, Blom, Fluitman, and Elwenspoek [12], Fabula, Wagner, and Schmidt [13], and Funk, Fabula, Flik and Larmer [14] have reported on work with bulk micromachined piezoelectric resonators, where a clamped-clamped beam-like structure on the silicon substrate is electrostatically driven in its first resonance mode and sensed capacitively. Prak, Elwenspoek, and Fluitman [15] developed a method to design the input/output electrodes for selectively exciting or sensing modes. Abdalla, Reddy, Faris and Gürdal [16] worked on the optimal design of the thickness and width for beams with different boundary conditions for maximum pull-in voltage. Turner, Miller, Hartwell, Macdonald, Strogartz, Adams and Zhang [17], [18] have investigated a parametrically driven torsional oscillator (Figure 1.3). Raskin, Brown, Khuri-Yakub and Rebeiz [19] worked on a parametric amplifier. DeVoe [20], [21] proposed a device that was an order of magnitude smaller than what was previously reported for bulk-micromachined devices by using surface micromachined piezoelectric filters in a process compatible with backend CMOS

processing. In this work, the center frequencies of the resonator reached up to 1.18 MHz. In Figure 1.4, a piezoelectric resonator structure reported in this work is shown. Kumar, Li, Calhoun, Boudreaux and DeVoe [22] fabricated piezoelectric $Al_{0.3}Ga_{0.7}As$ microstructures.

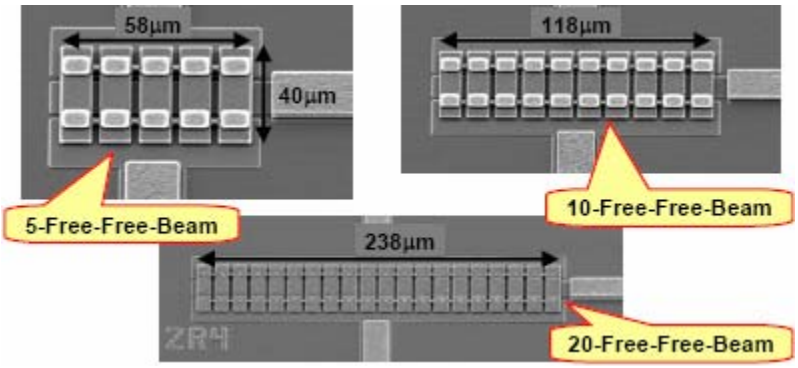

Figure 1.2: Scanning Electron Microscope (SEM) image of mechanically coupled micromechanical resonator arrays with varying number of coupled free-free beams [9].

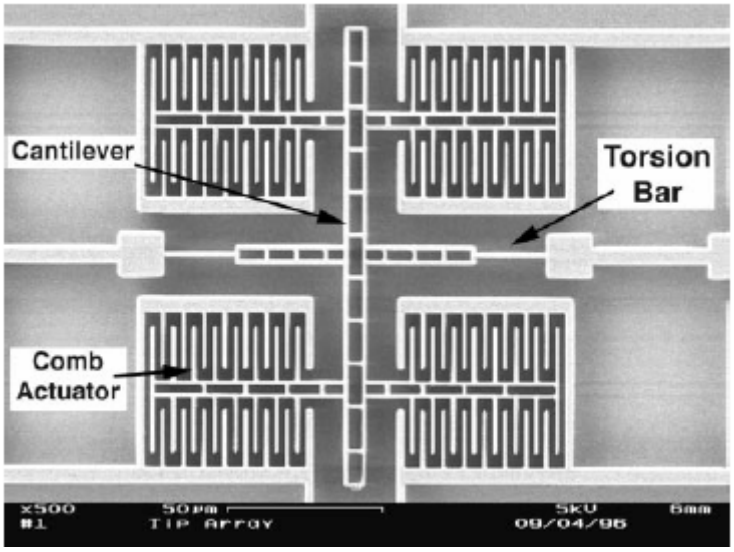

Figure 1.3: SEM image of a torsional oscillator [17].

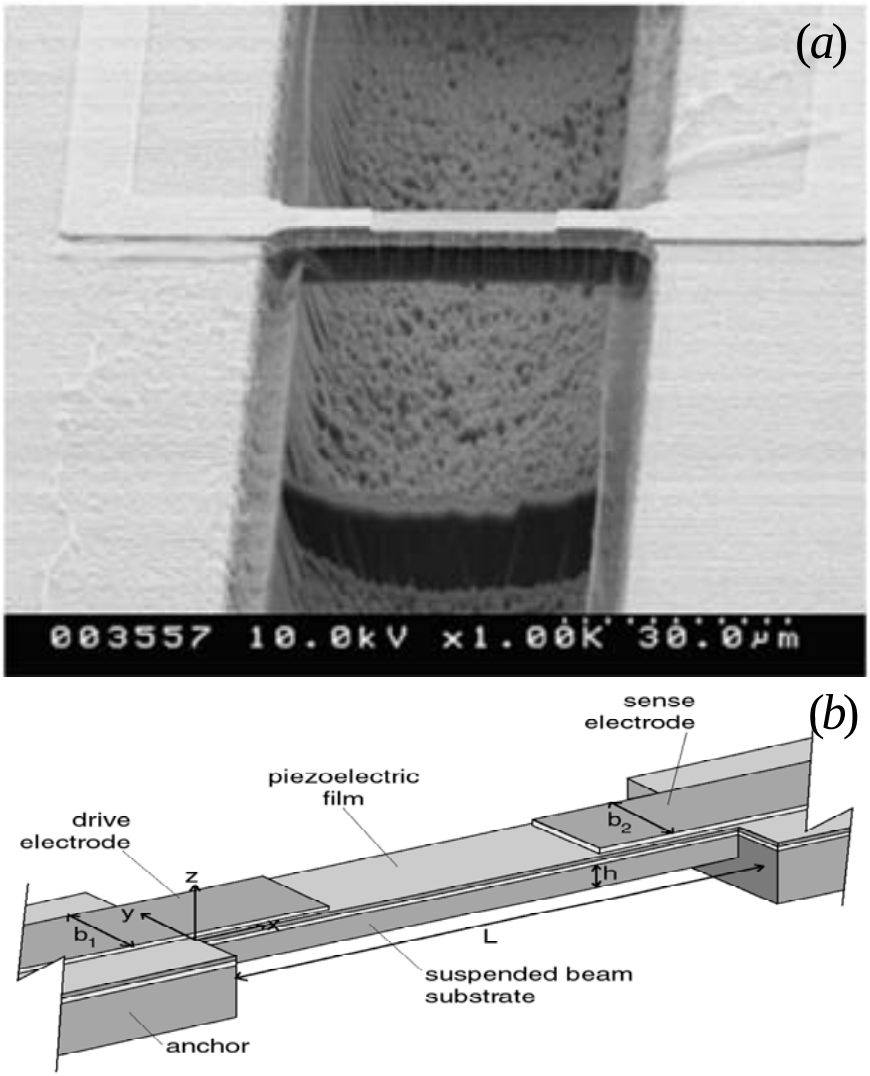

Figure 1.4: (a) SEM of a 50 µm PZT microresonator [23] and (b) a schematic showing the details of the device structure [21].

1.1.2. Nonlinearities and Phenomena in Microresonators

Nonlinearities in microscale and nanoscale resonators have long been observed and reported with respect to variation in the drive voltage, excitation frequency, and temperature parameters.

Husain, Hone, Postma, Huang, Drake, Barbic, Scherer and Roukes [24] reported that a very low driving power is needed to bring a bottom-up Pt nanowire resonator into the nonlinear regime. Piekarski *et al* [23] reported nonlinear Düffing-like behavior in an 80μm clamped-clamped PZT resonator when the driving voltage exceeded a certain value (shown in Figure 1.5).

By varying the operating temperature, Piekarski *et al* [23] reported that the resonant frequency initially decreases and then increases beyond a certain threshold temperature for an 80 μm clamped-clamped PZT driven resonator, while Nguyen *et al* [4] reported the reverse trend in frequency shift for electrostatic free-free and clamped-clamped beams. Paul and Baltes [25] studied a thermomechanically buckled plate structure.

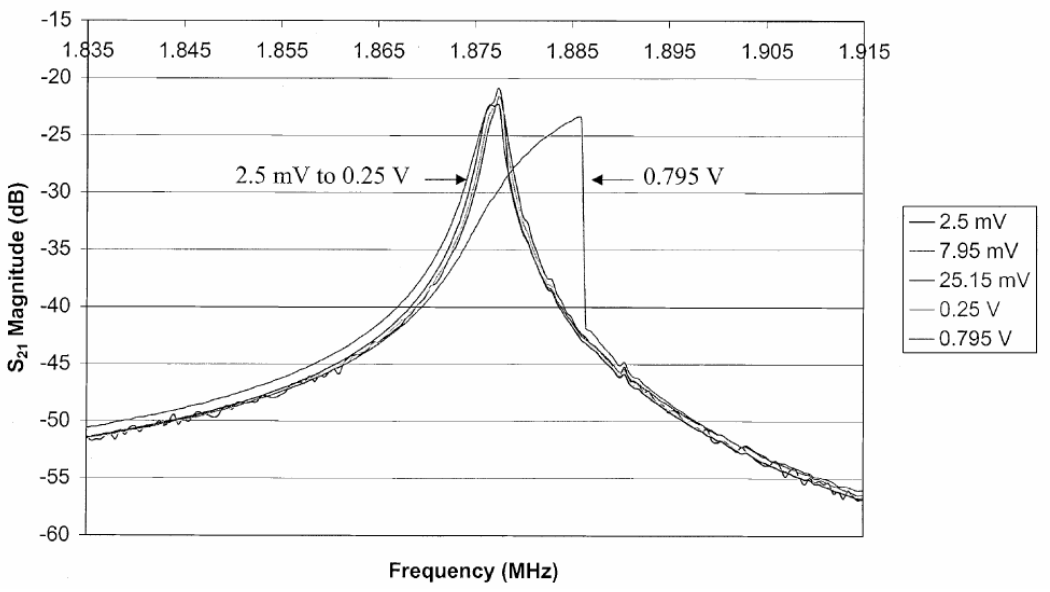

Figure 1.5: Effect of drive voltage on an 80um clamped-clamped PZT resonator's response magnitude [23].

Currano [26] reported the unusual spatial displacement pattern observed in 200 μm and 400 μm PZT clamped-clamped resonators. Li and Balachandran [27] also observed nonlinear response spectra in the same devices for harmonic driving signals close to the first resonance frequencies.

Shaw, Turner, Rhoads, Baskaran and Zhang [28], [29] reported the nonlinear nature of responses in a parametrically excited resonator; they discuss the dependence of the bandwidth on the excitation amplitude; the existence of non-trivial responses outside of the passband; and the nonlinear input/output relationship, as well as higher order resonances that occur in the resonator.

In clamped-clamped MEMS structures, stress could be one of the reasons. DeVoe reported that in his PZT resonators the compressive residual stress between SiO_2 layer and the wafer caused the resonator to buckle up (Figure 1.6). Vangob [30], Yang and Kim [31], as well as Wagner, Quenzer, Hoerschelmann, Lisec and Juerss [32] also reported residual compressive stresses leading to buckled beams or membranes.

Different from the source of nonlinearity in a clamped-clamped MEMS structure, Postma, Kozinsky, Husain and Roukes's work [33] revealed that for cantilevers, the nonlinearity generally sets in at larger amplitude than in the clamped-clamped beams. This is because the nonlinearity due to curvature has the dominant influence in the response of the fundamental mode of the cantilever [34].

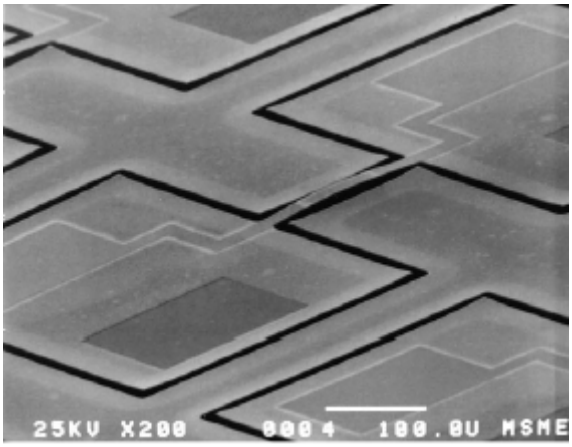

Figure 1.6: Bowing due to high compressive stress in single-beam resonators with SiO_2 layer [21].

The third-order intermodulation distortion caused by parametric excitation or capacitive nonlinearity for electrostatically driven flexural-mode beams can also be other sources of the nonlinearity [4], [28], [29].

Susceptibility to contamination may be one explanation offered for nonlinear frequency-temperature relations. Nguyen *et al* [4] explained the observation by using a mass-removal-based model, where the frequency initially raises by burning off contaminants that adsorb onto the resonator surfaces and ceases to increase when all of the contaminants are removed; due to a negative Young's modulus temperature coefficient, the expected decrease in frequency with temperature is observed.

1.1.3. Buckling Analysis for MEMS Devices

As mentioned in the previous section, either intrinsic or thermal stress induced buckling phenomena has long been reported in MEMS field [30], [31], [32], [35], and correspondingly, analysis and applications of buckling have been reported.

Qiu, Lang and Slocum [36] worked on analysis of a bistable mechanism and studied the snap through problem of a statically buckled microbeam. Fang and Wickert [37], [38] analytically studied the static post-buckling problem of a micromachined beam. Chiao and Lin [39] worked on thermal stress induced self-buckling micromachined beams. Brand, Hornung, Baltes and Hafner [40] reported the observation of a smooth quasibuckling transition rather than a sharp Euler buckling in their micro-membrane device. These studies on post-buckled microstructures have by and large focused on the static case, and in all of these cases, the structures were modeled as uniform beams. Li, Balachandran, and Preidikman [41], [42], [27] presented nonlinear dynamic studies on piezoelectrically actuated microresonators with axially stepwise varying properties, where the oscillations are modeled to occur around a post-buckled position.

1.2. Objectives and Scope of this Work

The goal of this work is to develop a refined nonlinear model for a composite beam with axially varying properties and distributed actuation and apply it to microstructures with finite stepwise axially varying properties (FSAVP). Through this

application, it is intended to describe the nonlinear behavior of piezoelectric microresonators. Specific objectives of this dissertation work are as follows:

1. Experimental characterization of the nonlinear behavior of Lead Zirconate Titanate (PZT) microresonators

2. Development of a nonlinear beam model with Euler-Bernoulli assumption that takes in to account axial elongation caused by external forces and transverse displacement

3. Determination of solutions for free and forced vibration problems of a FSAVP beam around a post-buckled equilibrium position, and comparisons of the model predictions with experimental data

Experimental studies have been carried out with the 200 μm and 400 μm PZT resonators, with frequencies ranging from 100 KHz to 500 KHz. In these structures, the microresonators are excited around their first natural frequency and the responses of these resonators has been experimentally studied. Nonlinear Düffing-like frequency-response behavior is observed for 200 μm PZT resonators, and unusual spatial vibration patterns and frequency response spectra are observed in the case of the 200 μm and 400 μm PZT resonators. An explanation for these phenomena is provided in this work.

The following features distinguish the current study from the previous efforts:

1. Development of a nonlinear beam model with a clear physical interpretation on how the axial strain influences the system dynamics and how the strain is also affected by external forces

2. Application of the model developed for a macroscale uniform beam to microscale beam-like composite structures with FSAVP

3. Presentation of the first evidence for occurrence for certain phenomena in the dynamics of microresonators can be caused by buckling

4. Development of a complete solution for static pre-buckling, critical-buckling, and post-buckling problems for an extensible beam.

1.3. Organization of Dissertation

In the next chapter, the experimental arrangement and the experimental observations are presented. A refined nonlinear beam model is then developed and applied to the microresonator with FSAVP in Chapter 3. Following this, in Chapter 4, the free and forced oscillations of such a beam about the post-buckling position are studied and obtained the numerical results are compared with experimental data. Finally, a complete solution for the static pre-buckling, critical-buckling and post-buckling problems of an axially extensional Euler-Bernoulli beam is presented in Chapter 5. Summary and suggestions for future work are included in Chapter 6. References are included at the end of the dissertation. Appendices are also included to provide additional details.

Chapter 2

2 Lead Zirconate Titanate (PZT) Microresonators

In this chapter, the structure of the microresonator is discussed and data obtained in experiments conducted with these resonators are presented. The experimental data presented in this chapter is used for comparison with model predictions in Chapter 4.

2.1. Microresonator Structure Description

Oscillations of microelectromechanical resonators fabricated as clamped-clamped composite structures are studied here. The resonators considered in this effort are based on the piezoelectric effect, as shown in Figure 1.4. The dimensions of the resonators considered in this study typically range in lengths from 50 μm to 400 μm, with a width of 20 μm and a total thickness less than 3 μm. The elastic substrate is SiO_2 layer, on the top of which a thin platinum electrode layer and a layer of sol-gel piezoelectric film are deposited in that order throughout the structure's length. To complete the structure, a platinum electrode layer that extends over one quarter of the length from each boundary is deposited as the top layer so that each resonator structure has three layers in the mid-span where the top electrode layer is absent and four layers elsewhere [21], [26]. Due to the asymmetry of the cross-section, the position of the piezoelectric layer is offset from the neutral axis, and in addition, residual stress may also be introduced in each layer during the fabrication process.

For comparisons between model predictions and the experimental results, particular attention is paid to a 200 μm long resonator. The thickness values for each layer are provided in Table 2.1. As discussed later in Chapter 3, each resonator is modeled as a composite beam with axial properties that vary stepwise from section to section. The axial stiffness, the bending stiffness, and the mass per unit length values are given in Table 2.2. Subscripts are used to indicate values associated with a particular section.

Table 2.1 - Thickness values for the 200 μm composite resonator.

SiO_2 [μm]	**Bottom Pt [μm]**	**PZT [μm]**	**Top Pt [μm]**
1.030	0.085	1.09	0.090

Table 2.2 - Axial stiffness, bending stiffness, and mass density values for the 200 μm long resonator.

EA_1 [N]	EA_2 [N]	EA_3 [N]
3.17	2.88	3.17
EI_1 [N·m^2]	EI_2 [N·m^2]	EI_3 [N·m^2]
1.39×10^{-12}	0.83×10^{-12}	1.39×10^{-12}
ρA_1 [Kg/m]	ρA_2 [Kg/m]	ρA_3 [Kg/m]
3.01×10^{-7}	2.68×10^{-7}	3.01×10^{-7}

2.2. Experiments and Observations

The experimental arrangement used to study forced oscillations of the resonator is shown in Figure 2.1 (a). The silicon wafer is first fixed in the chamber of Dessert Cryogenics vacuum probe station in the Maryland MEMS Laboratory. Later the resonator is electronically connected to a Hewlett Packard 4395A spectrum analyzer and a power supply by connecting the top electrode and bottom electrode of the input port with 2 single micro probes (Figure 2.1 (b)). The excitation signal fed into the input port of the resonator consists of a sinusoidal component and a DC bias offset, so that the static axial force and resonant frequency can be tuned as the resonator is excited. A laser vibrometer is connected to the microscope of the probe station to measure the transverse vibrations at the mid-point of the resonator (Figure 2.1 (c)).

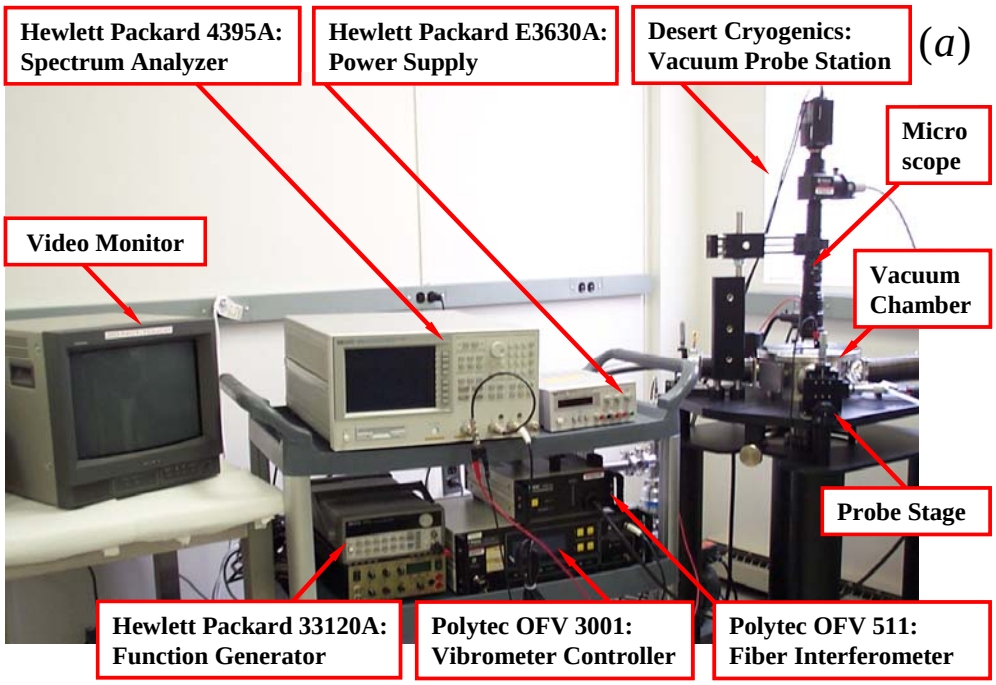

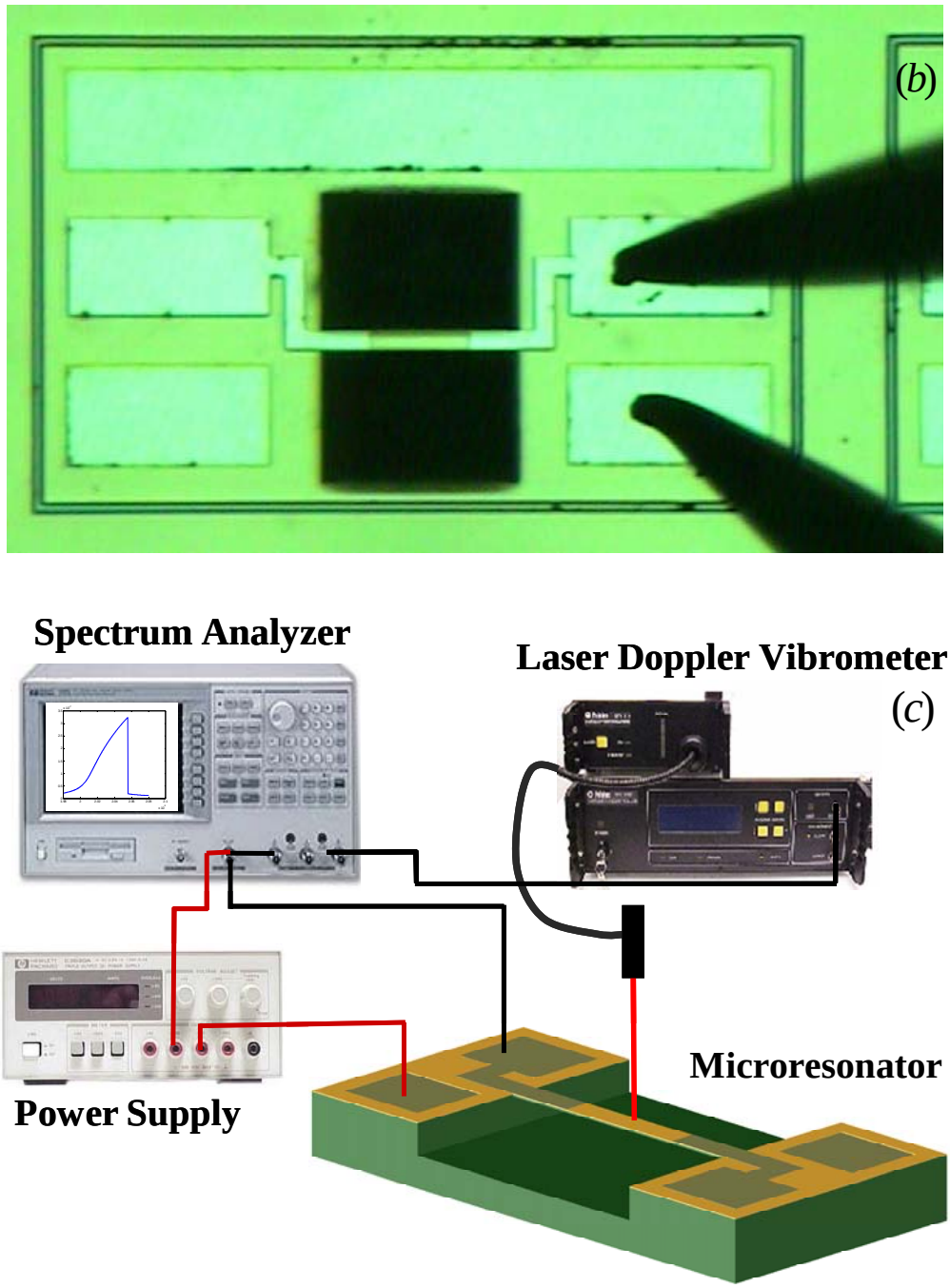

Figure 2.1: (a) Experimental arrangement in Maryland MEMS Laboratory; (b) an expanded view of the connection at the 200μm input port; and (c) sketch of how a laser vibrometer is positioned to examine transverse vibrations of resonator. The resonator is excited by signals input to the drive electrode.

The first natural frequency of a 200 μm resonator is experimentally determined to be close to 313 kHz, while the linear prediction obtained from the Euler-Bernoulli beam model of composite structure, without considering the axial force and the non-flat equilibrium position, is about 186 kHz.

In Figure 2.2 (a) a representative spatial response distribution of this resonator measured by a scanning laser vibrometer is shown. Although the sinusoidal excitation was closed to its measured first natural frequency of the resonator, the observed spatial pattern does not resemble that of a “typical” first mode shape of a clamped-clamped beam. Instead of a single extremum, three peaks appear in the spatial pattern with the peak on the left larger than the other two peaks. This spatial pattern has characteristics of a higher-order mode.

The amplitude of the vibration is typically a few hundred nanometers to 1 micrometer depending on the excitation level (Figure 2.2 (b)). Furthermore, a hardening type Düffing frequency amplitude response (Figure 2.2 (b)) and a nonlinear response spectrum is also observed. In Figure 2.2 (c), the response of a resonator to a sinusoidal input of 60mV with an excitation frequency close to the first natural frequency is shown. Apart from the driving frequency, higher harmonics are also observed.

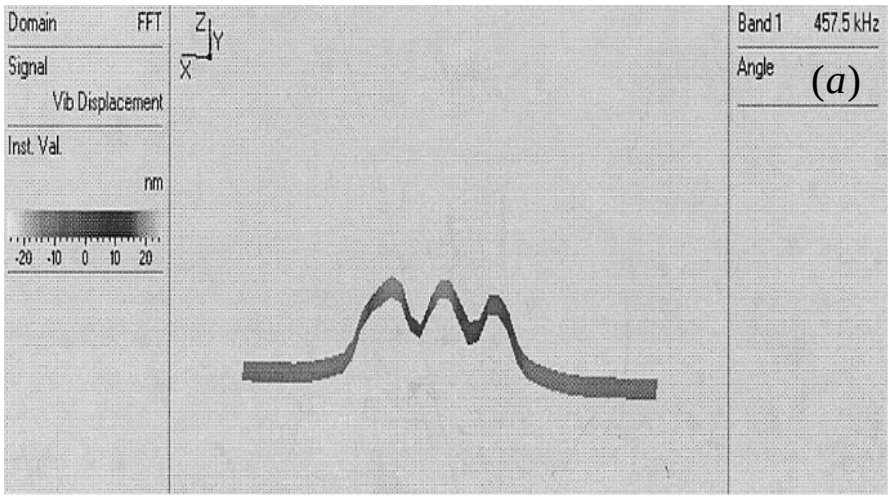
Domain FFT
Signal
Vib Displacement
Inst. Val.
nm
-20 -10 0 10 20
Z
Y
X
Band 1 457.5 kHz
Angle
(a)

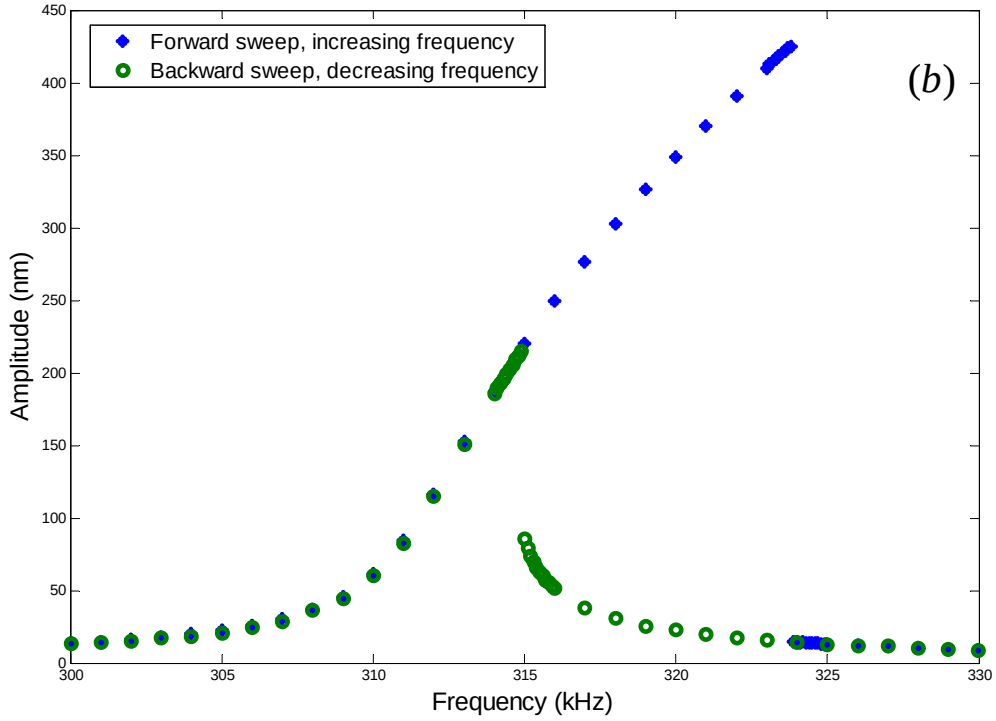
Forward sweep, increasing frequency
Backward sweep, decreasing frequency
(b)
Amplitude (nm)
Frequency (kHz)
0
50
100
150
200
250
300
350
400
450
300
305
310
315
320
325
330

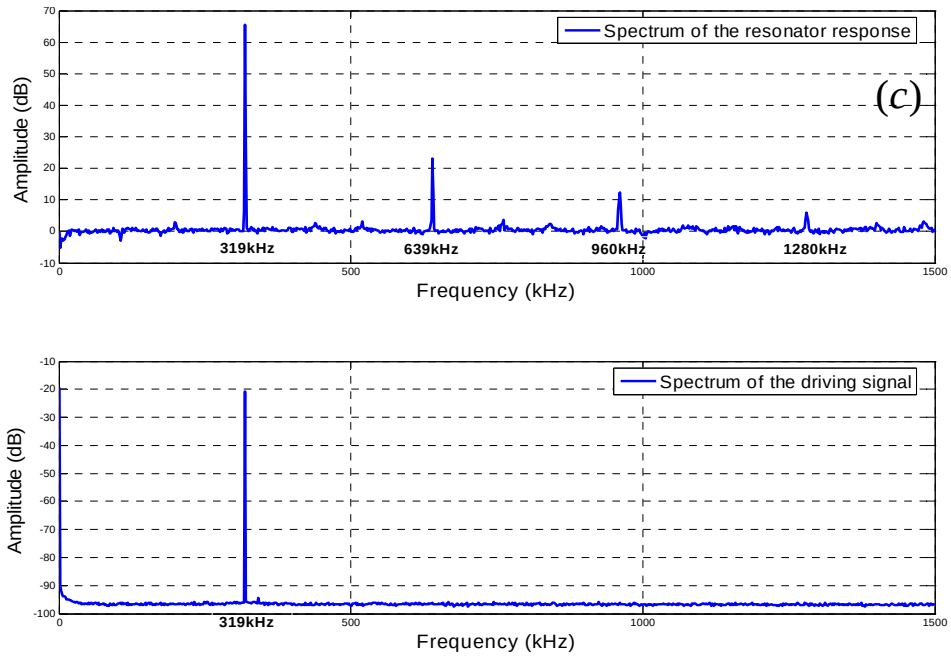

Figure 2.2: (a) Laser vibrometer measurement of a spatial pattern observed in experiments; (b) hardening Düffing type frequency response of a 200 μm PZT resonator to a sinusoidal input signal with an amplitude of 0.398V; and (c) spectrum of the laser vibrometer measurement at the mid-span of a 200 μm resonator (upper plot) when the excitation frequency is close to the first natural frequency. The presence of spatial harmonics distorts the spatial pattern from the typical mode shape associated with the fundamental mode of vibration of a clamped-clamped beam [26].

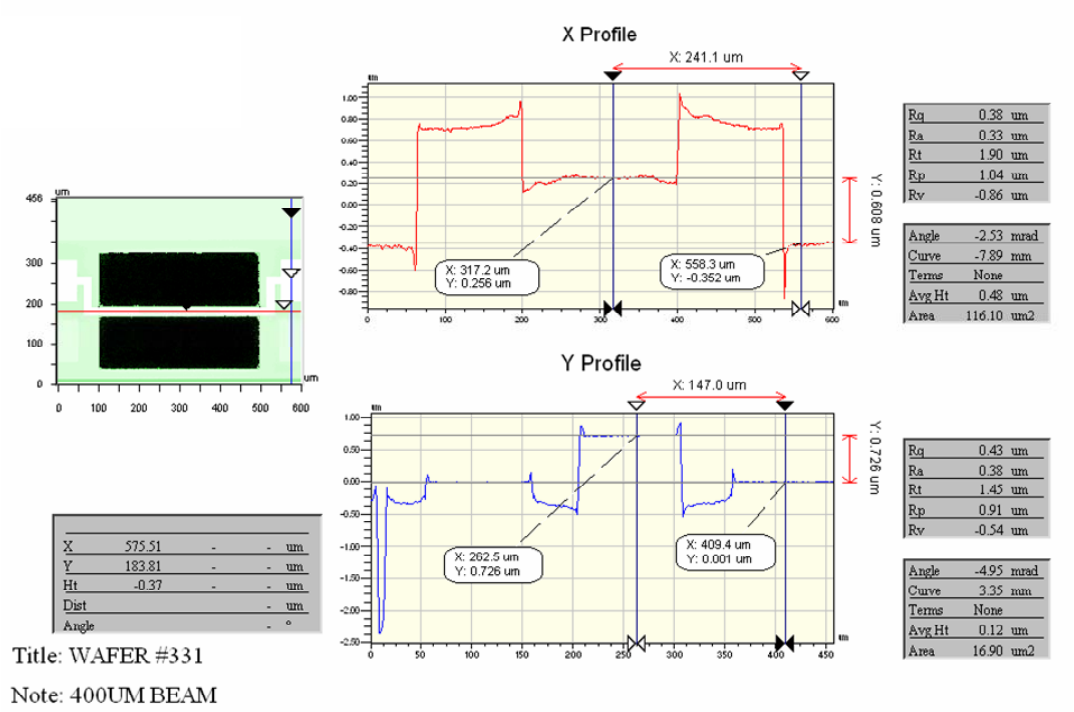

Figure 2.3: Contour of a 400 μm resonator showing a non-flat equilibrium position (Courtesy: B. Piekarski, ARL, Adelphi).

These experimental observations and supporting evidence from the U.S. Army Research Laboratory (ARL) (Figure 2.3) suggest that the oscillations may be taking place around a non-flat equilibrium position. In the later chapters, a hypothesis that the non-flat equilibrium position is caused by buckling is explored. This hypothesis is motivated by prior work conducted with buckled microstructures [43]-[46] and large-scale structures [47],[48]. These prior studies on electrostatically actuated micro-structures have by and large focused on the static case, and in all of these studies, the structures are modeled as uniform beams. The structures considered in this work, however, are piezoelectrically actuated microresonators with axially stepwise varying properties (Table 2.1 and Table 2.2).

In Chapter 3, a refined nonlinear model is developed to explain the experimental observations and to accurately predict the experimentally obtained value of the first natural frequency. In this development, a refined model for a uniform beam is first developed and later, this model is expanded to composite structures with stepwise varying properties. To use this model for predictions, static buckling of such beams is first studied. Free oscillations about a post-buckled equilibrium position and the response of the structure to a harmonic excitation close to the first natural frequency are then examined. This work is of general nature and it can be used to study buckling in any composite beam with axial properties that vary in a stepwise fashion across the structure's length. In Chapter 4, predictions for the responses of the considered microresonator are provided, compared with experimental observations, and discussed.

Chapter 3

3 Modeling of Microresonators

3.1. Composite Structure Properties

In Figure 3.1, the composite structure of the PZT resonator is shown. In general, for an n-layer laminate beam like structure, the effective bending stiffness EI , axial stiffness EA and the density per unit length ρA of the structure along the length of a composite structure can be determined as [49]

$$EI = D_{11} - \frac{B_{11}^2}{A_{11}}, \qquad EA = A_{11}, \qquad \rho A = \sum_{i=1}^{n} \rho_i \hat{b}_i \left(\hat{z}_i - \hat{z}_{i-1} \right) \tag{3.1}$$

where

$$\begin{aligned} A_{11} &= \sum_{i=2}^{n} E_i \hat{b}_i \left(\hat{z}_i - \hat{z}_{i-1} \right) \\ B_{11} &= \frac{1}{2} \sum_{i=2}^{n} E_i \hat{b}_i \left(\hat{z}_i^2 - \hat{z}_{i-1}^2 \right) \\ D_{11} &= \frac{1}{3} \sum_{i=2}^{n} E_i \hat{b}_i \left(\hat{z}_i^3 - \hat{z}_{i-1}^3 \right) \end{aligned} \tag{3.2}$$

where the subscript i represents the i^{th} layer of the composite structure, E_i is the Young's modulus of the i^{th} layer, ρ_i is the density of the i^{th} layer, $\hat{z}_i$ is the thickness of the i^{th} layer, and $\hat{b}_i$ is the width of the i^{th} layer.

For the 200 μm microresonator studied in this effort, the density and stiffness data are listed in Table 2.2.

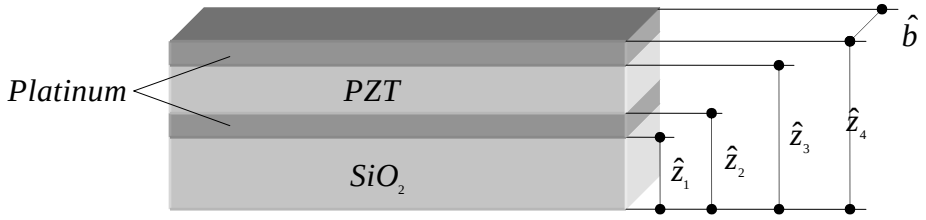

Figure 3.1: Sketch of the laminate structure of the PZT microresonator.

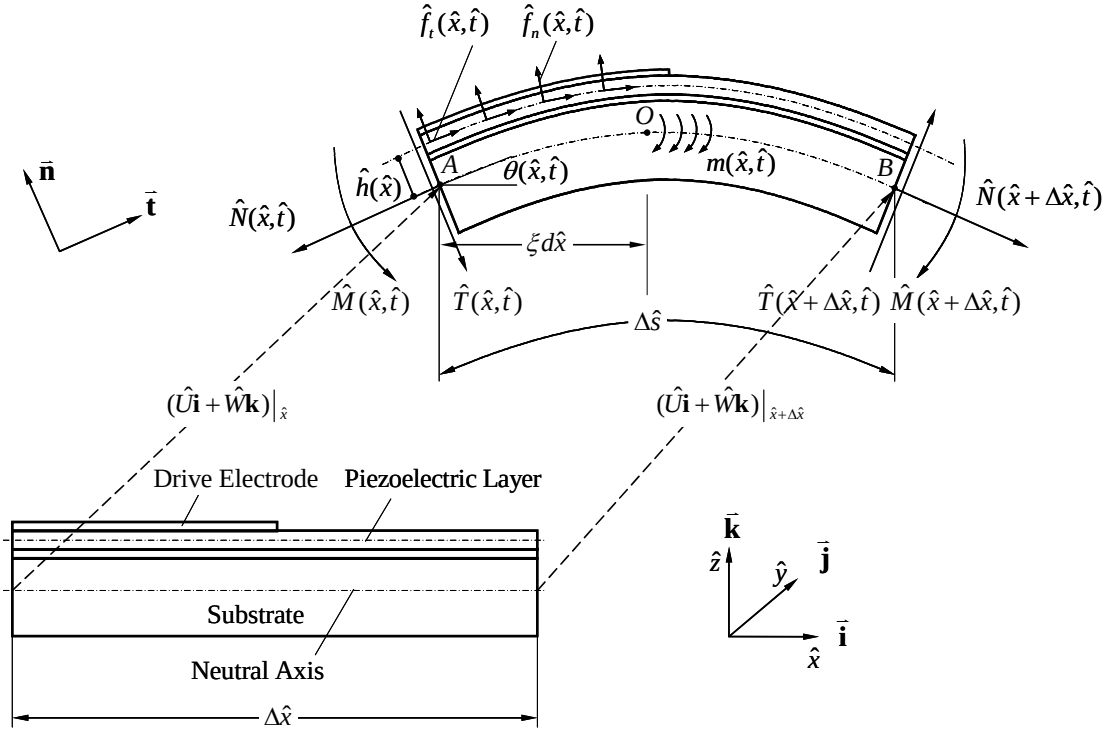

Figure 3.2: Free-body diagram of a infinitesimal beam section. *O* is the center of rotation for the deformed diagram, $\Delta\hat{x}$ is the length of the undeformed section and $\Delta\hat{s}$ is the length of deformed section.

3.2. General Governing Equations

To develop the model, the following assumption are made:

I. *Structure behaves as a uniform Euler-Bernoulli beam;*

II. *Axial and transverse displacements are "small" compared to the length;*

III. *Structure is initially straight, free from stresses and body forces (Figure 3.2);*

IV. *Axial and transverse displacements $\hat{U}$ and $\hat{W}$ satisfy $U = O(W^2)$ [50], this is explained later in this chapter;*

Proceeding along the lines of reference [50], ignoring the displacement along the $\vec{\mathbf{j}}$ direction in Figure 3.2, the force and moment equilibrium equations of the beam are determined to have the form

$$\begin{aligned}&\left(\hat{N}\vec{\mathbf{t}}\right)\Big|_{(\hat{x}+\Delta\hat{x},\hat{t})} - \left(\hat{N}\vec{\mathbf{t}}\right)\Big|_{(\hat{x},\hat{t})} + \left(\hat{T}\vec{\mathbf{n}}\right)\Big|_{(\hat{x}+\Delta\hat{x},\hat{t})} - \left(\hat{T}\vec{\mathbf{n}}\right)\Big|_{(\hat{x},\hat{t})} + \left[\hat{f}_t(\hat{x},\hat{t})\vec{\mathbf{t}}\right]\Delta\hat{s} + \left[\hat{f}_n(\hat{x},\hat{t})\vec{\mathbf{n}}\right]\Delta\hat{s} \\ &= \rho A(\hat{x},\hat{t})\left[\left(\frac{\partial^2\hat{U}(\hat{x},\hat{t})}{\partial\hat{t}^2} + 2\hat{c}\frac{\partial\hat{U}(\hat{x},\hat{t})}{\partial\hat{t}}\right)\vec{\mathbf{i}} + \left(\frac{\partial^2\hat{W}(\hat{x},\hat{t})}{\partial\hat{t}^2} + 2\hat{\mu}\frac{\partial\hat{W}(\hat{x},\hat{t})}{\partial\hat{t}}\right)\vec{\mathbf{k}}\right]\Delta\hat{x}\end{aligned} \tag{3.3}$$

$$\begin{aligned}&\left[\hat{M}\vec{\mathbf{j}}\right]\Big|_{(\hat{x}+\Delta\hat{x},\hat{t})} - \left[\hat{M}\vec{\mathbf{j}}\right]\Big|_{(\hat{x},\hat{t})} + \left[\hat{m}(\hat{x},\hat{t})\vec{\mathbf{j}}\right]\Delta\hat{s} + \left[\hat{T}(\hat{x},\hat{t})\vec{\mathbf{j}}\right]\Delta\hat{x} + \left[\hat{f}_n(\hat{x},\hat{t})\Delta\hat{s}\right](\xi\Delta\hat{x})\vec{\mathbf{j}} \\ &= \left[\hat{J}(\hat{x},\hat{t})\frac{\partial^2\theta(\hat{x},\hat{t})}{\partial\hat{t}^2}\vec{\mathbf{j}}\right]\Delta\hat{x}\end{aligned} \tag{3.4}$$

where $\vec{\mathbf{i}}$ and $\vec{\mathbf{k}}$, and $\vec{\mathbf{t}}$ and $\vec{\mathbf{n}}$ are the tangential and normal unit vectors associated with undeformed and deformed structures respectively. The carat symbol "^" has been used to indicate a dimensional variable; $\hat{x}$ is the spatial variable, $\Delta\hat{s}$ is the deformed

length of an originally infinitesimal beam section $\Delta\hat{x}$; $\hat{N}(\hat{x},\hat{t})$ is the axial force along the longitudinal direction, $\hat{M}(\hat{x},\hat{t})$ and $\hat{T}(\hat{x},\hat{t})$ are respectively the bending moment and shear force on the boundary of the infinitesimal section; $\hat{U}(\hat{x},\hat{t})$ and $\hat{W}(\hat{x},\hat{t})$ are respectively the axial and transverse displacements; $\hat{f}_t(\hat{x},\hat{t})$ and $\hat{f}_n(\hat{x},\hat{t})$ are the distributed excitations along the tangential and normal directions of the deformed beam; $\hat{m}(\hat{x},\hat{t})$ is the distributed moment; $\hat{J}(\hat{x},\hat{t})$ is the mass moment of inertia, $\theta(\hat{x},\hat{t})$ is the rigid body rotation; and $\xi\Delta\hat{x}$ is the distance from point *A* to the rotation center *O*. It is assumed that the system has viscous damping for motion along the $\vec{\mathbf{i}}$ and $\vec{\mathbf{k}}$ directions, and the respective damping coefficients are denoted by $\hat{c}$ and $\hat{\mu}$.

After ignoring the mass moment of inertia $\hat{J}(\hat{x},\hat{t})$ in Eq. (3.4), and substituting (3.4) into (3.3), and using Taylor-series expansions, the following equation of motion (EOM) is obtained

$$\begin{aligned}&\frac{\partial}{\partial\hat{x}}\left[\hat{N}\vec{\mathbf{t}}+\left(\frac{\partial\hat{M}}{\partial\hat{x}}+\hat{m}\frac{\partial\hat{s}}{\partial\hat{x}}\right)\vec{\mathbf{n}}\right]+\frac{\partial\hat{s}}{\partial\hat{x}}\left[\hat{f}_t\vec{\mathbf{t}}+\hat{f}_n\vec{\mathbf{n}}\right]\\&=\rho A\left[\frac{\partial^2\hat{U}}{\partial\hat{t}^2}+2\hat{c}\frac{\partial\hat{U}}{\partial\hat{t}}\right]\vec{\mathbf{i}}+\rho A\left[\frac{\partial^2\hat{W}}{\partial\hat{t}^2}+2\hat{\mu}\frac{\partial\hat{W}}{\partial\hat{t}}\right]\vec{\mathbf{k}}\end{aligned}\tag{3.5}$$

The deformed length $\Delta\hat{s}$ is associated with the axial and transverse displacement in the following form

$$\Delta\hat{s} = \sqrt{\left(1+\frac{\partial\hat{U}}{\partial\hat{x}}\right)^2 + \left(\frac{\partial\hat{W}}{\partial\hat{x}}\right)^2}\,\Delta\hat{x} \tag{3.6}$$

Also, from Figure 3.2, the tangential and normal vectors $\vec{\mathbf{t}}$ and $\vec{\mathbf{n}}$ have the form

$$\vec{\mathbf{t}} = \frac{\partial\hat{x}}{\partial\hat{s}}\left[\left(1+\frac{\partial\hat{U}}{\partial\hat{x}}\right)\vec{\mathbf{i}} + \frac{\partial\hat{W}}{\partial\hat{x}}\vec{\mathbf{k}}\right] \tag{3.7}$$

$$\vec{\mathbf{n}} = \frac{\partial\hat{x}}{\partial\hat{s}}\left[-\frac{\partial\hat{W}}{\partial\hat{x}}\vec{\mathbf{i}} + \left(1+\frac{\partial\hat{U}}{\partial\hat{x}}\right)\vec{\mathbf{k}}\right] \tag{3.8}$$

Next, substituting Eqs. (3.7) and (3.8) into (3.5), the equation of motions along the $\vec{\mathbf{i}}$ and $\vec{\mathbf{k}}$ directions can be obtained as

$$\begin{aligned}&\frac{\partial}{\partial\hat{x}}\left\{\hat{N}\frac{\partial\hat{x}}{\partial\hat{s}}\left(1+\frac{\partial\hat{U}}{\partial\hat{x}}\right) - \left[\frac{\partial\hat{M}}{\partial\hat{x}}\frac{\partial\hat{x}}{\partial\hat{s}} + \hat{m}\right]\frac{\partial\hat{W}}{\partial\hat{x}}\right\} + \hat{f}_t\left(1+\frac{\partial\hat{U}}{\partial\hat{x}}\right) - \hat{f}_n\frac{\partial\hat{W}}{\partial\hat{x}} \\ &= \rho A\frac{\partial^2\hat{U}}{\partial\hat{t}^2} + 2\hat{c}\frac{\partial\hat{U}}{\partial\hat{t}}\end{aligned} \tag{3.9}$$

$$\begin{aligned}&\frac{\partial}{\partial\hat{x}}\left\{\hat{N}\frac{\partial\hat{x}}{\partial\hat{s}}\frac{\partial\hat{W}}{\partial\hat{x}} + \left[\frac{\partial\hat{M}}{\partial\hat{x}}\frac{\partial\hat{x}}{\partial\hat{s}} + \hat{m}\right]\left(1+\frac{\partial\hat{U}}{\partial\hat{x}}\right)\right\} + \hat{f}_t\frac{\partial\hat{W}}{\partial\hat{x}} + \hat{f}_n\left(1+\frac{\partial\hat{U}}{\partial\hat{x}}\right) \\ &= \rho A\frac{\partial^2\hat{W}}{\partial\hat{t}^2} + 2\hat{\mu}\frac{\partial\hat{U}}{\partial\hat{t}}\end{aligned} \tag{3.10}$$

The bending moment $\hat{M}(\hat{x},\hat{t})$ and its expansion can be expressed as

$$\hat{M}(\hat{x},\hat{t}) \approx -\frac{\left[EI\dfrac{\partial^2 \hat{W}}{\partial \hat{x}^2}\right]}{\left[1+\left(\dfrac{\partial \hat{W}}{\partial \hat{x}}\right)^2\right]^{3/2}} = -EI\frac{\partial^2 \hat{W}}{\partial \hat{x}^2}\left[1-\frac{3}{2}\left(\frac{\partial \hat{W}}{\partial \hat{x}}\right)^2 + O\left(\hat{W}^4\right)\right] \tag{3.11}$$

The *Lagrangian* description of the axial force $\hat{N}(\hat{x},\hat{t})$ is given by

$$\hat{N}(\hat{x},\hat{t}) = EA\left(\frac{\partial \hat{s}(\hat{x},\hat{t})}{\partial \hat{x}} - 1\right) \tag{3.12}$$

After using Taylor-series expansions to expand $\partial \hat{x}/\partial \hat{s}$ and $\partial \hat{s}/\partial\, \hat{x}$ based on Eq. (3.6), one can obtain

$$\begin{aligned}
\frac{\partial \hat{x}}{\partial \hat{s}} &= 1-\frac{\partial \hat{U}}{\partial \hat{x}}+\left(\frac{\partial \hat{U}}{\partial \hat{x}}\right)^2-\frac{1}{2}\left(\frac{\partial \hat{W}}{\partial \hat{x}}\right)^2-\left(\frac{\partial \hat{U}}{\partial \hat{x}}\right)^3+\frac{3}{2}\left(\frac{\partial \hat{U}}{\partial \hat{x}}\right)\left(\frac{\partial \hat{W}}{\partial \hat{x}}\right)^2+H.O.T \\
\frac{\partial \hat{s}}{\partial \hat{x}} &= 1+\frac{\partial \hat{U}}{\partial \hat{x}}+\frac{1}{2}\left(\frac{\partial \hat{W}}{\partial \hat{x}}\right)^2-\frac{1}{2}\left(\frac{\partial \hat{U}}{\partial \hat{x}}\right)^3-\frac{1}{2}\left(\frac{\partial \hat{U}}{\partial \hat{x}}\right)\left(\frac{\partial \hat{W}}{\partial \hat{x}}\right)^2+H.O.T
\end{aligned} \tag{3.13}$$

where H.O.T stands for higher order terms. On substituting (3.11), (3.12) and (3.13), into (3.9) and (3.10), and neglecting terms with orders higher than $O\left(\hat{W}^3\right)$, one obtains

$$\rho A\frac{\partial^2\hat{U}}{\partial\hat{t}^2}+2\hat{c}\frac{\partial\hat{U}}{\partial\hat{t}}-\frac{\partial}{\partial\hat{x}}\left\{EA\left[\left(\frac{\partial\hat{U}}{\partial\hat{x}}\right)+\frac{1}{2}\left(\frac{\partial\hat{W}}{\partial\hat{x}}\right)^2-\frac{\partial\hat{U}}{\partial\hat{x}}\left(\frac{\partial\hat{W}}{\partial\hat{x}}\right)^2\right]\right.$$
$$\left.+\frac{\partial}{\partial\hat{x}}\left(EI\frac{\partial^2\hat{W}}{\partial\hat{x}^2}\right)\frac{\partial\hat{W}}{\partial\hat{x}}\left(1-\frac{\partial\hat{U}}{\partial\hat{x}}\right)\right\}=\hat{f}_t\left(1+\frac{\partial\hat{U}}{\partial\hat{x}}\right)-\hat{f}_n\frac{\partial\hat{W}}{\partial\hat{x}}-\frac{\partial}{\partial\hat{x}}\left(\hat{m}\frac{\partial\hat{W}}{\partial\hat{x}}\right) \tag{3.14}$$

$$\rho A\frac{\partial^2\hat{W}}{\partial\hat{t}^2}+2\hat{\mu}\frac{\partial\hat{U}}{\partial\hat{t}}-\frac{\partial}{\partial\hat{x}}\left[EA\hat{e}\frac{\partial\hat{W}}{\partial\hat{x}}\right]+\frac{\partial^2}{\partial\hat{x}^2}\left(EI\frac{\partial^2\hat{W}}{\partial\hat{x}^2}\right)=\frac{\partial}{\partial\hat{x}}\left\{\frac{1}{2}\frac{\partial}{\partial\hat{x}}\left(EI\frac{\partial^2\hat{W}}{\partial\hat{x}^2}\right)\right.$$
$$\left.\times\left(\frac{\partial\hat{W}}{\partial\hat{x}}\right)^2+\frac{3}{2}\frac{\partial}{\partial\hat{x}}\left[EI\frac{\partial^2\hat{W}}{\partial\hat{x}^2}\left(\frac{\partial\hat{W}}{\partial\hat{x}}\right)^2\right]+\hat{m}\left(1+\frac{\partial\hat{U}}{\partial\hat{x}}\right)\right\}+\hat{f}_t\frac{\partial\hat{W}}{\partial\hat{x}}+\hat{f}_n\left(1+\frac{\partial\hat{U}}{\partial\hat{x}}\right) \tag{3.15}$$

where $\hat{e}(\hat{x},\hat{t})$ represents the strain in *Euler* description [51]

$$\hat{e}(\hat{x},\hat{t})=1-\frac{\partial\hat{x}}{\partial\hat{s}}=\frac{\partial\hat{U}}{\partial\hat{x}}-\left(\frac{\partial\hat{U}}{\partial\hat{x}}\right)^2+\frac{1}{2}\left(\frac{\partial\hat{W}}{\partial\hat{x}}\right)^2 \tag{3.16}$$

For a uniform beam, ρA, EI, and EA are constant properties. Next, the governing equations of motion are rewritten by using the following dimensionless variables

$$x=\frac{\hat{x}}{l},\quad h=\frac{\hat{h}}{l},\quad W=\frac{\hat{W}}{l},\quad U=\frac{\hat{U}}{l},\quad t=\frac{\hat{t}}{l^2}\sqrt{\frac{EI}{\rho A}},\quad f_t=\frac{\hat{f}_t l^3}{EI}$$
$$f_n=\frac{\hat{f}_n l^3}{EI},\quad m=\frac{\hat{m}l^2}{EI},\quad \tilde{\mu}=\frac{\hat{\mu}\,l^2}{\sqrt{\rho A\cdot EI}},\quad \tilde{c}=\frac{\hat{c}\,l^2}{\sqrt{\rho A\cdot EI}} \tag{3.17}$$

where the characteristic length l is defined as the undeformed structure's length. The dimensionless forms of Eqs. (3.14) – (3.16) can be obtained as

$$\frac{\partial^2 U}{\partial t^2}+2\tilde{c}\frac{\partial U}{\partial t}-\frac{1}{r^2}\frac{\partial}{\partial x}\left[\frac{\partial U}{\partial x}+\frac{1}{2}\left(\frac{\partial W}{\partial x}\right)^2-\frac{\partial U}{\partial x}\left(\frac{\partial W}{\partial x}\right)^2\right]$$
$$=\frac{\partial}{\partial x}\left[\frac{\partial^3 W}{\partial x^3}\frac{\partial W}{\partial x}\left(1-\frac{\partial U}{\partial x}\right)\right]-\frac{\partial}{\partial x}\left[m\frac{\partial W}{\partial x}\right]+f_t\left(1+\frac{\partial U}{\partial x}\right)-f_n\frac{\partial W}{\partial x} \tag{3.18}$$

$$\frac{\partial^2 W}{\partial t^2}+2\tilde{\mu}\frac{\partial W}{\partial t}-\frac{1}{r^2}\frac{\partial}{\partial x}\left(e\frac{\partial W}{\partial x}\right)+\frac{\partial^4 W}{\partial x^4}=\frac{1}{2}\frac{\partial}{\partial x}\left[\frac{\partial^3 W}{\partial x^3}\left(\frac{\partial W}{\partial x}\right)^2\right]$$
$$+\frac{3}{2}\frac{\partial^2}{\partial x^2}\left[\frac{\partial^2 W}{\partial x^2}\left(\frac{\partial W}{\partial x}\right)^2\right]+\frac{\partial}{\partial x}\left[m\left(1+\frac{\partial U}{\partial x}\right)\right]+f_t\frac{\partial W}{\partial x}+f_n\left(1+\frac{\partial U}{\partial x}\right) \tag{3.19}$$

$$e(x,t)=\hat{e}=\frac{\partial U}{\partial x}-\left(\frac{\partial U}{\partial x}\right)^2+\frac{1}{2}\left(\frac{\partial W}{\partial x}\right)^2 \tag{3.20}$$

where $r=\sqrt{EI/EA}\,l^{-1}$ is the slenderness ratio.

For an Euler-Bernoulli uniform beam, the width and thickness are smaller than the beam length, and therefore, the slenderness ratio is usually small. For the parameter values given in Table 2.2, for the particular study of a 200 μm resonator, r for each section is of the order of 10^{-3}. It is first assumed that $U=O(W^2)$ [50], and with this assumption, the different quantities can be ordered as $U=O(W^2)$; $W=O(r)$; $e=O(r^2)$.

With the above ordering, keeping terms up to orders of $O(W^2)$ in (3.20), the Euler strain e is found to have the same expression as the *Green-Lagrange* strain ε_{11} [51]; that is

$$e = \left(1 - \frac{\partial \hat{x}}{\partial \hat{s}}\right) \approx \left(\frac{\partial \hat{s}}{\partial \hat{x}} - 1\right) = \frac{\partial U}{\partial x} + \frac{1}{2}\left(\frac{\partial W}{\partial x}\right)^2 + \ldots \tag{3.21}$$

Thus from Eq.(3.12), one obtains

$$\hat{N} = EAe \tag{3.22}$$

For further analysis, a booking keeping parameter ϵ is introduced and the different quatities of interest are written as

$$e = \epsilon^2 \hat{e}, \quad r = \epsilon \hat{r}, \quad W = \epsilon \hat{W}, \quad U = \epsilon^2 \hat{U} \tag{3.23}$$

After using the ordering given by (3.23), Eqs. (3.18) and (3.19) become,

$$\begin{aligned} &\epsilon^2 \frac{\partial^2 \hat{U}}{\partial t^2} + \epsilon^2 2\tilde{c}_k \frac{\partial \hat{U}}{\partial t} - \frac{1}{\epsilon^2 \hat{r}^2} \frac{\partial}{\partial x}\left[\epsilon^2 \hat{e} - \epsilon^4 \frac{\partial \hat{U}}{\partial x}\left(\frac{\partial \hat{W}}{\partial x}\right)^2\right] \\ &= \frac{\partial}{\partial x}\left[\epsilon^2 \frac{\partial^3 \hat{W}}{\partial x^3}\frac{\partial \hat{W}}{\partial x}\left(1 - \epsilon^2 \frac{\partial \hat{U}}{\partial x}\right)\right] - \epsilon \frac{\partial}{\partial x}\left[m \frac{\partial \hat{W}}{\partial x}\right] + f_t\left(1 + \epsilon^2 \frac{\partial \hat{U}}{\partial x}\right) - \epsilon f_n \frac{\partial \hat{W}}{\partial x} \end{aligned} \tag{3.24}$$

$$\begin{aligned} &\epsilon \frac{\partial^2 \hat{W}}{\partial t^2} + \epsilon 2\tilde{\mu} \frac{\partial \hat{W}}{\partial t} - \frac{1}{\epsilon^2 \hat{r}^2} \frac{\partial}{\partial x}\left(\epsilon^3 \hat{e} \frac{\partial \hat{W}}{\partial x}\right) + \epsilon \frac{\partial^4 \hat{W}}{\partial x^4} = \epsilon^3 \frac{1}{2} \frac{\partial}{\partial x}\left[\frac{\partial^3 \hat{W}}{\partial x^3}\left(\frac{\partial \hat{W}}{\partial x}\right)^2\right] \\ &+ \epsilon^3 \frac{3}{2} \frac{\partial^2}{\partial x^2}\left[\frac{\partial^2 \hat{W}}{\partial x^2}\left(\frac{\partial \hat{W}}{\partial x}\right)^2\right] + \frac{\partial}{\partial x}\left[m\left(1 + \epsilon^2 \frac{\partial \hat{U}}{\partial x}\right)\right] + \epsilon f_t \frac{\partial \hat{W}}{\partial x} + f_n\left(1 + \epsilon^2 \frac{\partial \hat{U}}{\partial x}\right) \end{aligned} \tag{3.25}$$

In Eq. (3.24), terms of $O(\epsilon^0)$ are retained, and in (3.25) terms up to $O(\epsilon)$ are retained, resulting in the following

$$-\frac{1}{\hat{r}^2}\frac{\partial \hat{e}}{\partial x} = f_t \tag{3.26}$$

$$\epsilon \frac{\partial^2 \hat{W}}{\partial t^2} + \epsilon 2\tilde{\mu}\frac{\partial \hat{W}}{\partial t} - \epsilon \frac{1}{\hat{r}^2}\left[\frac{\partial \hat{e}}{\partial x}\frac{\partial \hat{W}}{\partial x} + \hat{e}\frac{\partial^2 \hat{W}}{\partial x^2}\right] + \epsilon \frac{\partial^4 \hat{W}}{\partial x^4} = \frac{\partial m}{\partial x} + \epsilon f_t \frac{\partial \hat{W}}{\partial x} + f_n \tag{3.27}$$

With this ordering, the longitudinal dynamics is neglected and only the influence of the quasi-static motion along the axial direction is considered in developing the model for the transverse vibrations of the structure. After substituting (3.26) into (3.27), and absorbing the ordering parameter ϵ back into the different terms, one arrives at the following system of equations for an elastic beam

$$\frac{\partial}{\partial x}\left(\frac{e}{r^2}\right) + f_t(x,t) = 0 \tag{3.28}$$

$$\frac{\partial^2 W}{\partial t^2} + 2\tilde{\mu}\frac{\partial W}{\partial t} - \frac{e}{r^2}\frac{\partial^2 W}{\partial x^2} + \frac{\partial^4 W}{\partial x^4} = \frac{\partial m}{\partial x} + f_n \tag{3.29}$$

Here, it is important to note that (3.28) can also be written in the dimensional form

$$\frac{\partial \hat{N}(\hat{x},\hat{t})}{\partial \hat{x}} + \hat{f}_t(\hat{x},\hat{t}) = 0 \tag{3.30}$$

For the particular case of a clamped-clamped resonator, the associated boundary conditions are

$$W(x,t)=0, \quad \frac{\partial W(x,t)}{\partial x}=0 \quad \text{at} \quad x=0, \quad x=1. \tag{3.31}$$

Eqs. (3.21), (3.28) and (3.29) are the equations of motion of the beam. These equations capture the longitudinal elongation due to the axial/transverse displacements and external force fields. The form of (3.29) is similar to that of a classic linear model, except that the dimensionless axial force term here is replaced by the axial strain. This strain is expressed as a second-order nonlinear quantity and considered as a function of the position *x* and the time *t*. It is believed that Eq. (3.29) allows for a clear physical interpretation on how the axial strain interacts with the system dynamics. From Eq. (3.28), one can state that the system behaves in a quasi-static manner along the *x* direction.

3.3. Governing Equations for Beam with Stepwise Varying Properties

In this section, the EOM (3.28), (3.29), and (3.31) given for a uniform beam will be expanded to structures with finite stepwise varying properties.

Following the earlier work in the field of active structures [52], for the microresonators studied in this effort, the external actuation is modeled as (see Figure 3.2)

$$\begin{aligned} \hat{f}_t(\hat{x},\hat{t}) &= \hat{p}(\hat{t})\delta(\hat{x}-\hat{x}_m), \quad \hat{p}(\hat{t}) = \hat{p}_0 \cos\hat{\Omega}\hat{t}, \\ \hat{m}(\hat{x},\hat{t}) &= \hat{f}_t(\hat{x},\hat{t})\cdot\hat{h}(\hat{x}), \qquad \hat{f}_n(\hat{x},\hat{t}) = 0 \end{aligned} \tag{3.32}$$

where $\hat{p}_0$ is constant with the dimensions [N/m] and $\delta(\hat{x})$ is the *Dirac delta* function.

In sectional form, the axially varying properties and external excitation can be written as (see Figure 3.4)

$$\begin{aligned} \rho A(\hat{x}) &= \sum_{k=1}^{n} \rho A_k H_k(\hat{x}), & EA(\hat{x}) &= \sum_{k=1}^{n} EA_k H_k(\hat{x}), \\ EI(\hat{x}) &= \sum_{k=1}^{n} EI_k H_k(\hat{x}), & \hat{h}(\hat{x}) &= \sum_{k=1}^{n} \hat{h}_k H_k(\hat{x}), \\ \hat{f}_t(\hat{x},\hat{t}) &= \sum_{k=1}^{n} \hat{f}_{t,k}(\hat{x},\hat{t}) H_k(\hat{x}), & \hat{f}_n(\hat{x},\hat{t}) &= \sum_{k=1}^{n} \hat{f}_{n,k}(\hat{x},\hat{t}) H_k(\hat{x}), \\ \hat{m}(\hat{x},\hat{t}) &= \sum_{k=1}^{n} \hat{m}_k(\hat{x},\hat{t}) H_k(\hat{x}), \end{aligned} \tag{3.33}$$

where the subscript *k* represents the k^{th} section of the resonator. Furthermore, $\hat{h}(\hat{x})$ is the distance between the mid-layer of piezoelectric material and the structure's neutral axis; ρA_k , EI_k , EA_k , and $\hat{h}_k$ are constant properties of the resonator; and $H_k(\hat{x}) = \left[u\left(\hat{x}-\hat{x}_{k-1}\right) - u\left(\hat{x}-\hat{x}_k\right) \right]$, where $u(\hat{x})$ is the unit step function. For the particular structure considered in this study, $n = 3$ and $m = 1$. The structure extends from $\hat{x}_0 = 0$ to $\hat{x}_3 = l$.

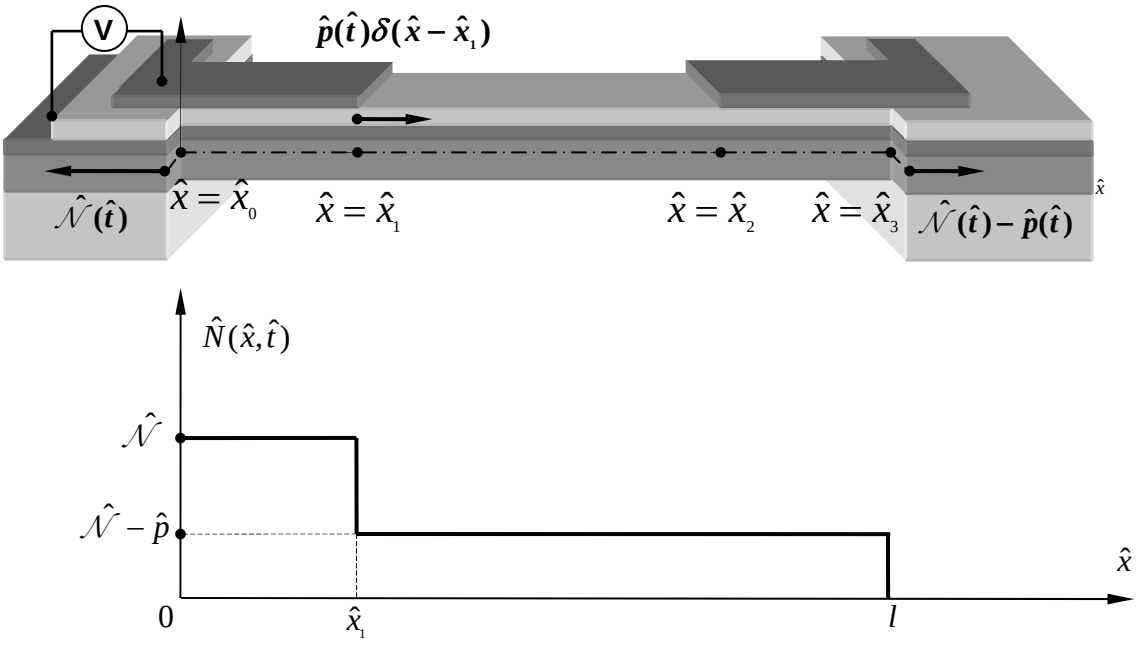

Figure 3.3: Sketch of the axial force increment introduced by external force along the axial direction.

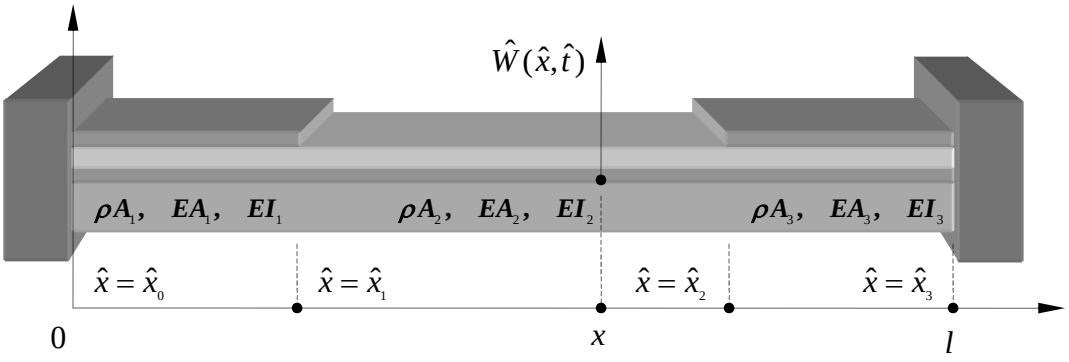

Figure 3.4: Clamped-clamped composite beam with axially varying characteristics.

With such properties, each section of the beam is regarded as a uniform beam. The EOM for each section can be written as

$$\frac{\partial}{\partial x}\left(\frac{e_k}{r_k^2}\right)+ f_{t,k}(x,t_k)=0 \tag{3.34}$$

$$\begin{aligned}&\frac{\partial^2 W_k}{\partial t_k^{\,2}}+2\tilde{\mu}_k\frac{\partial W_k}{\partial t_k}-\frac{e_k}{r_k^2}\frac{\partial^2 W_k}{\partial x^2}+\frac{\partial^4 W_k}{\partial x^4}=\tilde{F}_k\cos\Omega_k t_k,\\ &x\in[x_{k-1},x_k),\quad k=1,2,...,n.\end{aligned} \tag{3.35}$$

$$e_k=\frac{\partial U_k}{\partial x}+\frac{1}{2}\left(\frac{\partial W_k}{\partial x}\right)^2 \tag{3.36}$$

where

$$\tilde{F}_k(x)=\tilde{p}_k h_k\frac{\partial\delta(x-x_m)}{\partial x} \tag{3.37}$$

Making use of Eq. (3.32) in (3.34), it can be concluded that the axial strain e_k is a constant with respect to *x*. Further, from Eqs.(3.22) and (3.30), the axial force has the form (see Figure 3.3),

$$EA_k e_k=\hat{N}(\hat{t})=\hat{\mathcal{N}}(\hat{t})+\hat{p}(\hat{t}) \tag{3.38}$$

Here $\hat{\mathcal{N}}(\hat{t})$ represents the part of axial strain induced by sources other than those directly due to the external excitation, such as residual stresses and the displacement field.

Next, to obtain a more applicable formulation of axial strain e_k, Eq. (3.36) is spatially integrated and evaluated from $x = x_{k-1}$ to x_k to obtain

$$e_k(t_k) = \frac{U_k(x_k) - U_k(x_{k-1})}{(x_k - x_{k-1})} + \frac{1}{2(x_k - x_{k-1})} \int_{x_{k-1}}^{x_k} \left(\frac{\partial W_k}{\partial x} \right)^2 dx \tag{3.39}$$

It is noticed that from the displacement compatibility conditions that

$$U_k(x_k) = U_{k+1}(x_k), \quad W_k(x_k) = W_{k+1}(x_k) \tag{3.40}$$

Now, the following definitions are introduced

$$X_k = U_k(x_k), \qquad Y_k = \frac{EA_k}{2(x_k - x_{k-1})} \int_{x_{k-1}}^{x_k} \left(\frac{\partial W_k}{\partial x} \right)^2 dx, \qquad K_k = \frac{EA_k}{(x_k - x_{k-1})} \tag{3.41}$$

Then with the displacement compatibility condition (3.40), the force compatibility condition (3.38) can be written for the different sections as

$$\begin{aligned}
&K_1(X_1 - X_0) + Y_1 = K_2(X_2 - X_1) + Y_2 \\
&K_2(X_2 - X_1) + Y_2 = K_3(X_3 - X_2) + Y_3 \\
&\vdots \\
&K_m(X_m - X_{m-1}) + Y_m = K_{m+1}(X_{m+1} - X_m) + Y_{m+1} + \hat{p} \\
&K_{m+1}(X_{m+1} - X_m) + Y_{m+1} = K_{m+2}(X_{m+2} - X_{m+1}) + Y_{m+2} \\
&\vdots \\
&K_{n-1}(X_{n-1} - X_{n-2}) + Y_{n-1} = K_n(X_n - X_{n-1}) + Y_n
\end{aligned} \tag{3.42}$$

Writing (3.42) in matrix form, one arrives at

$$\{X\} = \mathrm{A} \cdot \left[\{Y\} + \{F\} \right] \tag{3.43}$$

where

$$\mathrm{A} = \left[A_{i,j} \right] = \begin{bmatrix} 1 & 0 & 0 & & & & & & \\ -K_1 & K_1 + K_2 & -K_2 & & & & & 0 & \\ & -K_2 & K_2 + K_3 & -K_3 & & & & & \\ & & \ddots & \ddots & \ddots & & & & \\ & & & -K_i & K_i + K_{i+1} & -K_{i+1} & & & \\ & & & & \ddots & \ddots & \ddots & & \\ & 0 & & & & -K_{n-1} & K_{n-1} + K_n & -K_n & \\ & & & & & 0 & 0 & 1 & \end{bmatrix}^{-1} \tag{3.44}$$

$$\{X\} = \begin{Bmatrix} X_0 \\ X_1 \\ X_2 \\ \vdots \\ X_m \\ \vdots \\ X_{n-1} \\ X_n \end{Bmatrix}, \quad \{Y\} = \begin{Bmatrix} X_0 \\ Y_2 - Y_1 \\ Y_3 - Y_2 \\ \vdots \\ Y_{m+1} - Y \\ \vdots \\ Y_n - X_{n-1} \\ X_n \end{Bmatrix}, \quad \{F\} = \begin{Bmatrix} 0 \\ 0 \\ 0 \\ \vdots \\ \hat{p} \\ \vdots \\ 0 \\ 0 \end{Bmatrix} \tag{3.45}$$

By solving system (3.43), the displacement vector $\{X\}$ can be obtained as

$$X_k = \left[A_{k+1,1} X_0 + A_{k+1,n+1} X_n \right] + A_{k+1,m+1} \hat{p} + \left\{ -A_{k+1,2} Y_1 + \left[\sum_{i=2}^{n-1} \left(A_{k+1,i} - A_{k+1,i+1} \right) Y_i \right] + A_{k+1,n} Y_n \right\} \tag{3.46}$$

$k = 1, 2, \ldots, n.$

In a general case, the boundary conditions can be described as

$$X_n - X_0 = \overline{\varepsilon} \tag{3.47}$$

where $\overline{(\ )}$ means the average value. Next, after defining

$$\begin{gathered}\overline{EA} = \left[\sum_{j=1}^{n} \frac{\left(x_j - x_{j-1}\right)}{EA_j}\right]^{-1}, \quad \overline{EA_2} = \left[\sum_{j=m+1}^{n} \frac{\left(x_j - x_{j-1}\right)}{EA_j}\right]^{-1}, \\ \overline{EA_1} = \left[\sum_{j=1}^{m} \frac{\left(x_j - x_{j-1}\right)}{EA_j}\right]^{-1}, \ \hat{N}_0 = \overline{EA} \cdot \overline{\varepsilon}, \ N_k = \frac{\hat{N}_0 l^2}{EI_k}\end{gathered} \tag{3.48}$$

and substituting (3.32), (3.40), (3.41), (3.46), and (3.48) back into (3.39), the axial strain e_k can be expressed as a function of transverse displacement

$$\begin{gathered}e_k(t_k) = r_k^2 N_k + r_k^2 q_k \tilde{p} \cos \Omega_k t_k + \left[\Lambda_k \sum_{i=1}^{n} \int_{x_{i-1}}^{x_i} \left(\frac{\partial W_i}{\partial x}\right)^2 dx\right], \\ x \in [x_{k-1}, x_k), \quad k = 1, 2, \ldots, n.\end{gathered} \tag{3.49}$$

where

$$q_k = \begin{cases} \dfrac{\overline{EA}}{\overline{EA_2}}, & k \le m \\ -\dfrac{\overline{EA}}{\overline{EA_1}}, & k > m \end{cases}, \quad \Lambda_k = \frac{\overline{EA}}{2EA_k} \tag{3.50}$$

$$\tilde{p}_k = \frac{\hat{p}_0 l^2}{EI_k}, \text{ and } \Omega_k = \sqrt{\frac{\rho A_k}{EI_k}}\, l^2 \hat{\Omega} \tag{3.51}$$

Equation (3.35) and (3.49) are applicable to the microresonators studied in this effort. They are different from the governing equations treated in previous work [47], [48], since the resonator has distributed excitation as well as varying properties. The displacement field of one section is coupled with the fields of all the sections. This equation along with the boundary conditions represent a nonlinear model that can be used to study transverse vibrations of beam-like structures with axially stepwise varying properties, coupled axial and transverse excitations, and sections with “small” slenderness ratio values, which are common in MEMS applications.

Chapter 4

4 Nonlinear Analysis

In this chapter, the model developed in Chapter 3 is studied and nonlinear analysis is carried out with this model. The static buckling problem is first solved with the hypothesis that the non-flat equilibrium position is caused by buckling, then the beam's free vibration around a buckled position is studied and finally, the forced oscillation case is studied. This analysis is of general nature, and at the end of this chapter, this analysis is applied to a microresonator

4.1. Static Buckling Problem

In this section, the static buckling problem is addressed. It is assumed that the dimensionless static buckling deflection of the resonator can be expressed as

$$\upsilon(x) = \sum_{k=1}^{n} \upsilon_k(x) H_k(x) \tag{4.1}$$

where $\upsilon_k(x)$ is the transverse displacement in the k^{th} section of the beam. For the static buckling analysis, the inertia, damping, and external actuation terms in (3.35) are dropped, and the static compressive axial forces $-\hat{P}_0$ and $-P_{0,k}$ are substituted for $\hat{N}_0$ and N_k in (3.48) respectively. After carrying these substitutions through and

making use of (3.49) in (3.35), the nonlinear equation governing the equilibrium of the beam subjected to a static axial force can be written as

$$\frac{d^4\upsilon_k}{dx^4}+\left\{P_{0,k}-\frac{\Lambda_k}{r_k^2}\sum_{i=1}^{3}\left[\int_{x_{i-1}}^{x_i}\left(\frac{d\upsilon_i}{dx}\right)^2 dx\right]\right\}\frac{d^2\upsilon_k}{dx^2}=0,\quad k=1,2,...,n. \tag{4.2}$$

The associated boundary conditions follow from (3.31) as

$$\upsilon_1(x)=0,\ \frac{d\upsilon_1(x)}{dx}=0\quad at\quad x=0,\qquad \upsilon_n(x)=0,\ \frac{d\upsilon_n(x)}{dx}=0\quad at\quad x=1. \tag{4.3}$$

In order to obtain the solution of (4.2), the critical buckling force must be first calculated by solving the linear buckling problem for this composite resonator with axially varying properties. To this end, neglecting the nonlinear term in (4.2) and substituting for the dimensionless buckling load $P_{0,k}$ with the critical buckling load $P_{c,k}$, the linear buckling problem associated with (4.1) – (4.3) is determined to be

$$\psi(x)=\sum_{k=1}^{n}\psi_k(x)H_k(x) \tag{4.4}$$

where $\psi_k(x)$ is governed by

$$\frac{d^4\psi_k}{dx^4}+\zeta_k^2\frac{d^2\psi_k}{dx^2}=0 \tag{4.5}$$

and

$$\psi_1(x)=0,\ \frac{d\psi_1(x)}{dx}=0 \quad at \quad x=x_0,$$
$$\psi_n(x)=0,\ \frac{d\psi_n(x)}{dx}=0 \quad at \quad x=x_n. \tag{4.6}$$

In Eq. (4.5), $\zeta_k^2 = P_{c,k} = \hat{P}_c\, l^2 / EI_k$ .The general solution of (4.5) is given by

$$\psi_k(x) = a_{1,k} + a_{2,k}x + a_{3,k}\cos(\zeta_k x) + a_{4,k}\sin(\zeta_k x) \tag{4.7}$$

To determine the arbitrary constants $a_{j,k}$ for $j=1,2,3,4$ and $k=1,2,...,n$, the following compatibility conditions are enforced [53] (see Figure 4.1)

$$\psi_{k-1}(x)=\psi_k(x), \qquad \frac{d\psi_{k-1}(x)}{dx}=\frac{d\psi_k(x)}{dx},$$
$$EI_{k-1}\frac{d^2\psi_{k-1}(x)}{dx^2}=EI_k\frac{d^2\psi_k(x)}{dx^2}, \quad EI_{k-1}\frac{d^3\psi_{k-1}(x)}{dx^3}=EI_k\frac{d^3\psi_k(x)}{dx^3}, \tag{4.8}$$
$$@\ x=x_{k-1}, \quad k=2,3,...,n.$$

After substituting (4.7) into (4.6) and (4.8), one obtains a set of twelve homogeneous algebraic equations that defines an eigenvalue problem for the $a_{j,k}$ and the eigenvalues ζ_k, which are functions of the critical buckling force. For a three-section beam model, the eigenvalue problem takes the form

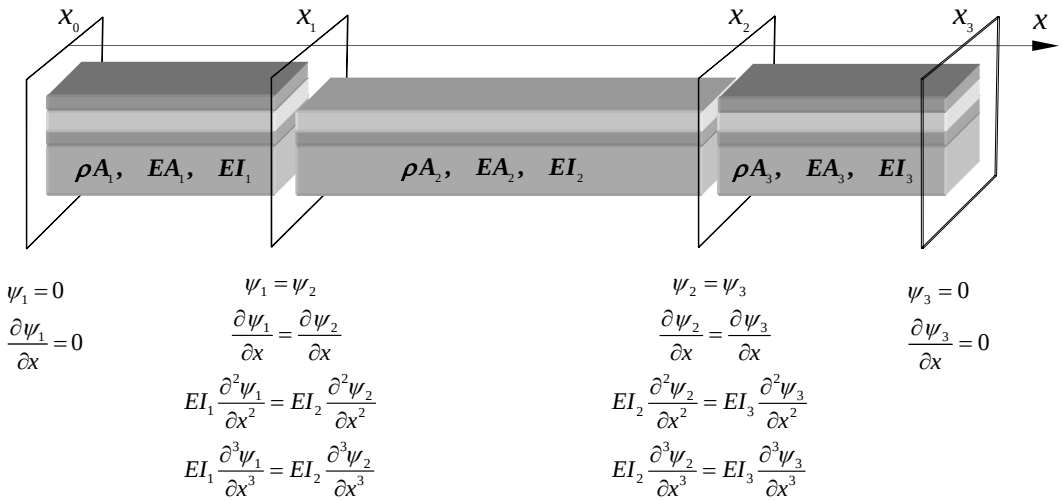

Figure 4.1: Boundary conditions and compatibility conditions for a clamped-clamped composite beam.

$$
\begin{bmatrix}
1 & 0 & 1 & 0 & & & & & & & & \\
0 & 1 & 0 & 1 & & & & & & & & \\
1 & x_1 & \cos\zeta_1 x_1 & \sin\zeta_1 x_1 & -1 & -x_1 & -\cos\zeta_2 x_1 & -\sin\zeta_2 x_1 & & & 0 & \\
0 & 1 & -\zeta_1 \sin\zeta_1 x_1 & \zeta_1 \cos\zeta_1 x_1 & 0 & -1 & \zeta_2 \sin\zeta_2 x_1 & -\zeta_2 \cos\zeta_2 x_1 & & & & \\
0 & 0 & -EI_1\zeta_1^2 \cos\zeta_1 x_1 & -EI_1\zeta_1^2 \sin\zeta_1 x_1 & 0 & 0 & EI_2\zeta_2^2 \cos\zeta_2 x_1 & EI_2\zeta_2^2 \sin\zeta_2 x_1 & & & & \\
0 & 0 & EI_1\zeta_1^3 \sin\zeta_1 x_1 & -EI_1\zeta_1^3 \cos\zeta_1 x_1 & 0 & 0 & -EI_2\zeta_2^3 \sin\zeta_2 x_1 & EI_2\zeta_2^3 \cos\zeta_2 x_1 & & & & \\
 & & & & 0 & 0 & EI_2\zeta_2^3 \sin\zeta_2 x_2 & -EI_2\zeta_2^3 \cos\zeta_2 x_2 & 0 & 0 & -EI_3\zeta_3^3 \sin\zeta_3 x_2 & EI_3\zeta_3^3 \cos\zeta_3 x_2 \\
 & & & & 0 & 0 & -EI_2\zeta_2^2 \cos\zeta_2 x_2 & -EI_2\zeta_2^2 \sin\zeta_2 x_2 & 0 & 0 & EI_3\zeta_3^2 \cos\zeta_3 x_2 & EI_3\zeta_3^2 \sin\zeta_3 x_2 \\
 & & & & 0 & 1 & -\zeta_2 \sin\zeta_2 x_2 & \zeta_2 \cos\zeta_2 x_2 & 0 & -1 & \zeta_3 \sin\zeta_3 x_2 & -\zeta_3 \cos\zeta_3 x_2 \\
 & & 0 & & 1 & x_2 & \cos\zeta_2 x_2 & \sin\zeta_2 x_2 & -1 & -x_2 & -\cos\zeta_3 x_2 & -\sin\zeta_3 x_2 \\
 & & & & & & & & 0 & 1 & -\zeta_3 \sin\zeta_3 & \zeta_3 \cos\zeta_3 \\
 & & & & & & & & 1 & 1 & \cos\zeta_3 & \sin\zeta_3
\end{bmatrix}
\times
\begin{Bmatrix}
a_{1,1} \\ a_{2,1} \\ a_{3,1} \\ a_{4,1} \\ a_{1,2} \\ a_{2,2} \\ a_{3,2} \\ a_{4,2} \\ a_{1,3} \\ a_{2,3} \\ a_{3,3} \\ a_{4,3}
\end{Bmatrix} = 0
\tag{4.9}
$$

At this point it is convenient to introduce a new constant quantity, $\hat{Q}_c$, defined as

$$\hat{Q}_c = EA_k \cdot e_{c,k} \tag{4.10}$$

where $e_{c,k}$ is a measure of the longitudinal extension.

$$e_{c,k} = \Lambda_k \sum_{i=1}^{n} \left[\int_{x_{i-1}}^{x_i} \left(\frac{d\psi_i}{dx} \right)^2 dx \right] \tag{4.11}$$

After determining the critical buckling force, the post-buckling problem is considered. When the compressive axial force is larger than the critical buckling force, the linear buckling problem given by (4.5) cannot be used to study the beam's deformation. The nonlinear equation given by (4.2) needs to be considered. For solving (4.2), following reference [47], it is assumed that

$$\upsilon_k(x) = b_k \psi_k(x) \tag{4.12}$$

where b_k is a non-dimensional factor, which is called the buckling factor. On substituting (4.5), (4.11), and (4.12) into (4.2), the result is

$$b_k^2 = \frac{r_k^2 \left(P_{0,k} - P_{c,k} \right)}{e_{c,k}} \tag{4.13}$$

On substituting (4.10) into (4.13) and returning it to dimensional form, it is found that b_k is a constant with respect to $\hat{x}$ for all the sections; that is,

$$b^2 = \frac{\left(\hat{P}_0 - \hat{P}_c\right)}{\hat{Q}_c} \tag{4.14}$$

Therefore the solution of (4.2) can be written as

$$\upsilon_k(x) = b\psi_k(x) \tag{4.15}$$

Here, it's important to note the fact that if the beam span is $\hat{x} \in (0,\ l)$ at critical buckling situation, then after buckling, the beam shall have a shorter span; that is, $x \in (0, x_n)$, where $x_n < l$. Therefore (4.12) is only an approximation to calculate the buckling factor b based on an *assumption* that the actual buckling force $\hat{P}_0$ is *slightly* higher than the critical buckling force $\hat{P}_c$, so that the change of the span is negligible and the buckling displacement $\upsilon(x)$ can be approximately expressed as the critical mode shape $\psi(x)$ times an amplitude term, as shown in (4.12). A complete solution for the static pre-buckling, critical-buckling, and post-buckling cases is given in Chapter 5.

4.2. Free Vibrations about Post-Buckling Position

Free oscillations of the undamped resonator modeled as a beam with axially varying properties are considered in this section. The equation of motion of an undamped, unforced beam subjected to an axial load is given by

$$\frac{\partial^2 w_k}{\partial t_k^{\,2}} + \left\{ P_{0,k} - \frac{\Lambda_k}{r_k^2} \left[\sum_{i=1}^{n} \int_{x_{i-1}}^{x_i} \left(\frac{\partial w_i}{\partial x} \right)^2 dx \right] \right\} \frac{\partial^2 w_k}{\partial x^2} + \frac{\partial^4 w_k}{\partial x^4} = 0, \qquad k = 1, 2, ..., n. \tag{4.16}$$

where w_k is the overall transverse displacement in the free vibration case. The corresponding boundary and compatibility conditions are similar in form to those given by (4.6) and (4.8). The solution of this system can be written as the sum of a static component and a dynamic component [41] (see Figure 4.2)

$$w_k(x, t_k) = b\, \psi_k(x) + v_k(x, t_k) \tag{4.17}$$

where $v_k(x, t_k)$ is the k^{th} component of the dynamic deflection, $\psi_k(x)$ is the k^{th} component of the static buckling mode shape $\psi(x)$, and b is the buckling level factor defined by (4.14).

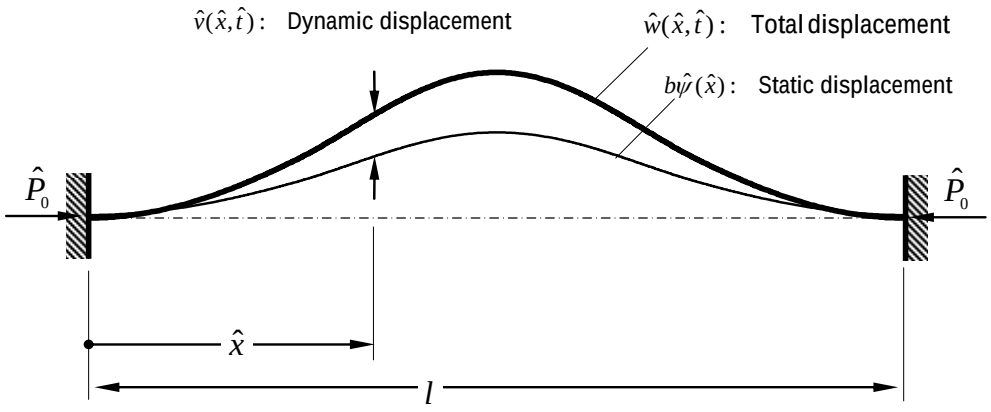

Figure 4.2: Buckled beam configuration.

Next, the natural frequencies $\hat{\omega}$ and mode shapes associated with free oscillations around the post-buckled position $b\psi(x)$ are examined. To find the natural frequencies and mode shapes, (4.17) is first substituted into (4.16), it is assumed that $\left|v_k(x,t_k)\right| << \left|b\,\psi_k(x)\right|$, and the separation of variables is used to have

$$v_k(x,t_k) = \phi_k(x)\, e^{i\omega_k t_k} \tag{4.18}$$

where $\phi_k(x)$ is the mode shape and ω_k is the frequency quantity associated with section $k = 1, 2, ..., n.$, which is defined in the same way as (3.51). Here, it's necessary to keep in mind that $\omega_k t_k = \hat{\omega}\,\hat{t}$. On substituting (4.5), (4.13) and (4.18) into (4.16), the following equation is obtained:

$$-\omega_k^2\phi_k + P_{c,k}\frac{d^2\phi_k}{dx^2} + \frac{d^4\phi_k}{dx^4} = \frac{2b^2\Lambda_k}{r_k^2}\frac{d^2\psi_k}{dx^2}\left[\sum_{i=1}^{n}\int_{x_{i-1}}^{x_i}\left(\frac{d\psi_i}{dx}\frac{d\phi_i}{dx}\right)dx\right] \tag{4.19}$$

The general solution of (4.19) is composed of a homogeneous solution $\phi_{h,k}(x)$ and a particular solution $\phi_{p,k}(x)$

$$\phi_k(x) = \phi_{h,k}(x) + \phi_{p,k}(x) \tag{4.20}$$

The homogeneous solution is given by

$$\phi_{h,k}(x) = C_{1,k}\sin\left(\lambda_{1,k}x\right) + C_{2,k}\cos\left(\lambda_{1,k}x\right) + C_{3,k}\sinh\left(\lambda_{2,k}x\right) + C_{4,k}\cosh\left(\lambda_{2,k}x\right) \tag{4.21}$$

where

$$\lambda_{1,k} = \sqrt{\frac{1}{2}\left(P_{c,k} + \sqrt{P_{c,k}^2 + 4\omega_k^2}\right)}, \quad \lambda_{2,k} = \sqrt{\frac{1}{2}\left(-P_{c,k} + \sqrt{P_{c,k}^2 + 4\omega_k^2}\right)} \tag{4.22}$$

The particular solution can be obtained by solving the equation obtained after substituting (4.20) and (4.21) into (4.19), that is,

$$\begin{aligned} &-\omega_k^2\phi_{p,k} + P_{c,k}\frac{d^2\phi_{p,k}}{dx^2} + \frac{d^4\phi_{p,k}}{dx^4} - \frac{2b^2\Lambda_k}{r_k^2}\frac{d^2\psi_k}{dx^2}\left[\sum_{i=1}^{n}\int_{x_{i-1}}^{x_i}\left(\frac{d\psi_i}{dx}\frac{d\phi_{p,i}}{dx}\right)dx\right] \\ &= \frac{2b^2\Lambda_k}{r_k^2}\frac{d^2\psi_k}{dx^2}\left[\sum_{i=1}^{n}\int_{x_{i-1}}^{x_i}\left(\frac{d\psi_i}{dx}\frac{d\phi_{h,i}}{dx}\right)dx\right] \end{aligned} \tag{4.23}$$

It follows that the solution of (4.23) can be written as

$$\phi_{p,k} = C_{5,k}\left[a_{3,k}\cos\left(\zeta_k x\right) + a_{4,k}\sin\left(\zeta_k x\right)\right] \tag{4.24}$$

where the $C_{5,k}$ are constants. Making use of (4.23) and (4.24), the relations between the constants $C_{j,k}$, $j=1,2,...,5$ are obtained as

$$\sum_{i=1}^{n}\left(B_{1,i}C_{1,i}+B_{2,i}C_{2,i}+B_{3,i}C_{3,i}+B_{4,i}C_{4,i}+D_{k,i}C_{5,i}\right)=0 \tag{4.25}$$

where the $B_{j,i}$ s and $D_{k,i}$ are constant values ($j=1,2,3,4.$ $k=1,2,...n.$), which are given by

$$B_{1,i} = \left\{ a_{2,i} \sin\left(\lambda_{1,i} x\right) + a_{3,i} \zeta_i \lambda_{1,i} \left[\frac{\cos\left[\left(\zeta_i - \lambda_{1,i}\right) x\right]}{2\left(\zeta_i - \lambda_{1,i}\right)} + \frac{\cos\left[\left(\zeta_i + \lambda_{1,i}\right) x\right]}{2\left(\zeta_i + \lambda_{1,i}\right)} \right] \right.$$
$$\left. + a_{4,i} \zeta_i \lambda_{1,i} \left[\frac{\sin\left[\left(\zeta_i - \lambda_{1,i}\right) x\right]}{2\left(\zeta_i - \lambda_{1,i}\right)} + \frac{\sin\left[\left(\zeta_i + \lambda_{1,i}\right) x\right]}{2\left(\zeta_i + \lambda_{1,i}\right)} \right] \right\} \Bigg|_{x_{i-1}}^{x_i}$$

$$B_{2,i} = \left\{ a_{2,i} \cos\left(\lambda_{1,i} x\right) + a_{3,i} \zeta_i \lambda_{1,i} \left[\frac{\sin\left[\left(\zeta_i - \lambda_{1,i}\right) x\right]}{2\left(\zeta_i - \lambda_{1,i}\right)} - \frac{\sin\left[\left(\zeta_i + \lambda_{1,i}\right) x\right]}{2\left(\zeta_i + \lambda_{1,i}\right)} \right] \right.$$
$$\left. + a_{4,i} \zeta_i \lambda_{1,i} \left[\frac{-\cos\left[\left(\zeta_i - \lambda_{1,i}\right) x\right]}{2\left(\zeta_i - \lambda_{1,i}\right)} + \frac{\cos\left[\left(\zeta_i + \lambda_{1,i}\right) x\right]}{2\left(\zeta_i + \lambda_{1,i}\right)} \right] \right\} \Bigg|_{x_{i-1}}^{x_i}$$

$$B_{3,i} = \left\{ a_{2,i} \sinh\left(\lambda_{2,i} x\right) - \frac{a_{3,i} \zeta_i \lambda_{2,i}}{\lambda_{2,i}^2 + \zeta_i^2} \left[\lambda_{2,i} \sin\left(\zeta_i x\right) \sinh\left(\lambda_{2,i} x\right) - \zeta_i \cos\left(\zeta_i x\right) \cosh\left(\lambda_{2,i} x\right) \right] \right.$$
$$\left. + \frac{a_{4,i} \zeta_i \lambda_{2,i}}{\lambda_{2,i}^2 + \zeta_i^2} \left[\lambda_{2,i} \cos\left(\zeta_i x\right) \sinh\left(\lambda_{2,i} x\right) + \zeta_i \sin\left(\zeta_i x\right) \cosh\left(\lambda_{2,i} x\right) \right] \right\} \Bigg|_{x_{i-1}}^{x_i} \tag{4.26}$$

$$B_{4,i} = \left\{ a_{2,i} \cosh\left(\lambda_{2,i} x\right) - \frac{a_{3,i} \zeta_i \lambda_{2,i}}{\lambda_{2,i}^2 + \zeta_i^2} \left[\lambda_{2,i} \sin\left(\zeta_i x\right) \cosh\left(\lambda_{2,i} x\right) - \zeta_i \cos\left(\zeta_i x\right) \sinh\left(\lambda_{2,i} x\right) \right] \right.$$
$$\left. + \frac{a_{4,i} \zeta_i \lambda_{2,i}}{\lambda_{2,i}^2 + \zeta_i^2} \left[\lambda_{2,i} \cos\left(\zeta_i x\right) \cosh\left(\lambda_{2,i} x\right) + \zeta_i \sin\left(\zeta_i x\right) \sinh\left(\lambda_{2,i} x\right) \right] \right\} \Bigg|_{x_{i-1}}^{x_i}$$

$$D_{k,i} = \left\{ \frac{a_{3,i}^2 + a_{4,i}^2}{2} \zeta_i^2 x - \frac{a_{3,i}^2 - a_{4,i}^2}{4} \zeta_i \sin\left(2\zeta_i x\right) + a_{2,i} a_{3,i} \cos\left(\zeta_i x\right) + a_{2,i} a_{4,i} \sin\left(\zeta_i x\right) \right.$$
$$\left. + \frac{a_{3,i} a_{4,i}}{2} \zeta_i \cos\left(2\zeta_i x\right) \right\} \Bigg|_{x_{i-1}}^{x_i} - \frac{r_k^2 \delta_{ik}}{2 b^2 \zeta_k^2 \Lambda_k} \omega_k^2$$

Equation (4.25) along with the associated boundary conditions and compatibility conditions forms an eigenvalue problem for the $C_{j,i}$ and the natural frequencies ω_k.

After determining these values for $C_{j,i}$, the expression for the free vibration mode shape of the post-buckled beam with axially varying properties can be determined as

$$\phi(x) = \sum_{k=1}^{n} \phi_k(x) H_k(x) \tag{4.27}$$

4.3. Forced Oscillations

Forced oscillations of the resonator modeled as a beam with axially varying properties are considered in this section. The nonlinear equation of motion is given by (3.35), and (3.49), the boundary conditions are given by (3.31), and the displacement compatibility conditions are similar as form those given by (4.8). For solving (3.35), it is assumed that

$$W_k(x,t_k) = b\psi_k(x) + \eta_k(x,t_k) \tag{4.28}$$

where the $\eta_k(x,t_k)$ represent the dynamic deflection and $b\psi_k(x)$ is the static post-buckling position given by (4.15). On substituting (3.49), (4.5), (4.11), (4.13) and (4.28) into (3.35), one obtains

$$\begin{aligned}
&\ddot{\eta}_k + P_{c,k}\eta_k' + \eta_k^{iv} - \frac{2b^2\Lambda_k}{r_k^2}\left[\sum_{i=1}^{n}\left\langle \psi_i', \eta_i' \right\rangle_i\right]\psi_k'' = \left[\tilde{F}_k + q_k\tilde{p}_k\left(b\psi_k'' + \eta_k''\right)\right]\cos\Omega_k t_k \\
&-2\tilde{\mu}_k\dot{\eta}_k + \frac{2b\Lambda_k}{r_k^2}\left[\sum_{i=1}^{n}\left\langle \psi_i', \eta_i' \right\rangle_i\right]\eta_k'' + \frac{\Lambda_k}{r_k^2}\left[\sum_{i=1}^{n}\left\langle \eta_i', \eta_i' \right\rangle_i\right]\eta_k'' + \frac{b\Lambda_k}{r_k^2}\left[\sum_{i=1}^{n}\left\langle \eta_i', \eta_i' \right\rangle_i\right]\psi_k'' \\
&k = 1, 2, ..., n.
\end{aligned} \tag{4.29}$$

From here onwards, the following notations and expressions are used for convenience:

$$(\dot{}) = \partial/\partial t_k \ , \ (\ )' = \partial/\partial x \, , \langle a,b \rangle_i = \int_{x_{i-1}}^{x_i} (a \cdot b)\, dx \, , \text{and } \langle a,b \rangle = \int_{x_0}^{x_n} (a \cdot b)\, dx \qquad (4.30)$$

The corresponding boundary conditions and the compatibility conditions follow the same form as given by (4.6) and (4.8), that is,

$$\begin{aligned} &\eta_1 = 0, \qquad \eta_1' = 0 \quad at \quad x = x_0, \\ &\eta_n = 0, \qquad \eta_n' = 0 \quad at \quad x = x_n. \end{aligned} \qquad (4.31)$$

$$\begin{aligned} &\eta_{k-1} = \eta_k, \qquad EI_{k-1}\eta_{k-1}'' = EI_k \eta_k'', \\ &\eta_{k-1}' = \eta_k', \qquad EI_{k-1}\eta_{k-1}''' = EI_k \eta_k''', \qquad at \ x = x_{k-1}, \quad k = 2,3,...,n. \end{aligned} \qquad (4.32)$$

Next, assuming that the system is a weakly nonlinear system with weak damping and weak forcing, the method of multiple scales [54], [55] is used to obtain for an approximate solution of (4.29). The basic approach follows that presented in earlier work [56], but here, the application is directed towards a composite microscale structure with axially varying properties. Different time scales are introduced by using a small, dimensionless book-keeping parameter ε as

$$T_{0k} = t_k, \quad T_{1k} = \varepsilon t_k, \quad T_{2k} = \varepsilon^2 t_k, \quad ... \qquad (4.33)$$

and correspondingly, the derivatives take the form

$$\frac{\partial}{\partial t_k} = D_{0k} + \varepsilon D_{1k} + \varepsilon^2 D_{2k} + ..., \quad D_{ik} = \frac{\partial}{\partial T_{ik}} \tag{4.34}$$

It is noted that

$$D_{ik} = l^2 \sqrt{\frac{\rho A_k}{EI_k}} \hat{D}_i \text{ and } \hat{D}_i = \frac{\partial}{\partial \hat{T}_i} \tag{4.35}$$

for the purposes of the ensuing the frequency-response derivation. To balance the effect of nonlinearity, damping, and excitation, the following scaling is also introduced:

$$\tilde{p}_k = \varepsilon^3 p_k, \quad \tilde{\mu}_k = \varepsilon^2 \mu_k \tag{4.36}$$

With this scaling, the sources of secular terms will arise at $O(\varepsilon^3)$. The approximate solution is then expanded as

$$\begin{aligned} \eta_k(x,t_k) = \varepsilon \eta_{1k}(x,T_{0k},T_{1k},T_{2k}) + \varepsilon^2 \eta_{2k}(x,T_{0k},T_{1k},T_{2k}) \\ + \varepsilon^3 \eta_{3k}(x,T_{0k},T_{1k},T_{2k}) + ... \end{aligned} \tag{4.37}$$

Introducing (4.33)-(4.37) into (4.29), rewriting the excitation term in polar form, and collecting terms of the same power of ε, the following hierarchy of equations is obtained:

$O(\varepsilon)$:

$$\mathcal{L}(\eta_{1k}) = D_{0k}^2\eta_k + P_{c,k}\eta_{1k}'' + \eta_{1k}^{iv} - \frac{2b^2\Lambda_k}{r_k^2}\left[\sum_{i=1}^{n}\left\langle \psi_i', \eta_{1i}'\right\rangle_i\right]\psi_k'' = 0 \tag{4.38}$$

$O(\varepsilon^2)$:

$$\mathcal{L}(\eta_{2k}) = \frac{2b\Lambda_k}{r_k^2}\left[\sum_{i=1}^{n}\left\langle \psi_i', \eta_{1i}'\right\rangle_i\right]\eta_{1k}'' + \frac{b\Lambda_k}{r_k^2}\left[\sum_{i=1}^{n}\left\langle \eta_{1i}', \eta_{1i}'\right\rangle_i\right]\psi_k'' - 2D_{0k}D_{1k}\eta_{1k} \tag{4.39}$$

$O(\varepsilon^3)$:

$$\begin{aligned}\mathcal{L}(\eta_{3k}) = &-2\mu_k D_{0k}\eta_{1k} - 2D_{0k}D_{1k}\eta_{2k} - \left(D_{1k}^2 + 2D_{0k}D_{2k}\right)\eta_{1k} \\ &+ \frac{2b\Lambda_k}{r_k^2}\left[\sum_{i=1}^{n}\left\langle \psi_i', \eta_{1i}'\right\rangle_i\right]\eta_{2k}'' + \frac{2b\Lambda_k}{r_k^2}\left[\sum_{i=1}^{n}\left\langle \psi_i', \eta_{2i}'\right\rangle_i\right]\eta_{1k}'' \\ &+ \frac{\Lambda_k}{r_k^2}\left[\sum_{i=1}^{n}\left\langle \eta_{1i}', \eta_{1i}'\right\rangle_i\right]\eta_{1k}'' + \frac{2b\Lambda_k}{r_k^2}\left[\sum_{i=1}^{n}\left\langle \eta_{1i}', \eta_{2i}'\right\rangle_i\right]\psi_k'' \\ &+ \left[\frac{1}{2}F_k e^{j\Omega_k t_k} + c.c.\right]\end{aligned} \tag{4.40}$$

where *c.c.* stands for complex conjugate of the preceding terms and

$$F_k = p_k h_k \frac{\partial\delta(x - x_m)}{\partial x} + bq_k p_k \psi_k'' \tag{4.41}$$

The corresponding boundary conditions and compatibility conditions at all orders follow the same form as that of (4.31) and (4.32).

When the excitation frequency is close to the first natural frequency, namely

$$\hat{\Omega} = \hat{\omega}_1 + \varepsilon^2\hat{\sigma} \text{ , or } \Omega_k = \omega_{1k} + \varepsilon^2\sigma_k \tag{4.42}$$

the solution of (4.38) can be approximated to consist of an amplitude $A_{1k}(T_{1k}, T_{2k})$ with the first mode shape of the free vibrations around the post-buckled position $\phi_{1k}(x)$,which is given by (4.20), (4.21), and (4.24). For the sake of continuity, the displacement at the connecting point of two sections has to be the same; that is

$$A_{1k}\phi_{1,k}(x_k) = A_{1k+1}\phi_{1,k+1}(x_k) \tag{4.43}$$

Also, the compatibility conditions of $\phi_{1k}(x)$ require that

$$\phi_{1,k}(x_k) = \phi_{1,k+1}(x_k) \tag{4.44}$$

Hence, it follows that the amplitude in (4.43) has to be independent of the section number. Therefore, one can write the solution of (4.38) as

$$\eta_{1k} = \phi_{1k}(x)\left[A_1(T_{1k}, T_{2k})e^{j\omega_{1k}T_{0k}} + \bar{A}_1(T_{1k}, T_{2k})e^{-j\omega_{1k}T_{0k}} \right] \tag{4.45}$$

where A_1 and $\bar{A}_1$ are the complex amplitude and its complex conjugate, which can be written in a polar form as, $A_1(T_{1k}, T_{2k}) = \frac{1}{2}ae^{j\beta}$.

Next to solve Eq. (4.39), (4.45) is first substituted into (4.39), resulting in

$$\begin{aligned}\mathcal{L}(\eta_{2k}) = {} & \frac{2b\Lambda_k}{r_k^2}\left[\sum_{i=1}^{n}\left\langle \psi_i', \phi_{1i}'\right\rangle_i \left(A_1 e^{j\omega_{1i}T_{0i}} + c.c.\right)\right]\phi_{1k}''\left(A_1 e^{j\omega_{1k}T_{0k}} + c.c.\right) \\ & + \frac{b\Lambda_k}{r_k^2}\left[\sum_{i=1}^{n}\left\langle \phi_i', \phi_{1i}'\right\rangle_i \left(A_1^2 e^{j2\omega_{1i}T_{0i}} + A_1\bar{A}_1 + c.c.\right)\right]\psi_k'' \\ & - j2\omega_{1k}\phi_{1k}\left[\left(D_{1k}A_1\right)e^{j\omega_{1k}T_{0k}} - \left(D_{1k}\bar{A}_1\right)e^{-j\omega_{1k}T_{0k}}\right]\end{aligned} \tag{4.46}$$

From (3.17) and (3.51), also

$$\omega_k T_{0k} = \hat{\omega}\hat{t}, \quad n \in N^1 \tag{4.47}$$

Therefore,

$$\left[\sum_{i=1}^{n}(\cdot)_i e^{j\omega_i T_{0i}}\right] = \left[\sum_{i=1}^{n}(\cdot)_i\right]e^{j\omega_k T_{0k}} \tag{4.48}$$

Making use of (4.48) in (4.46), the right-hand side of (4.39) can be expressed as the summation of sources of the non-secular terms and secular terms (S.T.),

$$\mathcal{L}(\eta_{2k}) = b\Psi_k(x)\left[A_1^2 e^{j2\omega_{1k}T_{0k}} + A_1\bar{A}_1 + c.c.\right] + \text{S.T.} \tag{4.49}$$

where,

$$\begin{aligned}\Psi_k(x) = {} & \frac{2\Lambda_k}{r_k^2}\left[\sum_{i=1}^{n}\left\langle \psi_i', \phi_{1i}'\right\rangle_i\right]\phi_{1k}'' + \frac{\Lambda_k}{r_k^2}\left[\sum_{i=1}^{n}\left\langle \phi_{1i}', \phi_{1i}'\right\rangle_i\right]\psi_k'' \\ \text{S.T.} = {} & -j2\omega_{1k}\phi_{1k}\left[\left(D_{1k}A_1\right)e^{j\omega_{1k}T_{0k}} - \left(D_{1k}\bar{A}_1\right)e^{-j\omega_{1k}T_{0k}}\right]\end{aligned} \tag{4.50}$$

Setting the sum of the secular terms to zero one obtains that the amplitude term is only a function of the time scale T_2; that is

$$A_1 = A_1(T_{2k}) \tag{4.51}$$

Next, to solve (4.49), it is assumed that the approximate solution for the spatial term of $\eta_{2k}(x,t_k)$ is a weighted summation of the free-oscillation mode shapes given by (4.20), (4.21), and (4.24). This leads to

$$\eta_{2k} = bA_1\bar{A}_1\Phi_{1k}(x) + bA_1^2\Phi_{2k}(x)e^{j2\omega_{1k}T_{0k}} + c.c. \tag{4.52}$$

where $\Phi_{1k}(x)$ and $\Phi_{2k}(x)$ are defined as

$$\Phi_{1k}(x) = \sum_{r=1}^{\infty} T_r\phi_{rk}, \qquad \Phi_{2k}(x) = \sum_{r=1}^{\infty} S_r\phi_{rk}, \tag{4.53}$$

On substituting (4.52) into (4.49), one first obtains the decoupled differential equations for $\Phi_{1k}(x)$ and $\Phi_{2k}(x)$

$$P_{c,k}\Phi''_{1k} + \Phi^{iv}_{1k} - \frac{2b^2\Lambda_k}{r_k^2}\left[\sum_{i=1}^{n}\left\langle\psi'_i, \Phi'_{1i}\right\rangle_i\right]\psi''_k = \Psi_k \tag{4.54}$$

$$-(2\omega_{1k})^2\Phi_{2k} + P_{c,k}\Phi''_{2k} + \Phi^{iv}_{2k} - \frac{2b^2\Lambda_k}{r_k^2}\left[\sum_{i=1}^{n}\left\langle\psi'_i, \Phi'_{2i}\right\rangle_i\right]\psi''_k = \Psi_k \tag{4.55}$$

Then making use of (4.53) in (4.54) and (4.55)

$$\sum_{r=1}^{\infty} T_r \left\{ P_{c,k}\phi_{rk}'' + \phi_{rk}^{iv} - \frac{2b^2\Lambda_k}{r_k^2}\left[\sum_{i=1}^{n}\left\langle \psi_i', \phi_{rk}' \right\rangle_i\right]\psi_k'' \right\} = \Psi_k \tag{4.56}$$

$$\sum_{r=1}^{\infty} S_r \left\{ -(2\omega_{1k})^2\phi_{rk} + P_{c,k}\phi_{rk}'' + \phi_{rk}^{iv} - \frac{2b^2\Lambda_k}{r_k^2}\left[\sum_{i=1}^{n}\left\langle \psi_i', \phi_{rk}' \right\rangle_i\right]\psi_k'' \right\} = \Psi_k \tag{4.57}$$

Equations (4.56) and (4.57) can be further simplified by applying (4.19), and this leads to

$$\sum_{r=1}^{\infty} T_r \omega_{rk}^2 \phi_{rk} = \Psi_k \tag{4.58}$$

$$\sum_{r=1}^{\infty} S_r \left[\omega_{rk}^2 - (2\omega_{1k})^2 \right]\phi_{rk} = \Psi_k \tag{4.59}$$

Next, multiplying by $\frac{EI_k}{\rho A_k l^4}$ on both sides of these equations, using properties given in (3.51), one obtains

$$\sum_{r=1}^{\infty} T_r \hat{\omega}_r^2 \phi_{rk} = \frac{EI_k}{\rho A_k l^4}\Psi_k \tag{4.60}$$

$$\sum_{r=1}^{\infty} S_r \left[\hat{\omega}_r^2 - (2\hat{\omega}_1)^2 \right]\phi_{rk} = \frac{EI_k}{\rho A_k l^4}\Psi_k \tag{4.61}$$

It is mentioned that as a stepwise function defined as in (4.27), any two functions $\varphi(x)$ and $\vartheta(x)$ have the following property

$$\langle \varphi, \vartheta \rangle = \sum_{k=1}^{n} \langle \varphi_k, \vartheta_k \rangle_k \tag{4.62}$$

One can operate on this inner product in (4.58) and (4.59) with the p^{th} free vibration mode shape $\phi_p(x)$ throughout $x \in (x_0, x_n)$ by using the partial inner product through the k^{th} section $x \in (x_{k-1}, x_k)$, and then summing up all the sections together. This results in

$$\sum_{r=1}^{\infty} T_r \hat{\omega}_r^2 \left[\sum_{k=1}^{n} \langle \phi_{rk}, \phi_{pk} \rangle_k \right] = \sum_{k=1}^{n} \frac{EI_k}{\rho A_k l^4} \langle \Psi_k, \phi_{pk} \rangle_k \tag{4.63}$$

$$\sum_{r=1}^{\infty} S_r \left[\hat{\omega}_r^2 - (2\hat{\omega}_1)^2 \right] \left[\sum_{k=1}^{n} \langle \phi_{rk}, \phi_{pk} \rangle_k \right] = \sum_{k=1}^{n} \frac{EI_k}{\rho A_k l^4} \langle \Psi_k, \phi_{pk} \rangle_k \tag{4.64}$$

Next, making use of the orthogonal prosperities of $\phi(x)$, (4.63) and (4.64) become

$$T_p \hat{\omega}_p^2 \sum_{k=1}^{n} \langle \phi_{pk}, \phi_{pk} \rangle_k = \sum_{k=1}^{n} \left[\frac{EI_k}{\rho A_k l^4} \langle \Psi_k, \phi_{pk} \rangle_k \right] \tag{4.65}$$

$$S_p \left[\hat{\omega}_p^2 - (2\hat{\omega}_1)^2 \right] \sum_{k=1}^{n} \langle \phi_{pk}, \phi_{pk} \rangle_k = \sum_{k=1}^{n} \left[\frac{EI_k}{\rho A_k l^4} \langle \Psi_k, \phi_{pk} \rangle_k \right] \tag{4.66}$$

After substituting (4.50) into (4.65) and (4.66) and changing the subscript *p* back to *r* for consistency, the weighting factors T_r and S_r are obtained as

$$T_r = \frac{\langle \psi', \phi_1' \rangle \left[\sum_{k=1}^{n} \frac{\overline{EA}}{\rho A_k} \langle \phi_{1k}'', \phi_{rk} \rangle_k \right] + \langle \phi_1', \phi_1' \rangle \left[\sum_{k=1}^{n} \frac{\overline{EA}}{2\rho A_k} \langle \psi_k'', \phi_{rk} \rangle_k \right]}{\hat{\omega}_r^2 \langle \hat{\phi}_r, \hat{\phi}_r \rangle}$$

$$S_r = \frac{\langle \psi', \phi_1' \rangle \left[\sum_{k=1}^{n} \frac{\overline{EA}}{\rho A_k} \langle \phi_{1k}'', \phi_{rk} \rangle_k \right] + \langle \phi_1', \phi_1' \rangle \left[\sum_{k=1}^{n} \frac{\overline{EA}}{2\rho A_k} \langle \psi_k'', \phi_{rk} \rangle_k \right]}{\left[\hat{\omega}_r^2 - (2\hat{\omega}_1)^2 \right] \langle \hat{\phi}_r, \hat{\phi}_r \rangle} \tag{4.67}$$

Next, to solve (4.40), substituting (4.42), (4.45) and (4.52), one arrives at

$$\mathcal{L}(\eta_{3k}) = A_1^3 h_{1k}(x) e^{j3\omega_{1k} T_{0k}} + h_{2k}(x, T_{2k}) e^{j\omega_{1k} T_{0k}} + c.c. \tag{4.68}$$

where

$$h_{1k}(x) = \frac{2b^2 \Lambda_k}{r_k^2} \left[\Phi_{2k}'' \langle \psi', \phi_1' \rangle + \psi_k'' \langle \phi_1', \Phi_2' \rangle + \phi_{1k}'' \langle \psi', \Phi_2' \rangle + \frac{\phi_{1k}''}{2b^2} \langle \phi_1', \phi_1' \rangle \right] \tag{4.69}$$

$$h_{2k}(x, T_{2k}) = A_1^2 \bar{A}_1 g_k(x) - 2j\omega_{1k} \phi_{1k} \left[\mu_k A_1 + D_{2k} A_1 \right] + \frac{1}{2} F_k e^{j\sigma_k T_{2k}} \tag{4.70}$$

$$\begin{aligned} g_k(x) = \frac{2b^2 \Lambda_k}{r_k^2} \Big[& 2\Phi_{1k}'' \langle \psi', \phi_1' \rangle + \Phi_{2k}'' \langle \psi', \phi_1' \rangle + 2\phi_{1k}'' \langle \psi', \Phi_1' \rangle \\ & + \phi_{1k}'' \langle \psi', \Phi_2' \rangle + 2\psi_k'' \langle \phi_1', \Phi_1' \rangle + \psi_k'' \langle \phi_1', \Phi_2' \rangle + \frac{3}{2b^2} \phi_{1k}'' \langle \phi_1', \phi_1' \rangle \Big] \end{aligned} \tag{4.71}$$

The solvability condition [55] requires the right-hand side of (4.68) and it's boundary conditions be orthogonal to every solution of the corresponding homogenous adjoint problem from x = 0 to 1, which, from (4.18) and (4.27), is $\phi_{rk}(x) e^{\pm j\hat{\omega}_r \hat{t}}$ for the k^{th} section. Multiplying the right-hand side of (4.68) by $\phi_{1k}(x) e^{-j\hat{\omega}_1 \hat{t}}$ and spatially

integrating the result from $x = x_{k-1}$ to $x = x_k$, and adding all the three sections together, the following complex-valued modulation equation is obtained after setting the sum of the secular terms to zero:

$$\begin{aligned} &2j\left[\sum_{k=1}^{n}\left\langle\left(\mu_k A_1 + D_{2k}A_1\right)\omega_{1k}\phi_{1k}, \phi_{1k}\right\rangle_k\right] \\ &= \frac{1}{2}\left[\sum_{k=1}^{n}\left\langle F_k, \phi_{1k}\right\rangle_k\right]e^{j\hat{\sigma}\hat{T}_2} + A_1^2\bar{A}_1\left[\sum_{k=1}^{n}\left\langle g_k, \phi_{1k}\right\rangle_k\right] \end{aligned} \tag{4.72}$$

Further, substituting (3.17) and (4.35) into (4.72), and letting $\gamma = \hat{\sigma}\hat{T}_2 - \beta$, it is found that the approximate solution and frequency-response equation are given by

$$W = \sum_{k=1}^{n} W_k(x, t_k) H_k \tag{4.73}$$

$$\hat{\sigma} = -\hat{\alpha}_{nn}a^2 \pm \left(\frac{\mathcal{F}^2}{4\hat{\omega}_1^2 a^2} - \mathcal{C}^2\hat{\mu}^2\right)^{1/2} \tag{4.74}$$

where

$$\begin{aligned} W_k(x, t_k) = b\left[\psi_k(x) + \frac{1}{2}ba^2\Phi_{1k}(x)\right] + a\phi_{1k}(x)\cos(\Omega_k t_k - \gamma) \\ + \frac{1}{2}ba^2\Phi_{2k}(x)\cos\left[2(\Omega_k t_k - \gamma)\right] + \ldots \end{aligned} \tag{4.75}$$

$$\hat{\alpha}_{nn} = \frac{\sum_{k=1}^{n} \langle \phi_{1k}, g_k \rangle_k}{\left[8\hat{\omega}_1 \sum_{k=1}^{n} \frac{\rho A_k l^4}{EI_k} \langle \phi_{1k}, \phi_{1k} \rangle_k \right]},$$

$$\mathcal{F} = \frac{\sum_{k=1}^{n} \langle \phi_{1k}, F_k \rangle_k}{\left[\sum_{k=1}^{n} \frac{\rho A_k l^4}{EI_k} \langle \phi_{1k}, \phi_{1k} \rangle_k \right]}, \qquad (4.76)$$

$$\mathcal{C} = \frac{\sum_{k=1}^{n} \frac{1}{EI_k} \langle \phi_{1k}, \phi_{1k} \rangle_k}{\left[\sum_{k=1}^{n} \frac{\rho A_k}{EI_k} \langle \phi_{1k}, \phi_{1k} \rangle_k \right]}$$

4.4. Results and Discussion

In Figure 4.3 to Figure 4.5, the variations of a 200 μm PZT resonator's dynamic behaviors are shown with respect to the buckling factor *b* for free oscillations about the first, third, and fifth static buckling modes. When the resonator is oscillating around the fifth static buckling mode shape with *b* equal to 1.13×10^{-3}, the first natural frequency of the resonator is determined from the model as 314.4 kHz, this is close to the experimental result reported in Chapter 2. The corresponding deflection amplitude, which is derived from Eqs. (4.75), is $b\left[\psi(x)+\frac{1}{2}ba^2\Phi_1(x)\right]+a\phi_1(x)+\frac{1}{2}ba^2\Phi_2(x)$, this is shown in Figure 4.6 (a). Here it is important to note that for the same frequency value, the corresponding value of *b* depends on the resonator's stiffness and geometric properties as well as the normalization used to define the static critical buckling mode shape. For example, in this dissertation, the nondimensional static critical buckling

mode shape $\psi(x)$ is defined to satisfy $\int_0^1 \psi^2(x)\,dx = 1$. In Figure 4.6 (a), the amplitude value of mode shape $\phi_1(x)$ is tuned to be 10^{-3}, so that when turned back into dimensional form, the resonator's predicted dynamic displacement is of the same order as the measured displacement at the resonator's mid point. This forced oscillation spatial displacement pattern looks similar to the spatial pattern experimentally observed during forced oscillations, when the excitation frequency is close to the first natural frequency of the resonator (see Figure 2.1 (b)). The frequency-response curve shown in Figure 4.6 (b) resembles that of a Düffing oscillator with a hardening spring; again, this result is consistent with the experimental predictions. In Figure 4.7, simulations are conducted to assess the sensitivity of the nonlinear frequency response curve to geometrical parameters, such as the top electrode thickness. For different values of the top electrode thickness, the numerical value of $\hat{\alpha}_{nn}$ is found to vary, thus from Eq.(4.74) the system nonlinear hardening behavior varies.

The agreement between the analytical predictions and experimental data suggests that the hypothesis that the non-flat equilibrium position of the resonator is caused by buckling can be a valid one. Along with the work reported in references [41], [42], [27], the present study provides the first evidence of such a phenomenon in microscale resonators. In addition, the present work can be used as a basis to study buckling and oscillations of resonators with axially stepwise varying properties.

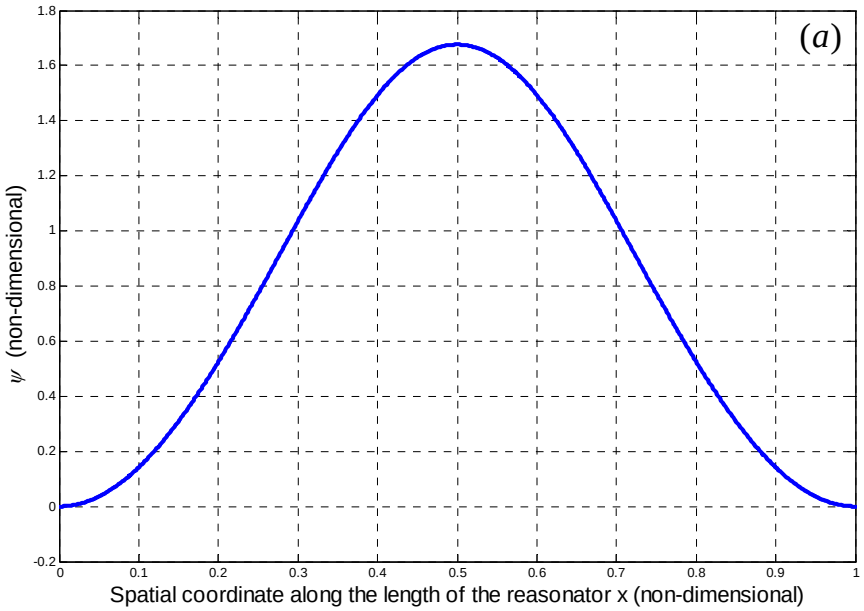
(a)
ψ (non-dimensional)
Spatial coordinate along the length of the reasonator x (non-dimensional)

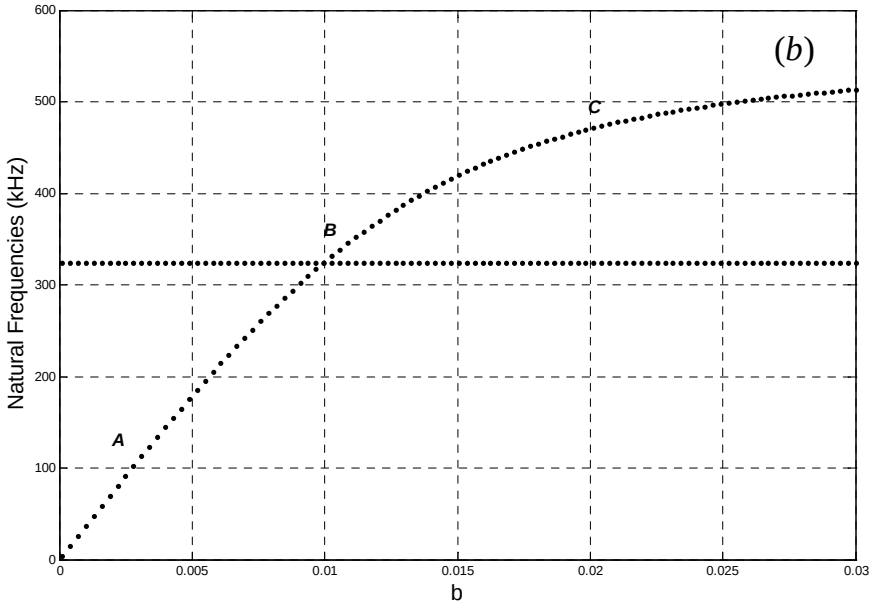
(b)
A
B
C
Natural Frequencies (kHz)
b

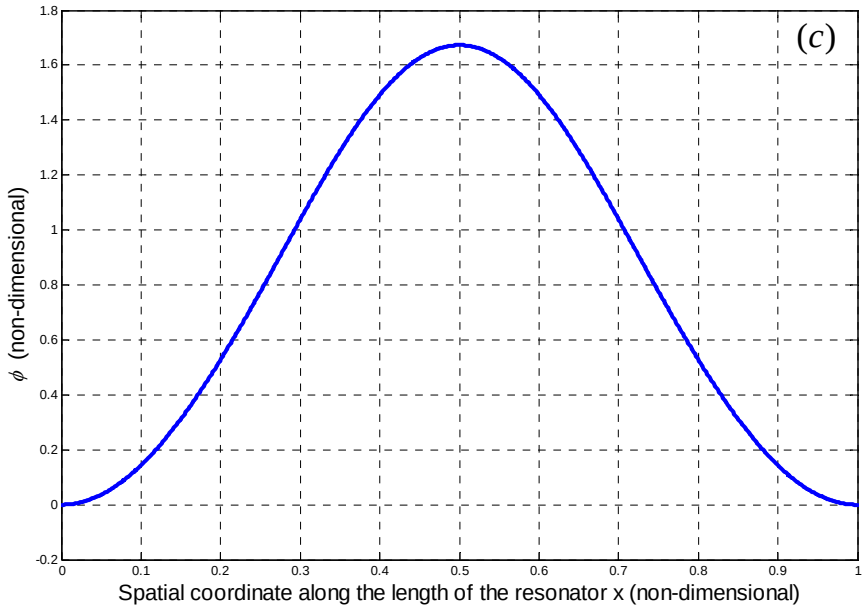
(c)
1.8
1.6
1.4
1.2
1
0.8
0.6
0.4
0.2
0
-0.2
0
0.1
0.2
0.3
0.4
0.5
0.6
0.7
0.8
0.9
1
ϕ (non-dimensional)
Spatial coordinate along the length of the resonator x (non-dimensional)

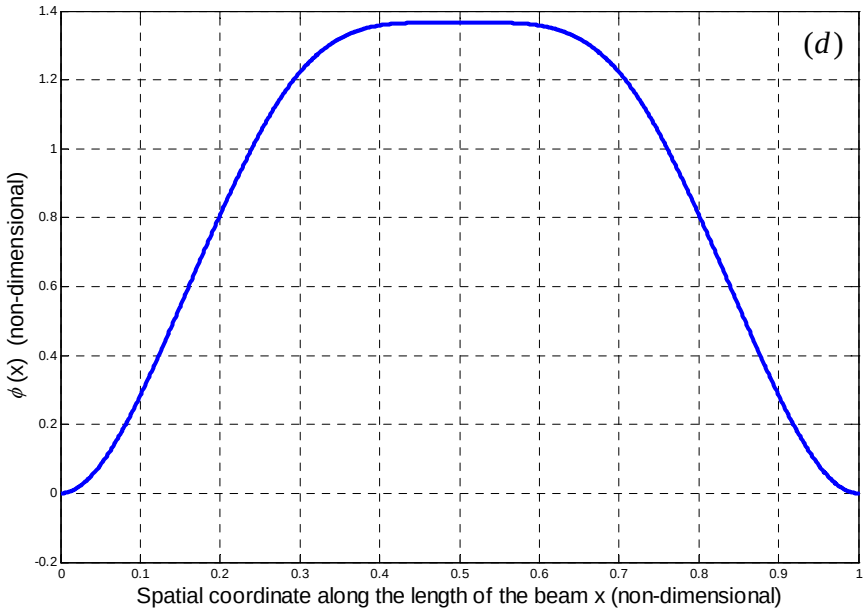
(d)
1.4
1.2
1
0.8
0.6
0.4
0.2
0
-0.2
0
0.1
0.2
0.3
0.4
0.5
0.6
0.7
0.8
0.9
1
ϕ (x) (non-dimensional)
Spatial coordinate along the length of the beam x (non-dimensional)

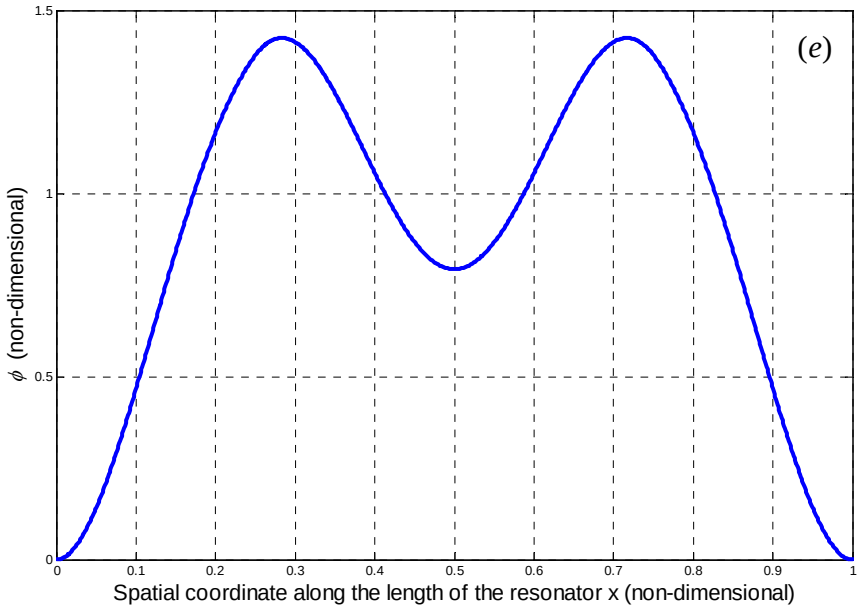

Figure 4.3: (a) The first static buckling mode shape of the 200μm PZT resonator, (b) the first and second natural frequencies versus b, (c) mode shape of free vibration at point A ($b = 1.0\times10^{-3}$) in the frequencies versus b plot, (d) mode shape of free vibration at point B ($b = 1.0\times10^{-2}$) in the frequencies versus b plot, and (e) mode shape of free vibration at point C ($b = 2.0\times10^{-2}$) in the frequencies versus b plot.

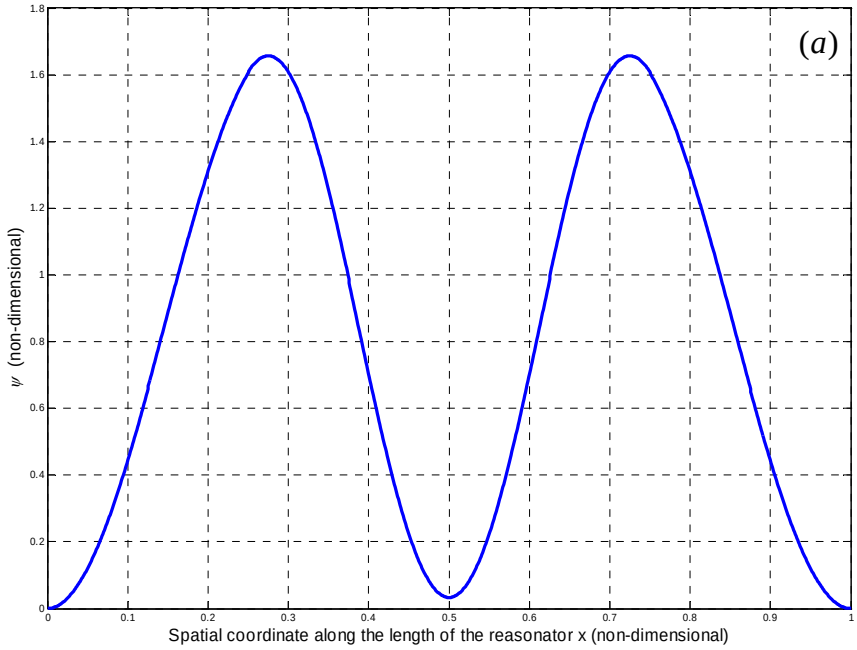
(a)
ψ (non-dimensional)
Spatial coordinate along the length of the reasonator x (non-dimensional)

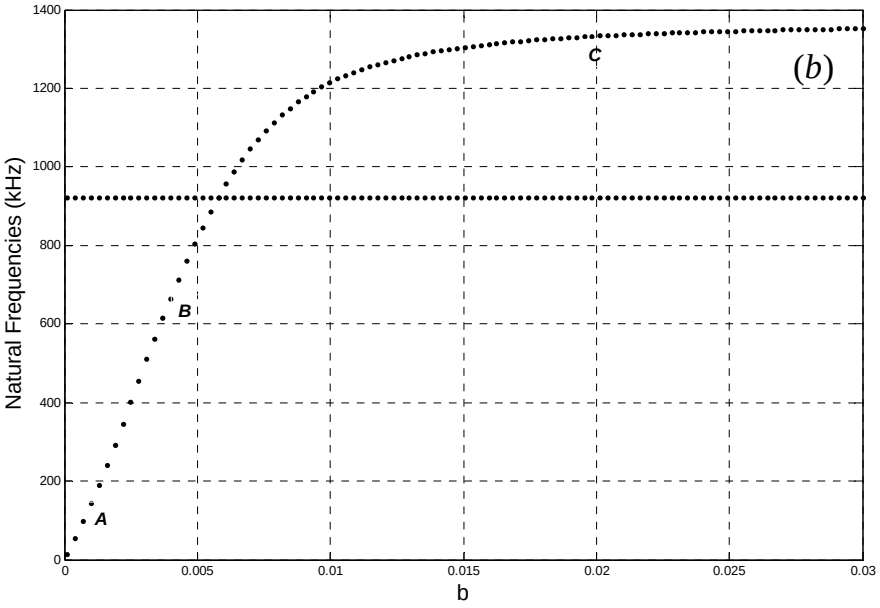
(b)
A
B
C
Natural Frequencies (kHz)
b

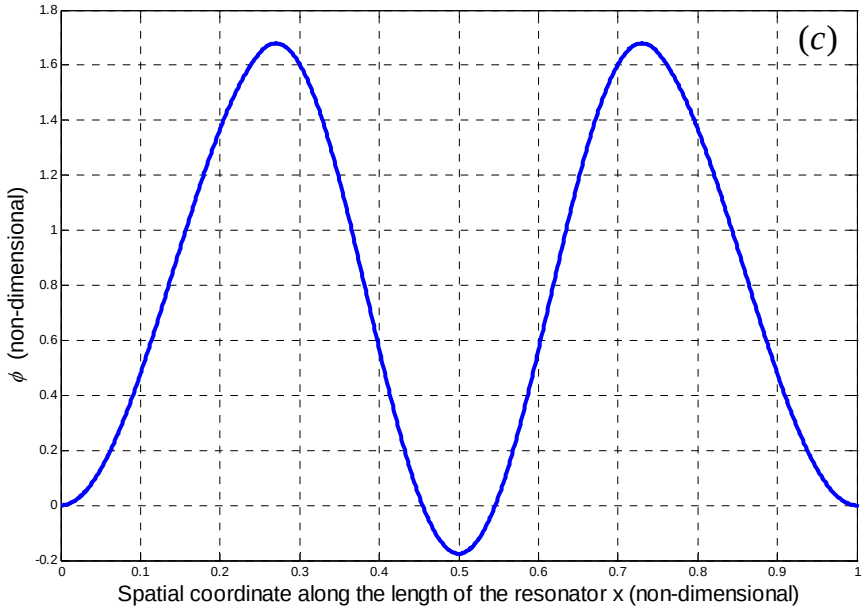
(c)
ϕ (non-dimensional)
Spatial coordinate along the length of the resonator x (non-dimensional)

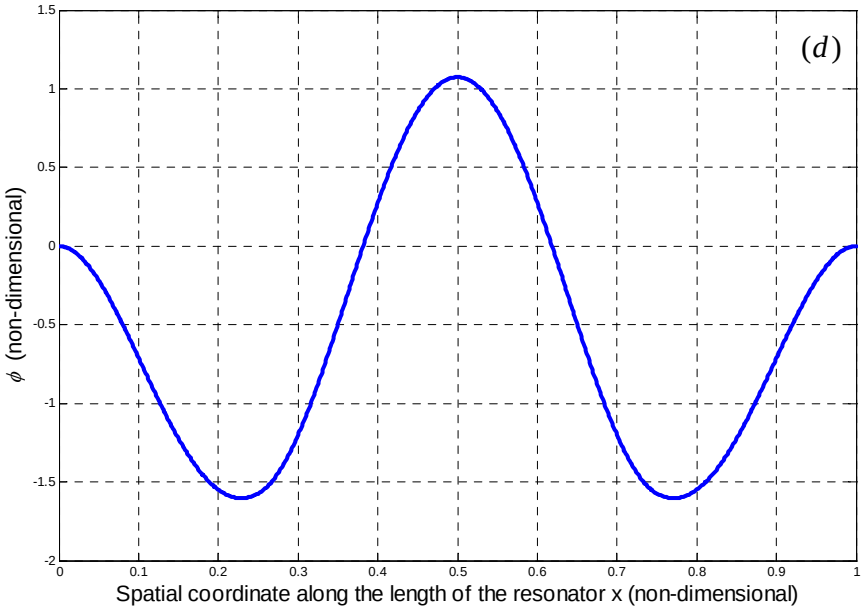
(d)
ϕ (non-dimensional)
Spatial coordinate along the length of the resonator x (non-dimensional)

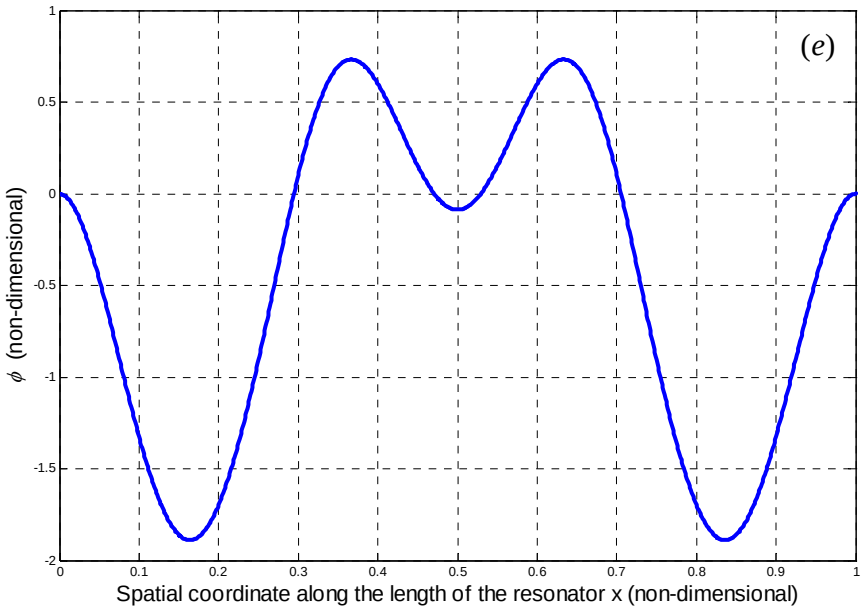

Figure 4.4: (a) The third static buckling mode shape of the 200μm PZT resonator, (b) the first and second natural frequencies versus b, (c) mode shape of free vibration at point A ($b = 1.0\times10^{-3}$) in the frequencies versus b plot, (d) mode shape of free vibration at point B ($b = 4.0\times10^{-3}$) in the frequencies versus b plot, and (e) mode shape of free vibration at point C ($b = 2.0\times10^{-2}$) in the frequencies versus b plot.

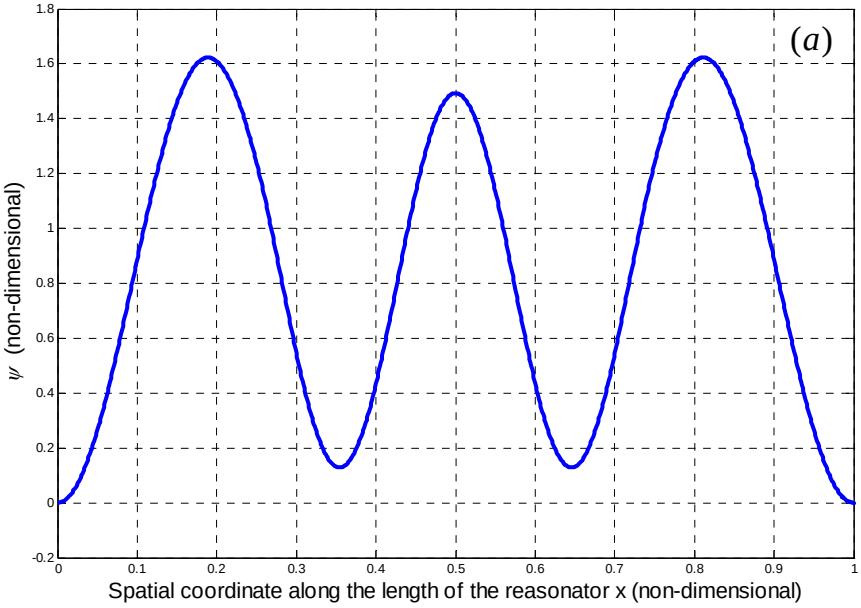
(a)
ψ (non-dimensional)
Spatial coordinate along the length of the reasonator x (non-dimensional)

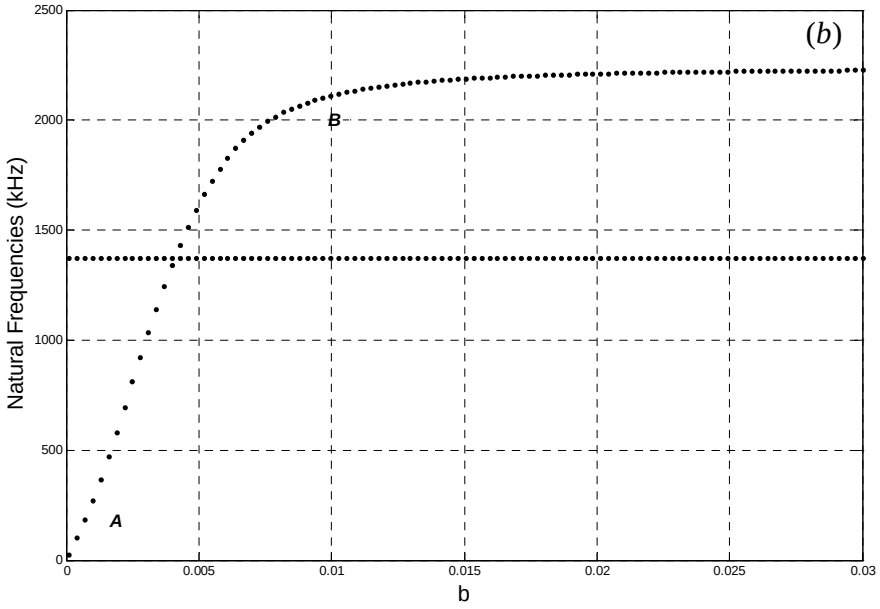
(b)
Natural Frequencies (kHz)
b
A
B

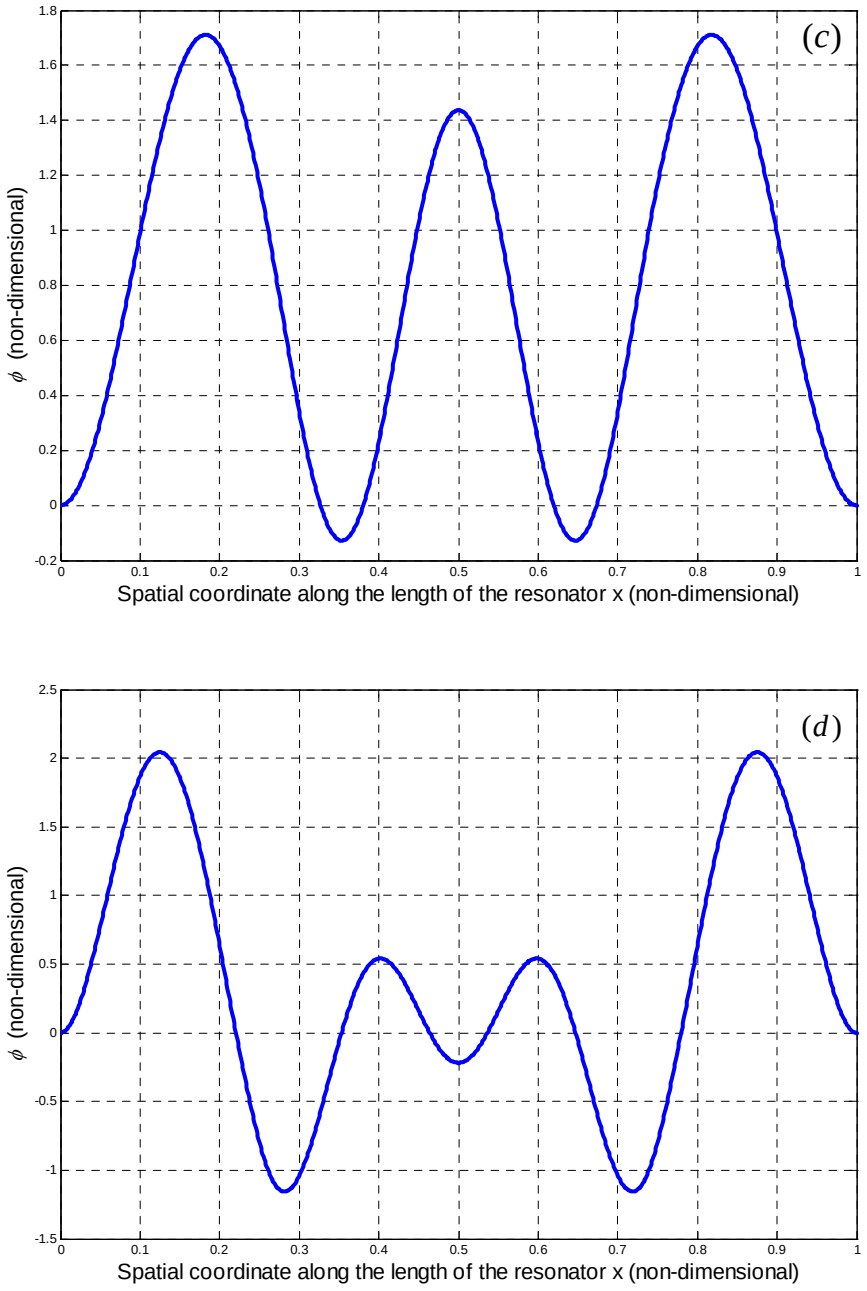

Figure 4.5: (a) The fifth static buckling mode shape of the 200μm PZT resonator, (b) the first and second natural frequencies versus *b*, (c) mode shape of free vibration at point *A* ($b = 1.0\times10^{-3}$) in the frequencies versus *b* plot, and (d) mode shape of free vibration at point *B* ($b = 1.0\times10^{-2}$) in the frequencies versus *b* plot.

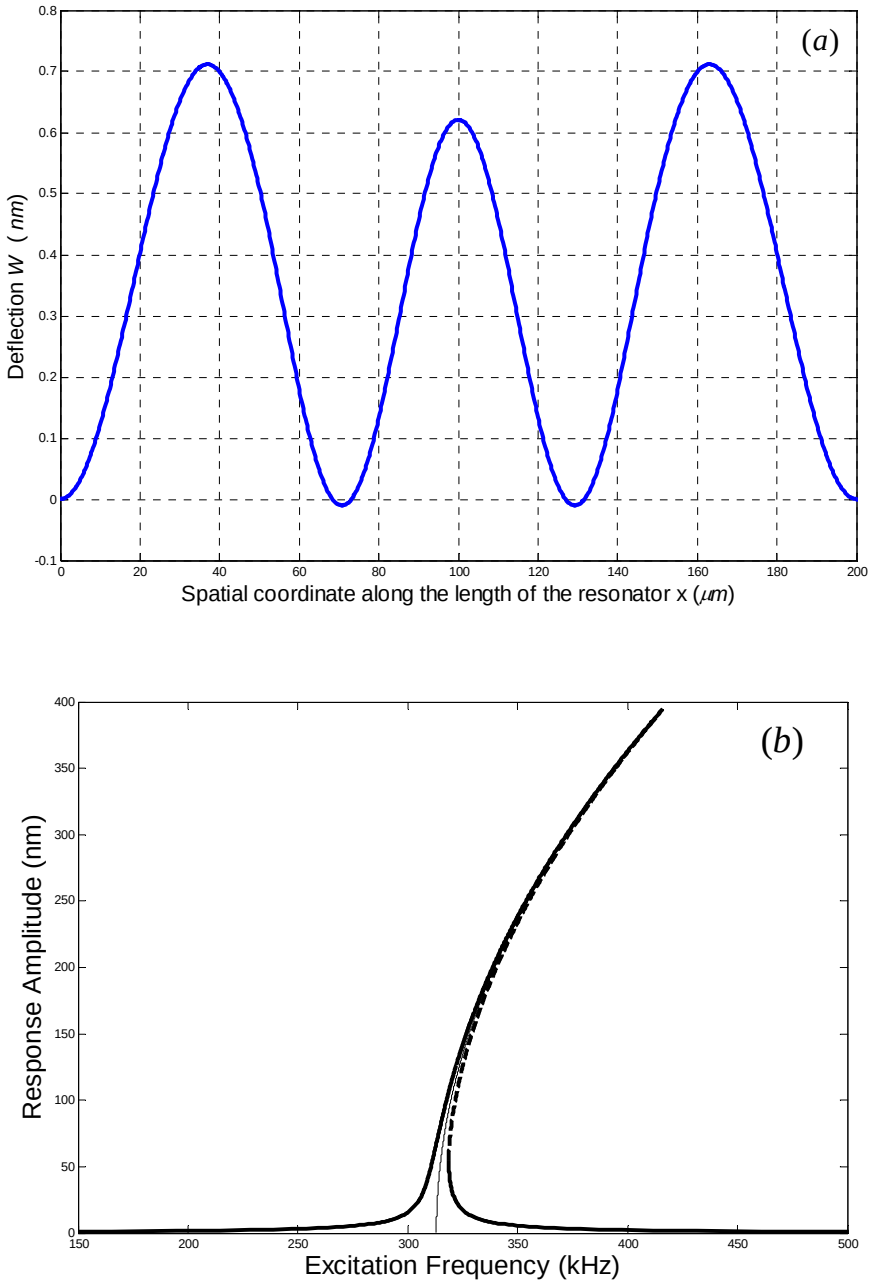

Figure 4.6: (a) Predicted spatial pattern when $b = 1.13\times10^{-3}$, the corresponding natural frequency is 314.4 kHz, and (b) analytical prediction for the frequency-response curve when $b = 1.13\times10^{-3}$ and $\hat{\mu} = 6.0\times10^{-2}$; the solid line represents a stable branch and the dashed line represents an unstable branch.

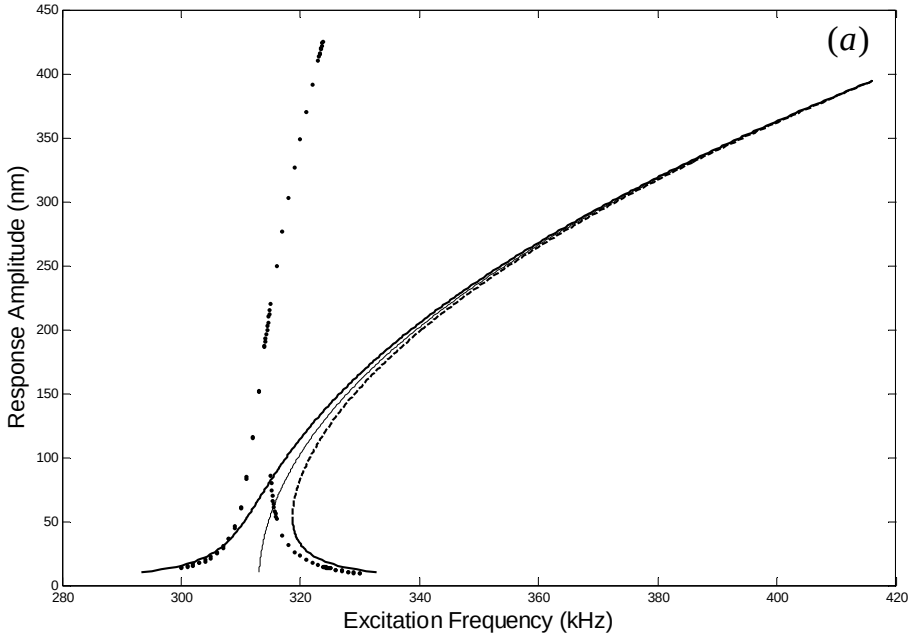
(a)
Response Amplitude (nm)
Excitation Frequency (kHz)
0
50
100
150
200
250
300
350
400
450
280
300
320
340
360
380
400
420

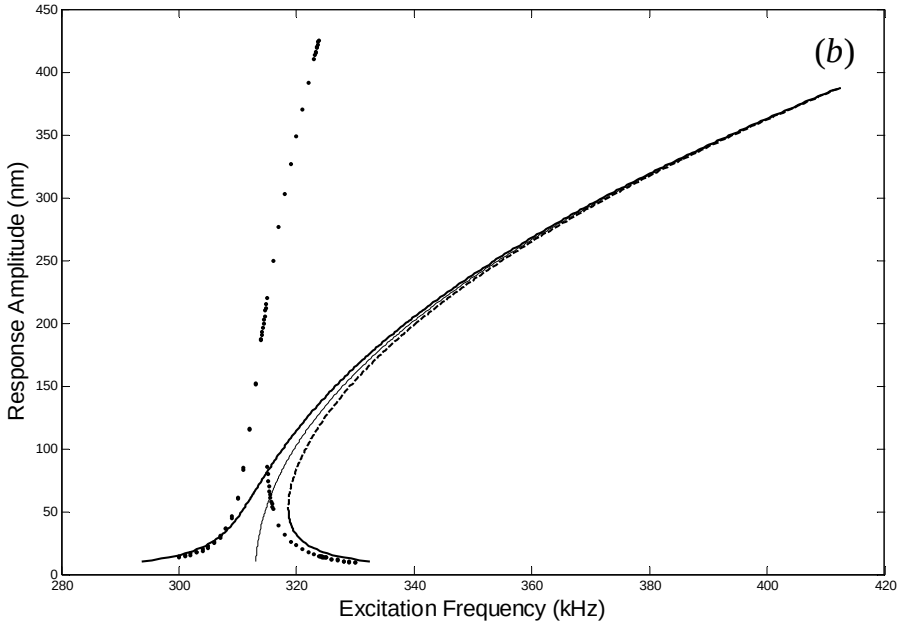
(b)
Response Amplitude (nm)
Excitation Frequency (kHz)
0
50
100
150
200
250
300
350
400
450
280
300
320
340
360
380
400
420

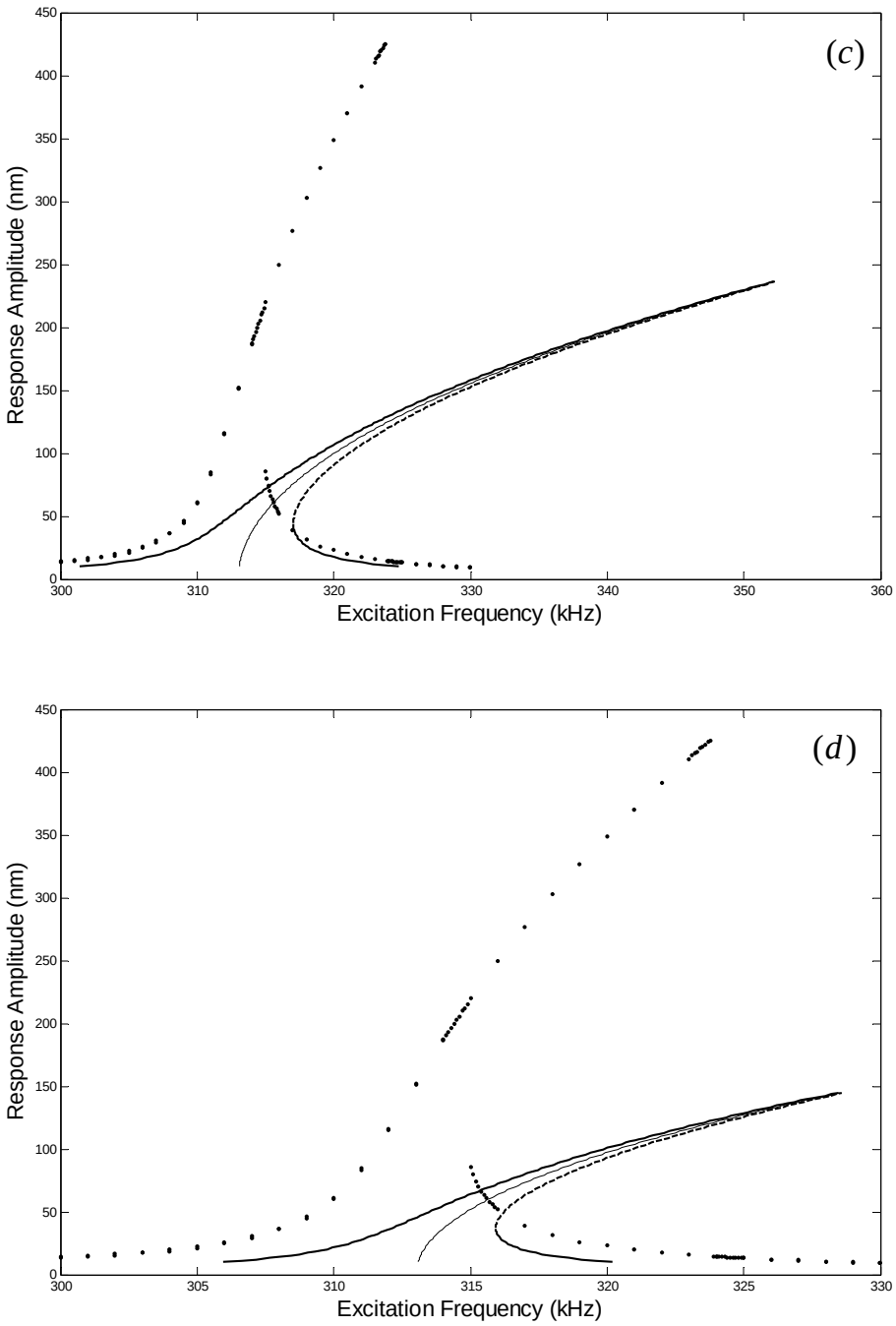

Figure 4.7: Comparison between experimental measurements and the predicted frequency responses. (a) top pt thickness is $90\,nm$, $\hat{\mu} = 8.0\times10^{-2}$, $b = 1.13\times10^{-3}$, and $\hat{\alpha}_{nn} = -4.98\times10^{11}$; (b) top pt thickness is $94\,nm$, $\hat{\mu} = 8.0\times10^{-2}$, $b = 1.13\times10^{-3}$, and $\hat{\alpha}_{nn} = -4.96\times10^{10}$. (c) top pt thickness is $140nm$, $\hat{\mu} = 8.0\times10^{-2}$, $b = 1.13\times10^{-3}$, and

$\hat{\alpha}_{nn} = -5.13\times10^{11}$; (d) top pt thickness is $160nm$, $\hat{\mu} = 8.0\times10^{-2}$, $b = 1.13\times10^{-3}$, and $\hat{\alpha}_{nn} = -5.37\times10^{11}$.

4.5. Other Comments

From Eq. (4.74), one can see that the nonlinear system has a hardening type of frequency response if $\hat{\alpha}_{nn} < 0$, and a softening type of frequency response if $\hat{\alpha}_{nn} > 0$. In Eqs. (4.76) and (4.71), $g(x)$ is a key quantity that determines the sign of $\hat{\alpha}_{nn}$ and one has to be careful in numerically determining this quantity. Due to an error in a MATLAB program that was written previously to determine $g(x)$, it was incorrectly predicted that the system exhibits a softening behavior for certain values of the electrode thickness (see the following article "Nonlinear Free and Forced Oscillations of Piezoelectric Resonators," in Journal of Micromechanics and Microengineering, Vol. 16, 2006, pp 356-367), the error in the simulation program has been since corrected. The current results indicate that the values of $\hat{\alpha}_{nn}$ are negative for all the previously considered electrode thicknesses. The frequency responses determined for different top electrode thickness values are shown in Figure 4.7. The author of this dissertation apologizes for this incorrect information provided earlier in the paper.

Chapter 5

5. Analysis of Buckling for Extensional Beams

In this chapter, a uniform beam under static axial force is studied (shown in Figure 5.1). A complete solution for the transverse displacement of this system is provided for pre-buckling, critical-buckling and post-buckling cases.

It is assume that the beam satisfies assumptions *I* - *IV* provided in Chapter 3. Then starting from the nonlinear EOM for a uniform *Euler-Bernoulli* beam given by Eqs. (3.28) and (3.29), for the static case shown in Figure 5.1, the governing equations become,

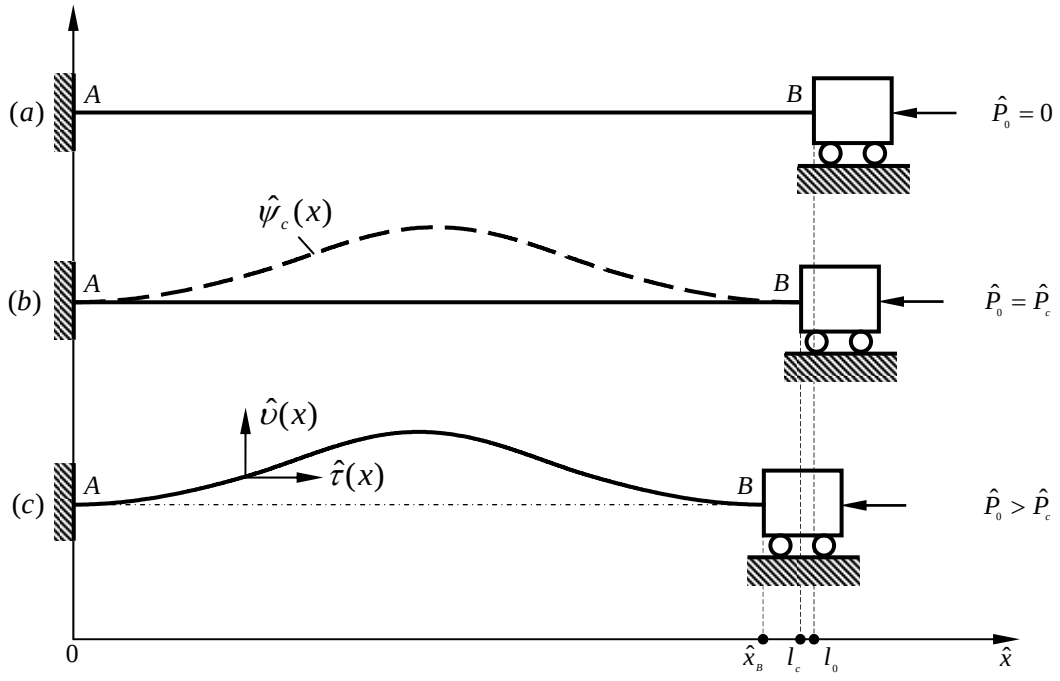

Figure 5.1: Sketches of a uniform beam subject to different axial forces: (*a*) zero axial force; (b) critical buckling force; and (*c*) post-buckling axial force.

$$\frac{d^4\upsilon}{dx^4} - \frac{e}{r^2}\frac{d^2\upsilon}{dx^2} = 0, \quad x \in \left(0, \quad x_B\right) \tag{5.1}$$

$$e = \frac{\partial \tau}{\partial x} + \frac{1}{2}\left(\frac{\partial \upsilon}{\partial x}\right)^2 = const. \tag{5.2}$$

where τ and υ are the dimensionless axial and transverse displacement for the static case (i.e., the case given by (3.17)). Next, the following notations are introduced

$$x = \frac{\hat{x}}{l_c}, \quad \upsilon = \frac{\hat{\upsilon}}{l_c}, \quad \tau = \frac{\hat{\tau}}{l_c}, \quad r^2 = \frac{EI}{EAl_c^2} \tag{5.3}$$

where l_c is the characteristic length to be defined later.

For the particular case of a clamped-clamped resonator, if we fix the left end and allow the right end to slide along the *x*-axis freely, then the associated *sliding boundary conditions* are

$$x_A \equiv 0,$$

$$\tau(x_A) = 0, \quad \tau(x_B) = x_B - \frac{l_0}{l_c} \tag{5.4}$$

$$\upsilon(x) = 0, \quad \frac{d\upsilon}{dx} = 0, \text{ at } x = x_A, \quad x = x_B$$

where l_0 is the length of the beam without the axial force.

Furthermore, (3.22) and (5.4) indicate that

$$e(x) = \left.\frac{\partial \pi}{\partial x}\right|_{x=0} = \frac{-\hat{P}_0}{EA} \tag{5.5}$$

On substituting this relation into (5.1), the governing equation for the transverse displacement becomes

$$\frac{d^4 \upsilon}{dx^4} + \zeta^2 \frac{d^2 \upsilon}{dx^2} = 0, \quad x \in \left(0, \quad x_B\right) \tag{5.6}$$

$$\zeta^2 = -\frac{e}{r^2} = P_0 = \frac{\hat{P}_0 \, l_c^2}{EI} \tag{5.7}$$

Note that the zero is always a solution of (5.6). The nonzero solution is given by

$$\upsilon(x) = a_1 + a_2 x + a_3 \cos(\zeta x) + a_4 \sin(\zeta x) \tag{5.8}$$

where the a_i are constants. Making use of the boundary conditions (5.4), the transverse displacement of the clamped-clamped uniform beam can be expressed as

$$\upsilon(x) = b\psi(x) \tag{5.9}$$

where b is the amplitude, namely the buckling factor, and $\psi(x)$ is the buckling mode shape corresponding to the axial force $\hat{P}_0$

$$\psi(x) = 1 - \cos(\zeta x)$$
$$\zeta x_B = 2n\pi, \quad n \in N^1 \tag{5.10}$$

Now, in Eqs. (5.9) and (5.10), there are 2 unknown quantities, the buckling factor b and the sliding end position x_B. Solving for these two quantities will give the full solution for the problem of interest. To this end, two additional equations regarding b and x_B need to be found.

First, the characteristic axial force $\hat{P}_c$ and the corresponding characteristic beam length l_c are defined as follows. Let

$$l_c = \left\{ l_c \in R^1 \mid l_c > 0 \right\}, \quad \hat{P}_c \in R^1 \tag{5.11}$$

and

$$\hat{P}_c = EA\left(\frac{l_0 - l_c}{l_0} \right)$$
$$\frac{\hat{P}_c l_c^2}{EI} = \zeta_c^2 = \left(2n\pi\right)^2, \quad n \in N^1 \tag{5.12}$$

Therefore, from (5.11) and (5.12), the initial length l_0 can be expressed by using the characteristic length l_c as

$$l_0 = \frac{l_c}{\left(1 - r^2 \zeta_c^2\right)} \tag{5.13}$$

From geometry, the length of the beam under axial force $\hat{P}_0$ is given by

$$l = \int_A^B d\hat{s} = \int_{\hat{x}_A}^{\hat{x}_B} \left(1+e\right) d\hat{x} = \int_{x_A}^{x_B} \left[1 + \frac{\partial \tau}{\partial x} + \frac{1}{2}\left(\frac{\partial \upsilon}{\partial x} \right)^2 \right] l_c dx = \left(2x_B - \frac{l_0}{l_c} + \frac{b^2}{4} \zeta^2 x_B \right) l_c \tag{5.14}$$

On the other hand, as the axial strain is a constant, according to Hooke's Law, the relation of axial force $\hat{P}_0$ with the length for a uniform beam can be written in dimensionless form as

$$P_0 = \zeta^2 = -\frac{1}{r^2}\left(\frac{l - l_0}{l_0}\right) \tag{5.15}$$

Next, by introducing a new parameter

$$\alpha^2 = \frac{P_0}{P_c} \tag{5.16}$$

and then making use of (5.7), (5.10), and (5.12) in (5.16), one obtains,

$$x_B = \frac{1}{\alpha} \tag{5.17}$$

On substituting Eqs. (5.13), (5.15), and (5.17) into (5.14), the buckling factor b can be expressed with respect to the buckling force α as

$$b^2 = \frac{4}{\alpha^2 \zeta_c^2}\left[\alpha\left(1+\frac{1}{1-r^2\zeta_c^2}\right)-\alpha^3 r^2 \zeta_c^2 - 2\right] \tag{5.18}$$

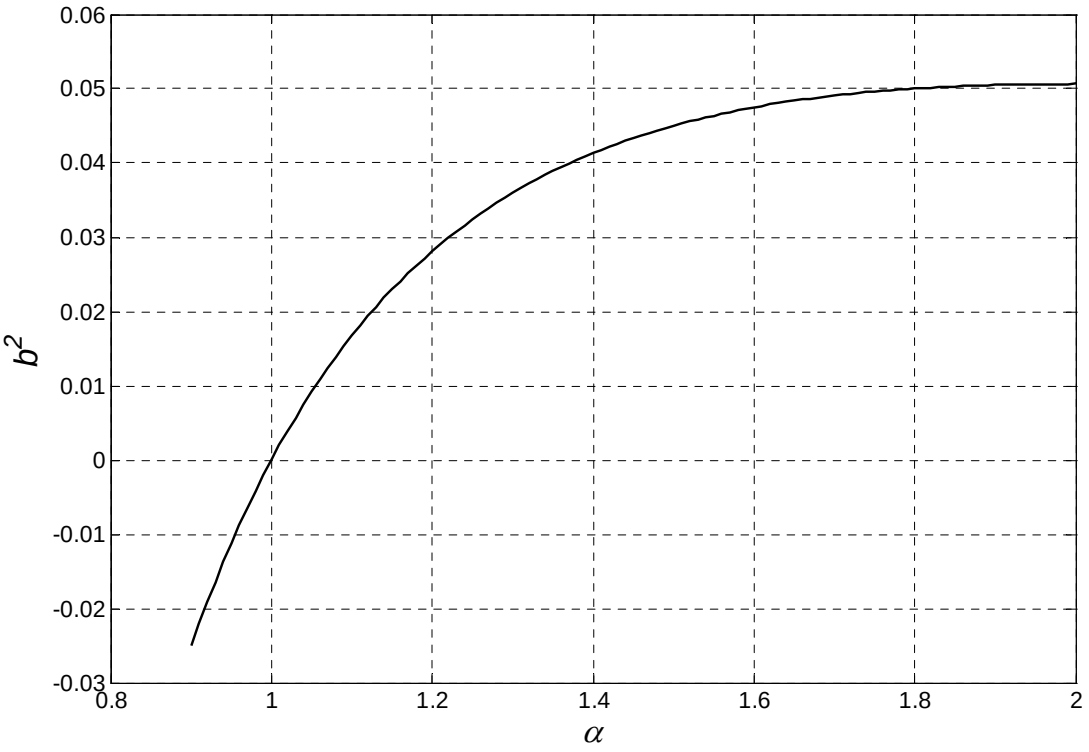

Figure 5.2: α versus b^2 for a beam with $r = 10^{-3}$.

As an example, in Figure 5.2 the variation of buckling factor b with respect to the axial force is shown. In this example, the slenderness ratio is chosen to be $r = 10^{-3}$.

Physically, if the nontrivial solution (5.10) exists, the buckling amplitude b has to be a real number. For $0 < \alpha < 1$, which means $0 < \hat{P}_0 < \hat{P}_c$ (Eq.(5.16)), $b^2 < 0$. One can conclude that in this case, (5.6) has only the zero solution, and the beam retains the flat position. In critical buckling case, $\alpha = 1$ and $b^2 = 0$, the solution exists but with a zero amplitude. For the post-buckling case, $\alpha > 1$ and $b^2 > 0$, the beam has 3 possible equilibrium positions: *i*) a zero displacement field, which is apparently possible but

not a stable equilibrium position, and *ii*) two nonzero transverse displacement fields with the same amplitude but different signs.

Chapter 6

6. Summary and Suggestions for Future Work

In this chapter, the research conducted during the course of the dissertation work is summarized, and conclusions and suggestions for future work are presented.

6.1. Dissertation Summary

In this dissertation, a study of the nonlinear behavior of PZT driven MEMS resonators fabricated as clamped-clamped structures is presented. Chapter 1 is composed of background information on the topics explored within this work, and the resonator structure along with the experimentally observed nonlinear dynamic behavior is presented in Chapter 2. In Chapters 3 and 4, a nonlinear model and the solutions of this model are developed for free and forced oscillations of a microresonator. Model predictions are also compared with experimental data at the end of Chapter 4. A complete solution for the static pre-buckling, critical-buckling, and post-buckling problems is developed for an axially elastic beam in Chapter 5.

The contributions of this research are summarized in the next three sections.

6.1.1. Nonlinear Modeling

A classic model for of Euler-Bernoulli beam assumes a constant value of the length and constant axial load in the beam. The refined model presented in Chapter 3 allows for the beam to be axially-extensional due to the axial/transverse vibrations and distribute external forces. In addition, it accounts for the axially varying properties.

Earlier work on this topic has been published by Nayfeh and Mook [50], but the model described in this dissertation is more complete and allows a clearer interpretation of the system behavior. This new nonlinear model includes parametric excitation as well as transverse excitation and distributed moment terms in the governing equations. For free vibration or forced vibration case without parametric excitation resulting in distributed tangent axial loads, the governing equation of motion of the beam can be simplified to the same form as the equation presented in the work of Nayfeh *et al* [50]. Second, the consideration of the axial strain is carried out in a comprehensive manner. The nonlinear axial strain is regarded as a function of the spatial variable $\hat{x}$ and time $\hat{t}$. It is described as to how the strain affects the system dynamics and is influenced by external force and transverse/axial displacements. It is believed that the model gives a clearer physical interpretation of the effect of axial strain on the system dynamics and it is believed to be the first comprehensive effort in this direction.

6.1.2. Model Application

Like many other MEMS devices, the microresonators studied in this dissertation are beam-like composite structures with "small" slenderness ratio values and with stepwise axially varying properties across the length. The laminate piezoelectric material causes the parametric and transverse excitations of the structure to be coupled. From Chapter 3 to Chapter 4, the presented nonlinear beam model in Chapter 3 is applied to the microresonators by taking into account all these structural properties together and seeking a solution for the nonlinear behavior under the assumption of buckling.

First, the equation of motion is treated on a section by section basis for the microresonator. The form for the axial strain $\hat{e}(\hat{x},\hat{t})$ is then simplified from a function of both the transverse displacement $\hat{W}_k(\hat{x},\hat{t})$ and axial displacement $\hat{U}_k(\hat{x},\hat{t})$ to a function of only the transverse displacement.

Next, proceeding along the lines of previous work [47], an approximate solution of the static buckling problem is developed. The buckling factor *b* is proved to be independent of the number of sections, allowing the post-buckling displacement to be expressed as the product of the whole critical buckling mode shape and a constant amplitude term.

Next, free and forced oscillation problems are solved for this composite stepwise distributed microsystem. This study is different from the previous works ([47], [48]) in that the resonator has axial excitation as well as varying beam properties causing the displacement field of one section to be coupled with other sections. Predictions

from this model are found to compare well with experimental data. This agreement provides the first evidence that buckling can be a reason for the non-flat equilibrium position of the microscale resonators. The model presented in Chapters 3 and 4 can be used as a basis to study various static and dynamic problems of beam structures with various excitations and beam properties. In addition, the unusual dynamic behavior is reported in Chapter 4 that within the same static buckling mode of the 200 μm long resonator, the same dynamic mode shape is different for different buckling factors *b*.

6.1.3. Static Buckling Problem

In Chapter 5, the limitation of the static post-buckling solution given in Chapter 4 is discussed. A modified model is then presented for the static buckling problem and a complete solution is developed for a uniform axially-extensible beam. This work addresses the pre-buckling, critical-buckling, and post-buckling problem at the same time. This effort to solve a buckling problem for extensional beams has not been previously carried out.

6.2. Suggestions for Future Work

Based on the analytical and experimental investigations conducted thus far, the following suggestions are made for future research work:

1. It is suggested that additional work be carried out to extend the work reported in Chapter 3 to give the model more generality. For example, modified models are needed for beam structures with continuously changing beam properties, as the recent experimental measurements show that residual stresses in the PZT microresonators cause not only the non-flat equilibrium

state lengthwise but also widthwise; the lengthwise varying warp of cross section makes the resonator bending stiffness a function of the spatial coordinate *x.*

2. Further studies are needed to justify the static buckling solution given in Chapter 5. Experimental data is needed from beams subject to different compressive axial forces. New issues are also brought up by the sliding boundary condition of this model, and we need to determine whether to use the *Lagrangian* description or *Eulerian* description in this problem.

3. Further research is needed to explore the reason for the 5th static buckling mode of the resonator determined in the predictions. A possible direction for this question might be to investigate the stability of a parametrically excited buckled beam with sliding boundary conditions. The analysis of the Kapitza pendulum by Kapitza [57] and a complete understanding of the question raised in the previous point might be useful for this study

4. Another suggestion for future research is the modeling of the piezoelectric layer of the resonator to predict the change in system dynamics and natural frequencies by tuning the axial strain through the application of a DC bias to the driving electrode

Appendices

MATLAB Programs and Subroutines

Free_Vib

```
clc;clear all;  close all;

ti = cputime;

%------------------------------------------------------------------------
%----                        Input  Zone                      --------
%------------------------------------------------------------------------
Beam_name  = 1;        %PZT=1,  AlGaAs=2
Wafer_name = 6;
Apply_V = 0;
BucklingFactor = 0.00113;
%-----------------------------

Static_Mode_No = 5;
Dynamic_Mode_No =1;
Image_Resol = 1000;
%-----------------------------

StaticBucklingLock = 1;
FreeVibrationLock  = 1;
ForceVibrationLock = 1;
%-----------------------------

fprintf( '************************************************************\n' );
fprintf( '** Free Vibrations of a MEMS Clamped-Clamped Resonator **\n');
fprintf( '***         Version 6.1     by  He   Li                **\n' );
fprintf( '************************************************************\n' );
fprintf( '\n\n' );

%------------------------------------------------------------------------
%----                    Data Preparation                    --------
%------------------------------------------------------------------------

%------------------     Beam Data  -----------------------------------
fprintf('*********   Resonator Geometry/Material/Stress Information
**********\n\n')
```

```
[Beam] = beam_structure ( Beam_name, Wafer_name, Apply_V );
P0_dim = Beam.AxF_dim;

EI = Beam.EI;
EA = Beam.EA;
pA = Beam.rho;
Length_dim = Beam.Length;

for i = 1 : Image_Resol+1        % every point in X-axis
   x_cord(i) = (i-1)/Image_Resol;
end

%--------------------     Non-Dimensionalize Data     ----------------------
P0 = P0_dim * Length_dim(4)^2 ./ EI;        %non-dim form of axial force
Lngth = Length_dim(1:3) / Length_dim(4);   %length of each section
Beam.AxF_nondim = P0;
Beam.Node = [0; Lngth(1); sum(Lngth(1:2)); sum(Lngth)]; % non-dim x position of
each node
Beam.NondimSection = Beam.Length(1:3)/Beam.Length(4);    %Non-dim Section
Length

fprintf('Length of the Resonator:       %g [um]\n\n',Length_dim(4)'*1e6)
fprintf('Density/UnitLength :          %e      %e      %e [kg/m]\n\n',pA')
fprintf('Bending Stiffness:            %e      %e      %e [Nm^2]\n\n',EI')
fprintf('Axial   Stiffness :           %e      %e      %e [N]\n\n',EA')
fprintf('Axial Stress:                 %e      %e      %e [N]\n\n\n\n',P0_dim')


%-------------------------------------------------------------------------
%----      Calculate the Static Critical Buckling Mode Shape       --------
%-------------------------------------------------------------------------

% To calculate the static critical buckling modeshape of a E-U beam

if StaticBucklingLock == 1
   fprintf( '         ---S T A T I C   B U C K L I N G ---\n\n')
   [P_cr W_st, static_eigVector] =Staticbuckleshape(Beam, Static_Mode_No,
Image_Resol);
   %P_cr is the critical buckling force, lamata^2
   %W_st is the normalized critial buckling mode shape
   Beam.Pcr_nondim = P_cr;
   Beam.Pcr_dim = P_cr.*EI/Length_dim(4)^2;     %dim form of P_critical [N]
   fprintf('The %gth/nd/st Static Bcukling Equlibrium Position\n\n', Static_Mode_No);
   fprintf('     Kesai = %g    %g    %g  \nPcr_nondim = %g    %g    %g      \n\n\n\n',...
         sqrt(P_cr),P_cr);
```

```
end


%-------------------------------------------------------------------------
%---- Calculate the Dynamic Mode Shape  upon PostBuckling Position --------
%-------------------------------------------------------------------------

if FreeVibrationLock == 1 & ForceVibrationLock ~= 1
   fprintf( '   ---  Dynamic Mode Shape  upon PostBuckling Position  ---\n\n');
   %###########THE DYNAMIC BUCKLED MODE SHAPE#############
   % clmnumber=12: FOR THE HOMOGENOUS EQUATION############
   % clmnumber=15: FOR THE NONHOMUGENOUS EQUATION ########
    [ W1_dy, wk, Beam] = dynamicdeflc( Beam, Dynamic_Mode_No,
BucklingFactor, Image_Resol, static_eigVector ) ;
   freq = wk*sqrt(EI(2)/pA(2))/Length_dim(4)^2/(2*pi);%wk is dimensionless
angular frequency
   ampl = 1e-003;
   Wdispl1 = BucklingFactor*W_st + ampl*W1_dy;
   Wdispl2 = BucklingFactor*W_st - ampl*W1_dy;
   fprintf('The %g Natural Frequency f = %g Hz\n\n', Dynamic_Mode_No, freq),
end

%-------------------------------------------------------------------------
%-----                Amplitude Calculation                --------
%-------------------------------------------------------------------------

if ForceVibrationLock == 1
   fprintf( '   ---  Amplitude Calculation  ---\n\n');
   %----calculation dynamic modeshape 1 ~ 10----
   w_drive = 300;
   Fi1 = 0;    Fi2 = 0;
   for mode = 1 : 3
      [ Ws_dyn(mode,:), wm(mode), Beam] = dynamicdeflc( Beam, mode,
BucklingFactor, Image_Resol, static_eigVector ) ;
      % Ws_dyn is a mxn matrix, representing modeshape from 1 -- m
   end
   W1_dy = Ws_dyn(1,:);
   wk = wm(1,1);
   for r = 1 : mode
      S(r) = Sm(W_st, Ws_dyn, wm, Beam, r);
      T(r) = Tm(W_st, Ws_dyn, wm, Beam, r);
      Fi1 = Fi1 + T(r)*Ws_dyn(r,:);
      Fi2 = Fi2 + S(r)*Ws_dyn(r,:);
   end
   g_x = gx(Beam, W_st, W1_dy, BucklingFactor, Fi1, Fi2);
```

```
   F = 40E-2;
   mu = 80E-3;
   i = 0;

   for a = 40e-6 : 3e-6 : 460e-5
      i = i + 1;
      A(i) = a;
      sgma(i,:) = Frequency_Response( Beam, W_st, W1_dy, g_x, F, a, mu, wk,
BucklingFactor );
   end
   % truncate the vector to keep values without image part
   m = 0;
   %Ampl = 0;
   %Sgma =0;
   for k = 1 : length(A)
      if imag(sgma(k,:)) == 0
         m = m+1;
         Sgma(m,:) = sgma(k,:);
         Ampl( m,:) = A(k);
      end
   end
   maxAmpl = max(abs(W1_dy))*Beam.Length(4);   %max value of W_dy in [m]
   Ampl = Ampl*maxAmpl*1E+009;                 % change Ampl in [nm]
   Sgma= Sgma/(2*pi)/1E+003;                   % change rad/s to kHz
   excit_freq = Sgma + 313;
end


%-------------------------------------------------------------------------
%-----                    Graph Ploting                    --------
%-------------------------------------------------------------------------
if StaticBucklingLock == 1 & ForceVibrationLock ~= 1
   plot(x_cord,W_st, 'linewidth',3)         %, x_cord, 0.2*(1-cos(2*pi*x_cord)));
   grid,xlabel('Spatial coordinate along the length of the reasonator x (non-
dimensional)','fontsize',16)
   ylabel('{\it{\psi}}  (non-dimensional)','fontsize',16);
   title('1st Static Critical Buckling Mode Shape','fontsize',18)
end

if FreeVibrationLock == 1 & ForceVibrationLock ~= 1
  figure(2)
   plot( x_cord,W1_dy, 'linewidth',3)
   grid,xlabel('Spatial coordinate along the length of the resonator x (non-
dimensional)','fontsize',16)
   ylabel('{\it{\phi}}  (non-dimensional)','fontsize',16)
end
```

```
if ForceVibrationLock == 1
   compare_w_exp_200(Ampl, excit_freq)
   end
tf = cputime;
el = tf - ti;
fprintf( '************************************************\n' );
fprintf( '  Elapsed CPU time (in seconds):        %g\n', el );
fprintf( '************************************************\n' );
```

function [Adyn, kesai, Lamata1, Lamata2, w2, a, Beam]=A_dynamic(wn,Beam, C, b)

```
%%%%%%%%%% THIS PROGRAM IS TO CALCULATE THE EIGENVALUE AND EIGENVECTOR OF THE DYNAMIC BUCKLING BEAM %%%%%%%

% the dynamic displacement is on the basis of a not-straight equilibrium
% position.
% the equations of B1 ~ B5 are based on those from the appendix of Journal paper

%PURPOSE : solve AX=0

% p1/p2 --------- the density of the material
% A1/A2 ---------       area of the cross section of the beam
% E1/E2 --------        the effective young's modulous of different section
% L ---------           the length of the beam, in this problem, L/4 are the electrod
% B1 --------           beita1 B1.^4=(w1.^2)*p1*A1/(E1*I1)
% B2 --------           beita2
% a ---------           the non=dimensional value at the junction point of different beam section, a=a/L
% A ---------           the 8x8 matrix that we are going to deal with
% w1/w2 -----           corresponding to the natural frequencies of different section of the beam, these are what we want in this problem

EI = Beam.EI;          %EI of each section, 3x1 vector
EA = Beam.EA;          %EA of each section, 3x1 vector
pA = Beam.rho;         %Line Densities of each section, 3x1 vector
SectionLength = Beam.NondimSection;%non-dim length of each section of the resonator, 3x1 vector
P_cr = Beam.Pcr_nondim;
SectionNo = length(SectionLength);
L = Beam.Length(4);     %over all non-dim length of the resonator, usually = 1

x(1) = 0;
for i = 1 : length(SectionLength)
```

```
   x(i+1) = x(i) + SectionLength(i);          %[0   .25   .75   1]
end

kesai = sqrt(P_cr);         %eigenvalues of the static buckling position
wk = sqrt(pA./EI)*sqrt(EI(2)/pA(2))*wn;
w2 = wk(2);
Lamata1 = sqrt(1/2*( P_cr+sqrt(P_cr.^2+4*wk.^2)));
Lamata2 = sqrt(1/2*(-P_cr+sqrt(P_cr.^2+4*wk.^2)));
N = length(C);          %divide C into a1~a4
a1 = C(1:4:N);          % C = [a1 a2 a3 a4 | a1 a2 a3 a4 | a1 a2 a3 a4 | ...]
a2 = C(2:4:N);
a3 = C(3:4:N);
a4 = C(4:4:N);
a  = [a1 a2 a3 a4];     % parameters of static displacment
delta = eye(SectionNo);

%---    construct qk & /\ik = A(ik) ----
K = EA ./ SectionLength;
EA_avg = sum(K.^-1)^-1;        % average stiffness EA of the whole 3 sections
EA_avg1= sum(K(1:1).^-1)^-1;   % average stiffness EA of the 1st section
EA_avg2= sum(K(2:3).^-1)^-1;   % average stiffness EA of the last 2 sections
%------------------
q(1) = EA_avg / EA_avg2;
q(2:3)=- EA_avg / EA_avg1;
%------------------
for k = 1 : SectionNo
   A(k) = EA_avg./(2*EA(k));
end
%############### THE PARAMETER OF B1--B5##################
D = zeros(SectionNo);
r2 = EI./(EA*L^2);
for i = 1 : SectionNo  % from the 1st section to the last section
    [bb1, bb2, bb3, bb4, bb5] = Bk( x(i+1),a(i,:), kesai(i), Lamata1(i), Lamata2(i));
   [b1, b2, b3, b4, b5] = Bk( x(i),a(i,:), kesai(i), Lamata1(i), Lamata2(i));
   B(1,i) = (bb1-b1);%Parameter(k)*(bb1 - b1);
   B(2,i) = (bb2 - b2);
   B(3,i) = (bb3 - b3);
   B(4,i) = (bb4 - b4);
   B(5,i) = (bb5 - b5);%/Parameter(k);
   for k = 1 : SectionNo
      D(k,i) = B(5,i) - delta(i,k)*r2(k)*(wk(k)^2)/(2*b^2*P_cr(k)*A(k));
   end
end

%##### THE EXPRESSION OF THE PARTICULAR SULUTION Fip######
```

```
%%%% THE EXPRESSION of MATRIX A(ij) FOR THE DYNAMIC
BUCKLING%%%%

Adyn=zeros(15,15);
%w(0)
Adyn(1,1)=sin(Lamata1(1)*x(1));
Adyn(1,2)=cos(Lamata1(1)*x(1));
Adyn(1,3)=sinh(Lamata2(1)*x(1));
Adyn(1,4)=cosh(Lamata2(1)*x(1));
Adyn(1,5)=a3(1)*cos(kesai(1)*x(1))+a4(1)*sin(kesai(1)*x(1));
%w(0)'
Adyn(2,1)= Lamata1(1)*cos(Lamata1(1)*x(1));
Adyn(2,2)=-Lamata1(1)*sin(Lamata1(1)*x(1));
Adyn(2,3)= Lamata2(1)*cosh(Lamata2(1)*x(1));
Adyn(2,4)= Lamata2(1)*sinh(Lamata2(1)*x(1));
Adyn(2,5)=-a3(1)*kesai(1)*sin(kesai(1)*x(1))+a4(1)*kesai(1)*cos(kesai(1)*x(1));
%w1 = w2
Adyn(3,1)= sin(Lamata1(1)*x(2));
Adyn(3,2)= cos(Lamata1(1)*x(2));
Adyn(3,3)= sinh(Lamata2(1)*x(2));
Adyn(3,4)= cosh(Lamata2(1)*x(2));
Adyn(3,5)=a3(1)*cos(kesai(1)*x(2))+a4(1)*sin(kesai(1)*x(2));
Adyn(3,6)=-sin(Lamata1(2)*x(2));
Adyn(3,7)=-cos(Lamata1(2)*x(2));
Adyn(3,8)=-sinh(Lamata2(2)*x(2));
Adyn(3,9)=-cosh(Lamata2(2)*x(2));
Adyn(3,10)=-a3(2)*cos(kesai(2)*x(2))-a4(2)*sin(kesai(2)*x(2));
%w1' = w2'
Adyn(4,1)= Lamata1(1)*cos(Lamata1(1)*x(2));
Adyn(4,2)=-Lamata1(1)*sin(Lamata1(1)*x(2));
Adyn(4,3)= Lamata2(1)*cosh(Lamata2(1)*x(2));
Adyn(4,4)= Lamata2(1)*sinh(Lamata2(1)*x(2));
Adyn(4,5)=-a3(1)*kesai(1)*sin(kesai(1)*x(2))+a4(1)*kesai(1)*cos(kesai(1)*x(2));
Adyn(4,6)=-Lamata1(2)*cos(Lamata1(2)*x(2));
Adyn(4,7)= Lamata1(2)*sin(Lamata1(2)*x(2));
Adyn(4,8)=-Lamata2(2)*cosh(Lamata2(2)*x(2));
Adyn(4,9)=-Lamata2(2)*sinh(Lamata2(2)*x(2));
Adyn(4,10)=a3(2)*kesai(2)*sin(kesai(2)*x(2))-a4(2)*kesai(2)*cos(kesai(2)*x(2));
%EI1 w1" = EI2 w2"
Adyn(5,1)=-(Lamata1(1).^2)*sin(Lamata1(1)*x(2))*EI(1);
Adyn(5,2)=-(Lamata1(1).^2)*cos(Lamata1(1)*x(2))*EI(1);
Adyn(5,3)= (Lamata2(1).^2)*sinh(Lamata2(1)*x(2))*EI(1);
Adyn(5,4)= (Lamata2(1).^2)*cosh(Lamata2(1)*x(2))*EI(1);
Adyn(5,5)=(-a3(1)*kesai(1).^2*cos(kesai(1)*x(2))-
a4(1)*kesai(1).^2*sin(kesai(1)*x(2)))*EI(1);
Adyn(5,6)= (Lamata1(2).^2)*sin(Lamata1(2)*x(2))*EI(2);
```

```
Adyn(5,7)= (Lamata1(2).^2)*cos(Lamata1(2)*x(2))*EI(2);
Adyn(5,8)=-(Lamata2(2).^2)*sinh(Lamata2(2)*x(2))*EI(2);
Adyn(5,9)=-(Lamata2(2).^2)*cosh(Lamata2(2)*x(2))*EI(2);
Adyn(5,10)=(a3(2)*kesai(2).^2*cos(kesai(2)*x(2))+a4(2)*kesai(2).^2*sin(kesai(2)*x
(2)))*EI(2);
%EI1 w1''' = EI2 w2'''
Adyn(6,1)=-(Lamata1(1).^3)*cos(Lamata1(1)*x(2))*EI(1);
Adyn(6,2)= (Lamata1(1).^3)*sin(Lamata1(1)*x(2))*EI(1);
Adyn(6,3)= (Lamata2(1).^3)*cosh(Lamata2(1)*x(2))*EI(1);
Adyn(6,4)= (Lamata2(1).^3)*sinh(Lamata2(1)*x(2))*EI(1);
Adyn(6,5)= (a3(1)*kesai(1).^3*sin(kesai(1)*x(2))-
a4(1)*kesai(1).^3*cos(kesai(1)*x(2)))*EI(1);
Adyn(6,6)= (Lamata1(2).^3)*cos(Lamata1(2)*x(2))*EI(2);
Adyn(6,7)=-(Lamata1(2).^3)*sin(Lamata1(2)*x(2))*EI(2);
Adyn(6,8)=-(Lamata2(2).^3)*cosh(Lamata2(2)*x(2))*EI(2);
Adyn(6,9)=-(Lamata2(2).^3)*sinh(Lamata2(2)*x(2))*EI(2);
Adyn(6,10)=(-
a3(2)*kesai(2).^3*sin(kesai(2)*x(2))+a4(2)*kesai(2).^3*cos(kesai(2)*x(2)))*EI(2);
%w2 = w3
Adyn(7,6)= sin(Lamata1(2)*x(3));
Adyn(7,7)= cos(Lamata1(2)*x(3));
Adyn(7,8)= sinh(Lamata2(2)*x(3));
Adyn(7,9)= cosh(Lamata2(2)*x(3));
Adyn(7,10)= a3(2)*cos(kesai(2)*x(3))+a4(2)*sin(kesai(2)*x(3));
Adyn(7,11)=-sin(Lamata1(3)*x(3));
Adyn(7,12)=-cos(Lamata1(3)*x(3));
Adyn(7,13)=-sinh(Lamata2(3)*x(3));
Adyn(7,14)=-cosh(Lamata2(3)*x(3));
Adyn(7,15)= -a3(3)*cos(kesai(3)*x(3))-a4(3)*sin(kesai(3)*x(3));
%w2' = w3'
Adyn(8,6)= Lamata1(2)*cos(Lamata1(2)*x(3));
Adyn(8,7)=-Lamata1(2)*sin(Lamata1(2)*x(3));
Adyn(8,8)= Lamata2(2)*cosh(Lamata2(2)*x(3));
Adyn(8,9)= Lamata2(2)*sinh(Lamata2(2)*x(3));
Adyn(8,10)=-a3(2)*kesai(2)*sin(kesai(2)*x(3))+a4(2)*kesai(2)*cos(kesai(2)*x(3));
Adyn(8,11)=-Lamata1(3)*cos(Lamata1(3)*x(3));
Adyn(8,12)= Lamata1(3)*sin(Lamata1(3)*x(3));
Adyn(8,13)=-Lamata2(3)*cosh(Lamata2(3)*x(3));
Adyn(8,14)=-Lamata2(3)*sinh(Lamata2(3)*x(3));
Adyn(8,15)= a3(3)*kesai(3)*sin(kesai(3)*x(3))-a4(3)*kesai(3)*cos(kesai(3)*x(3));
%EI2 w2'' = EI3 w3''
Adyn(9,6)=-(Lamata1(2).^2)*sin(Lamata1(2)*x(3))*EI(2);
Adyn(9,7)=-(Lamata1(2).^2)*cos(Lamata1(2)*x(3))*EI(2);
Adyn(9,8)= (Lamata2(2).^2)*sinh(Lamata2(2)*x(3))*EI(2);
Adyn(9,9)= (Lamata2(2).^2)*cosh(Lamata2(2)*x(3))*EI(2);
```

```
Adyn(9,10)=(-a3(2)*kesai(2).^2*cos(kesai(2)*x(3))-
a4(2)*kesai(2).^2*sin(kesai(2)*x(3)))*EI(2);
Adyn(9,11)= (Lamata1(3).^2)*sin(Lamata1(3)*x(3))*EI(3);
Adyn(9,12)= (Lamata1(3).^2)*cos(Lamata1(3)*x(3))*EI(3);
Adyn(9,13)=-(Lamata2(3).^2)*sinh(Lamata2(3)*x(3))*EI(3);
Adyn(9,14)=-(Lamata2(3).^2)*cosh(Lamata2(3)*x(3))*EI(3);
Adyn(9,15)=( a3(3)*kesai(3).^2*cos(kesai(3)*x(3))+a4(3)*kesai(3).^2*sin(kesai(3)*
x(3)))*EI(3);
%EI2 w2''' = EI1 w1'''
Adyn(10,6)= -(Lamata1(2).^3)*cos(  Lamata1(2)*x(3))*EI(2);
Adyn(10,7)=  (Lamata1(2).^3)*sin(  Lamata1(2)*x(3))*EI(2);
Adyn(10,8)=  (Lamata2(2).^3)*cosh( Lamata2(2)*x(3))*EI(2);
Adyn(10,9)=  (Lamata2(2).^3)*sinh( Lamata2(2)*x(3))*EI(2);
Adyn(10,10)=  (a3(2)*kesai(2).^3*sin(kesai(2)*x(3))-
a4(2)*kesai(2).^3*cos(kesai(2)*x(3)))*EI(2);
Adyn(10,11)=  (Lamata1(3).^3)*cos( Lamata1(3)*x(3))*EI(3);
Adyn(10,12)=-(Lamata1(3).^3)*sin( Lamata1(3)*x(3))*EI(3);
Adyn(10,13)=-(Lamata2(3).^3)*cosh(Lamata2(3)*x(3))*EI(3);
Adyn(10,14)=-(Lamata2(3).^3)*sinh(Lamata2(3)*x(3))*EI(3);
Adyn(10,15)=(-
a3(3)*kesai(3).^3*sin(kesai(3)*x(3))+a4(3)*kesai(3).^3*cos(kesai(3)*x(3)))*EI(3);
%w3(1) = 0
Adyn(11,11)= sin(Lamata1(3)*x(4));
Adyn(11,12)=cos(Lamata1(3)*x(4));
Adyn(11,13)=sinh(Lamata2(3)*x(4));
Adyn(11,14)=cosh(Lamata2(3)*x(4));
Adyn(11,15)=a3(3)*cos(kesai(3)*x(4))+a4(3)*sin(kesai(3)*x(4));
%w3(1)' = 0
Adyn(12,11)= Lamata1(3)*cos(Lamata1(3)*x(4));
Adyn(12,12)=-Lamata1(3)*sin(Lamata1(3)*x(4));
Adyn(12,13)=Lamata2(3)*cosh(Lamata2(3)*x(4));
Adyn(12,14)=Lamata2(3)*sinh(Lamata2(3)*x(4));
Adyn(12,15)=-a3(3)*kesai(3)*sin(kesai(3)*x(4))+a4(3)*kesai(3)*cos(kesai(3)*x(4));

Adyn(13:15,1) = B(1,1);
Adyn(13:15,2) = B(2,1);
Adyn(13:15,3) = B(3,1);
Adyn(13:15,4) = B(4,1);
Adyn(13:15,5) = D(1:3,1);
Adyn(13:15,6) = B(1,2);
Adyn(13:15,7) = B(2,2);
Adyn(13:15,8) = B(3,2);
Adyn(13:15,9) = B(4,2);
Adyn(13:15,10)= D(1:3,2);
Adyn(13:15,11)= B(1,3);
Adyn(13:15,12)= B(2,3);
```

```
Adyn(13:15,13)= B(3,3);
Adyn(13:15,14)= B(4,3);
Adyn(13:15,15)= D(1:3,3);


%-----  Normalize each row to avoid ill-conditioned matrix  ----------
for i = 1 : size(Adyn,1)
   Ampl = norm(Adyn(i,:));
   Adyn(i,:) = Adyn(i,:)/Ampl;
end

%%%%%% EXPRESSION Adyn ENDED%%%%%
y=det(Adyn);
Beam.EA_avg = EA_avg;
Beam.EA_avg1= EA_avg1;
Beam.EA_avg2= EA_avg2;
Beam.Bk = B;
Beam.Dk = D;
Beam.Aik = A;
Beam.q = q;
```

function [determinantA, A] = A_static(lamata2, EI, x, Length)

```
%%%%%%%%%%%% THIS PROGRAM IS TO CALCULATE THE
EIGENVALUE AND EIGENVECTOR OF THE STATIC BUCKLING BEAM
%%%%%%%
%PURPOSE : solve AX=0
% p1/p2 --------- the density of the material
% A1/A2 ---------      area of the cross section of the beam
% E1/E2 --------       the effective young's modulous of different section
% L ---------          the length of the beam, in this problem, L/4 are the electrod
% B1 --------          beita1 B1.^4=(w1.^2)*p1*A1/(E1*I1)
% B2 --------          beita2
% a ---------          the non=dimensional value at the junction point of different
beam section, a=a/L
% A ---------          the 8x8 matrix that we are going to deal with
% w1/w2 -----          corresponding to the natural frequencies of different section of
the beam, these are what we want in this problem
%%%% GIVE THE BASIC PARAMETER OF THE BEAM%%%%
%-------------------------------------------------------------------------
EI1=EI(1);  EI2=EI(2);  EI3=EI(3);
%-------------------------------------------------------------------------
lamata1=lamata2 * sqrt(EI2/EI1);
lamata3=lamata2 * sqrt(EI2/EI3);
%-----------------   THE EXPRESSION of MATRIX A(ij)   --------------------
A=zeros(12,12);
% boundary conditions at x=0, x=L
```

```
A(1,1)=1;
%W(0)=0
A(1,2)=x(1);
A(1,3)=cos(lamata1*x(1));
A(1,4)=sin(lamata1*x(1));
A(2,1)=0;
%W'(0)=0
A(2,2)=1;
A(2,3)=-lamata1*sin(lamata1*x(1));
A(2,4)=lamata1*cos(lamata1*x(1));
A(3,1)=1;
%W1(a)=W2(a)
A(3,2)=x(2);
A(3,3)=cos(lamata1*x(2));
A(3,4)=sin(lamata1*x(2));
A(3,5)=-1;
A(3,6)=-x(2);
A(3,7)=-cos(lamata2*x(2));
A(3,8)=-sin(lamata2*x(2));
A(4,1)=0;
%W1'(a)=W2'(a)
A(4,2)=1;
A(4,3)=-lamata1*sin(lamata1*x(2));
A(4,4)= lamata1*cos(lamata1*x(2));
A(4,5)=-0;
A(4,6)=-1;
A(4,7)= lamata2*sin(lamata2*x(2));
A(4,8)=-lamata2*cos(lamata2*x(2));
A(5,1)=0;                          %EI1*W1" = EI2*W2"
A(5,2)=0;
A(5,3)=-(lamata1.^2)*cos(lamata1*x(2));
A(5,4)=-(lamata1.^2)*sin(lamata1*x(2));
A(5,5)=0;
A(5,6)=0;
A(5,7)= (lamata2.^2)*cos(lamata2*x(2))*EI2/EI1;
A(5,8)= (lamata2.^2)*sin(lamata2*x(2))*EI2/EI1;
A(6,1)=0;                          %EI1*W1'" = EI2*W2'"
A(6,2)=0;
A(6,3)=(lamata1.^3)*sin(lamata1*x(2));
A(6,4)=-(lamata1.^3)*cos(lamata1*x(2));
A(6,5)=0;
A(6,6)=0;
A(6,7)=-(lamata2.^3)*sin(lamata2*x(2))*EI2/EI1;
A(6,8)=(lamata2.^3)*cos(lamata2*x(2))*EI2/EI1;
A(7,5)=1;
A(7,6)=x(3);
```

```
A(7,7)=cos(lamata2*x(3));
A(7,8)=sin(lamata2*x(3));
A(7,9)=-1;
A(7,10)=-x(3);
A(7,11)=-cos(lamata3*x(3));
A(7,12)=-sin(lamata3*x(3));
A(8,5)=0;
A(8,6)=1;
A(8,7)=-lamata2*sin(lamata2*x(3));
A(8,8)=lamata2*cos(lamata2*x(3));
A(8,9)=0;
A(8,10)=-1;
A(8,11)=lamata3*sin(lamata3*x(3));
A(8,12)=-lamata3*cos(lamata3*x(3));
A(9,5)=0;
A(9,6)=0;
A(9,7)=-(lamata2.^2)*cos(lamata2*x(3))*EI2/EI3;
A(9,8)=-(lamata2.^2)*sin(lamata2*x(3))*EI2/EI3;
A(9,9)=0;
A(9,10)=0;
A(9,11)=(lamata3.^2)*cos(lamata3*x(3));
A(9,12)=(lamata3.^2)*sin(lamata3*x(3));
A(10,5)=0;
A(10,6)=0;
A(10,7)=(lamata2.^3)*sin(lamata2*x(3))*EI2/EI3;
A(10,8)=-(lamata2.^3)*cos(lamata2*x(3))*EI2/EI3;
A(10,9)=0;
A(10,10)=0;
A(10,11)=-(lamata3.^3)*sin(lamata3*x(3));
A(10,12)=(lamata3.^3)*cos(lamata3*x(3));
A(11,9)=0;                          %W3'(x4) = 0
A(11,10)=1;
A(11,11)=-lamata3*sin(lamata3*x(4));
A(11,12)=lamata3*cos(lamata3*x(4));
A(12,9)=1;                          %W3(x4)=0
A(12,10)=x(4);
A(12,11)=cos(lamata3*x(4));
A(12,12)=sin(lamata3*x(4));
determinantA = det(A);
```

function [Adyn, Lamata1, Lamata2] = Adyn_flat(wn,Beam)

```
%THIS PROGRAM IS TO CALCULATE THE EIGENVALUE AND
EIGENVECTOR OF THE
%STATICIALLY STRAIT BEAM WITH STRETCHING/COMPRESSING AXIAL
FORCE, IN CASE
```

```
%THE AXIAL FORCE IS COMPRESSING, THE FORCE SHOULD NOT
EXCEED THE BEAM'S
%CRITICAL BUCKLING FORCE
%PURPOSE : solve AX=0
% p1/p2 --------- the density of the material
% A1/A2 ---------       area of the cross section of the beam
% E1/E2 --------        the effective young's modulous of different section
% L ---------           the length of the beam, in this problem, L/4 are the electrod
% B1 --------           beita1 B1.^4=(w1.^2)*p1*A1/(E1*I1)
% B2 --------           beita2
% a ---------           the non=dimensional value at the junction point of different
beam section, a=a/L
% A ---------           the 8x8 matrix that we are going to deal with
% w1/w2 -----           corresponding to the natural frequencies of different section of
the beam, these are what we want in this problem
EI = Beam.EI;          %EI of each section, 3x1 vector
EA = Beam.EA;          %EA of each section, 3x1 vector
pA = Beam.rho;         %Line Densities of each section, 3x1 vector
Lngth = Beam.NondimSection;%non-dim length of each section of the resonator, 3x1
vector
P = Beam.AxF_nondim;    %the axial force of the beam,not be used in this program,
3x1 vector
L = sum(Lngth);            %over all non-dim length of the resonator, usually = 1
x = Beam.Node;   %[0   .25   .75   1]
%kesai = sqrt(P);         %eigenvalues of the static buckling position
wk = sqrt(pA./EI)*sqrt(EI(2)/pA(2))*wn; %non-dim natural freq of each section
Lamata1 = sqrt(1/2*(-P+sqrt(P.^2+4*wk.^2)));
Lamata2 = sqrt(1/2*( P+sqrt(P.^2+4*wk.^2)));
%%%% THE EXPRESSION of MATRIX A(ij) FOR THE DYNAMIC
BUCKLING%%%%
Adyn=zeros(12,12);
Adyn(1,1)=sin(Lamata1(1)*x(1));
Adyn(1,2)=cos(Lamata1(1)*x(1));
Adyn(1,3)=sinh(Lamata2(1)*x(1));
Adyn(1,4)=cosh(Lamata2(1)*x(1));
Adyn(2,1)= Lamata1(1)*cos(Lamata1(1)*x(1));
Adyn(2,2)=-Lamata1(1)*sin(Lamata1(1)*x(1));
Adyn(2,3)= Lamata2(1)*cosh(Lamata2(1)*x(1));
Adyn(2,4)= Lamata2(1)*sinh(Lamata2(1)*x(1));
Adyn(3,1)= sin(Lamata1(1)*x(2));
Adyn(3,2)= cos(Lamata1(1)*x(2));
Adyn(3,3)= sinh(Lamata2(1)*x(2));
Adyn(3,4)= cosh(Lamata2(1)*x(2));
Adyn(3,5)=-sin(Lamata1(2)*x(2));
Adyn(3,6)=-cos(Lamata1(2)*x(2));
Adyn(3,7)=-sinh(Lamata2(2)*x(2));
```

```
Adyn(3,8)=-cosh(Lamata2(2)*x(2));
Adyn(4,1)= Lamata1(1)*cos(Lamata1(1)*x(2));
Adyn(4,2)=-Lamata1(1)*sin(Lamata1(1)*x(2));
Adyn(4,3)= Lamata2(1)*cosh(Lamata2(1)*x(2));
Adyn(4,4)= Lamata2(1)*sinh(Lamata2(1)*x(2));
Adyn(4,5)=-Lamata1(2)*cos(Lamata1(2)*x(2));
Adyn(4,6)= Lamata1(2)*sin(Lamata1(2)*x(2));
Adyn(4,7)=-Lamata2(2)*cosh(Lamata2(2)*x(2));
Adyn(4,8)=-Lamata2(2)*sinh(Lamata2(2)*x(2));
Adyn(5,1)=-(Lamata1(1).^2)*sin(Lamata1(1)*x(2))*EI(1)/EI(2);
Adyn(5,2)=-(Lamata1(1).^2)*cos(Lamata1(1)*x(2))*EI(1)/EI(2);
Adyn(5,3)= (Lamata2(1).^2)*sinh(Lamata2(1)*x(2))*EI(1)/EI(2);
Adyn(5,4)= (Lamata2(1).^2)*cosh(Lamata2(1)*x(2))*EI(1)/EI(2);
Adyn(5,5)= (Lamata1(2).^2)*sin(Lamata1(2)*x(2));
Adyn(5,6)= (Lamata1(2).^2)*cos(Lamata1(2)*x(2));
Adyn(5,7)=-(Lamata2(2).^2)*sinh(Lamata2(2)*x(2));
Adyn(5,8)=-(Lamata2(2).^2)*cosh(Lamata2(2)*x(2));
Adyn(6,1)=-(Lamata1(1).^3)*cos(Lamata1(1)*x(2))*EI(1)/EI(2);
Adyn(6,2)= (Lamata1(1).^3)*sin(Lamata1(1)*x(2))*EI(1)/EI(2);
Adyn(6,3)= (Lamata2(1).^3)*cosh(Lamata2(1)*x(2))*EI(1)/EI(2);
Adyn(6,4)= (Lamata2(1).^3)*sinh(Lamata2(1)*x(2))*EI(1)/EI(2);
Adyn(6,5)= (Lamata1(2).^3)*cos(Lamata1(2)*x(2));
Adyn(6,6)=-(Lamata1(2).^3)*sin(Lamata1(2)*x(2));
Adyn(6,7)=-(Lamata2(2).^3)*cosh(Lamata2(2)*x(2));
Adyn(6,8)=-(Lamata2(2).^3)*sinh(Lamata2(2)*x(2));
Adyn(7,5)= sin(Lamata1(2)*x(3));
Adyn(7,6)= cos(Lamata1(2)*x(3));
Adyn(7,7)= sinh(Lamata2(2)*x(3));
Adyn(7,8)= cosh(Lamata2(2)*x(3));
Adyn(7,9)=-sin(Lamata1(3)*x(3));
Adyn(7,10)=-cos(Lamata1(3)*x(3));
Adyn(7,11)=-sinh(Lamata2(3)*x(3));
Adyn(7,12)=-cosh(Lamata2(3)*x(3));
Adyn(8,5)= Lamata1(2)*cos(Lamata1(2)*x(3));
Adyn(8,6)=-Lamata1(2)*sin(Lamata1(2)*x(3));
Adyn(8,7)= Lamata2(2)*cosh(Lamata2(2)*x(3));
Adyn(8,8)= Lamata2(2)*sinh(Lamata2(2)*x(3));
Adyn(8,9)=-Lamata1(3)*cos(Lamata1(3)*x(3));
Adyn(8,10)= Lamata1(3)*sin(Lamata1(3)*x(3));
Adyn(8,11)=-Lamata2(3)*cosh(Lamata2(3)*x(3));
Adyn(8,12)=-Lamata2(3)*sinh(Lamata2(3)*x(3));
Adyn(9,5)=-(Lamata1(2).^2)*sin(Lamata1(2)*x(3))*EI(2)/EI(3);
Adyn(9,6)=-(Lamata1(2).^2)*cos(Lamata1(2)*x(3))*EI(2)/EI(3);
Adyn(9,7)= (Lamata2(2).^2)*sinh(Lamata2(2)*x(3))*EI(2)/EI(3);
Adyn(9,8)= (Lamata2(2).^2)*cosh(Lamata2(2)*x(3))*EI(2)/EI(3);
Adyn(9,9)= (Lamata1(3).^2)*sin(Lamata1(3)*x(3));
```

```
Adyn(9,10)= (Lamata1(3).^2)*cos(Lamata1(3)*x(3));
Adyn(9,11)=-(Lamata2(3).^2)*sinh(Lamata2(3)*x(3));
Adyn(9,12)=-(Lamata2(3).^2)*cosh(Lamata2(3)*x(3));
Adyn(10,5)= -(Lamata1(2).^3)*cos(  Lamata1(2)*x(3))*EI(2)/EI(3);
Adyn(10,6)=  (Lamata1(2).^3)*sin(  Lamata1(2)*x(3))*EI(2)/EI(3);
Adyn(10,7)=  (Lamata2(2).^3)*cosh( Lamata2(2)*x(3))*EI(2)/EI(3);
Adyn(10,8)=  (Lamata2(2).^3)*sinh( Lamata2(2)*x(3))*EI(2)/EI(3);
Adyn(10,9)=  (Lamata1(3).^3)*cos( Lamata1(3)*x(3));
Adyn(10,10)=-(Lamata1(3).^3)*sin( Lamata1(3)*x(3));
Adyn(10,11)=-(Lamata2(3).^3)*cosh(Lamata2(3)*x(3));
Adyn(10,12)=-(Lamata2(3).^3)*sinh(Lamata2(3)*x(3));
Adyn(11,9)= sin(Lamata1(3)*x(4));
Adyn(11,10)=cos(Lamata1(3)*x(4));
Adyn(11,11)=sinh(Lamata2(3)*x(4));
Adyn(11,12)=cosh(Lamata2(3)*x(4));
Adyn(12,9)= Lamata1(3)*cos(Lamata1(3)*x(4));
Adyn(12,10)=-Lamata1(3)*sin(Lamata1(3)*x(4));
Adyn(12,11)=Lamata2(3)*cosh(Lamata2(3)*x(4));
Adyn(12,12)=Lamata2(3)*sinh(Lamata2(3)*x(4));
%------    De- ill condition of the matrix  by normalize each row   -------
for i = 1 : size(Adyn,1)
   Ampl = norm(Adyn(i,:));
   %Adyn(i,:) = Adyn(i,:)/Ampl;
end
%%%%%% EXPRESSION Adyn ENDED%%%
```

function [Beam] = AlGaAs_beam (wafer_No, Apply_V)

```
%************ Material Properties ******************
E(1,:)=85e9;   d(1,:)=4.88e3;      thickness(1,:) = [2e-6];              thickness1(1,:) =
thickness(1,:); % AlGaAs : Si
E(2,:)=85e9;   d(2,:)=4.88e3;            thickness(2,:) = [1e-6];
         thickness1(2,:) = thickness(2,:);        % AlGaAs
E(3,:)=85e9;   d(3,:)=4.88e3;            thickness(3,:) = [0.5e-6];
         thickness1(3,:) = thickness(3,:)*0;     %AlGaAs : Si
nu = 0.3;
%********** Stress and Applied Voltages ***********
%     layer 1     layer 2           layer 3
stress = [ -80,            -80,              -80 ]' * 1e6;    % stress of each layer
d31    = [0, 1.13e-12, 0 ]';        % d31 is the piezoelectric coefficient of AlGaAs
Beam_angle = 39; % angle in Degree!!
%********** Structure Dimensions ******************
L = 200e-6;                      % the length of the beam, dimension is meter [m]
width = 15e-6;           % the width of the beam, [m]
Electr_posit = 0.25;
L1 = L * Electr_posit;                                  % Length of the 1st section
L2 = L * (1 - 2*Electr_posit);           % Length of the 2nd section
```

```
L3 = L * Electr_posit;                          % Length of the 3rd section
%************************************************
%Stress information
if wafer_No  <=  length( thickness(1,:) );      % if the wafer we choose is a valid
wafer
  resid_stress=stress( :,wafer_No )*(1-nu);%* cos((90-Beam_angle)/180*pi)^2;
        % Pa
  thick = [ thickness(:,wafer_No)      thickness1(:,wafer_No)
        thickness(:,wafer_No)];
  Length = [L1; L2; L3; L];
  Width = width;
  density = d;
else disp ('Wafer Number Exceeds the Number of Fabricated')
end
Beam.ResidualStress = resid_stress;
Beam.d31    = d31;
Beam.E = E;
Beam.Thickness = thick;
Beam.Width = Width;
Beam.LayerRho = density;
Beam.Length = Length;
Beam.nu = [nu; nu; nu];
```

function F = Average_F (residual_F, EA, Length)

```
% this function is to get the averaged axial force using a linear method
% without changing the dimensions
%residual_F     Axial force before the averaging,, Columnn Vector
%EA            Stiffness of each section in the beam, Columnn Vector
%Length        The length of each section, Columnn Vector;
K1 = EA(1)/Length(1);
K2 = EA(2)/Length(2);
K3 = EA(3)/Length(3);
K  = [  -1     K1                    0
           -1      -K2      K2
       -1      0       -K3  ];
U  = - K^-1 * residual_F;       %U = { P_average, U1, U2}' = { [N], [m], [m] }'
F = U(1);
```

function [Beam] = beam_structure(Beam_Name, wafer_No, Apply_V)

```
function [Beam] = beam_structure( Beam_Name, wafer_No, Apply_V )

%%%% GIVE THE BASIC PARAMETER OF THE BEAM%%%
% p1/p2 --------- the density of the material
% A1/A2 ---------       area of the cross section of the beam
% E1/E2 --------        the effective young's modulous of different section
% L ---------           the length of the beam, in this problem, L/4 are the electrod
```

```
% B1 --------            beita1 B1.^4=(w1.^2)*p1*A1/(E1*I1)
% B2 --------            beita2
% a ---------            the non=dimensional value at the junction point of different
beam section, a=a/L
% A ---------            the 8x8 matrix that we are going to deal with
% w1/w2 -----            corresponding to the natural frequencies of different section of
the beam, these are what we want in this problem
% Lamata                                the lamata in dynamic mode

%********** Material Properties *****************
[ Beam ] =  Choose_beam( Beam_Name, wafer_No , Apply_V);
%-------------------------------------------------------------------------
ResidStress=Beam.ResidualStress;
d31=Beam.d31;
E=Beam.E ;
Thickness=Beam.Thickness;
Width=Beam.Width;
density=Beam.LayerRho;
Length=Beam.Length;
%-------------------------------------------------------------------------
%%%%% CALCULATE THE 'EIs' AND 'pAs' OF EACH SECTION OF THE
BEAM%%%%%%%%%
[EI1,pA1]=getEI(E, density, Thickness(: , 1), Width);
[EI2,pA2]=getEI(E, density, Thickness(: , 2), Width);
[EI3,pA3]=getEI(E, density, Thickness(: , 3), Width);
EI = [ EI1; EI2; EI3 ];
pA = [ pA1; pA2; pA3 ];
EA1 = get_EA( E, Thickness(: , 1), Width);
EA2 = get_EA( E, Thickness(: , 2), Width);
EA3 = get_EA( E, Thickness(: , 3), Width);
EA = [ EA1; EA2; EA3];
n = size(Length,1);
rk = sqrt(EI./EA/Length(n)^2);
P1 = ResidStress' * Thickness(:,1) * Width;
P2 = ResidStress' * Thickness(:,2) * Width;
P3 = ResidStress' * Thickness(:,3) * Width;
P00 = (P1+P2+P3)/3;
P0 = [ P00; P00; P00 ];
%-------------------------------------------------------------------------
Beam.AxF_dim    = P0;
Beam.EI = EI;
Beam.EA = EA;
Beam.rho = pA;
Beam.r = rk;
%-------------------------------------------------------------------------
```

function [B1k, B2k, B3k, B4k, B5k] = Bk(x, a, kesai, Lamata1, Lamata2)

```
a1 = a(:,1);
a2 = a(:,2);
a3 = a(:,3);
a4 = a(:,4);
B1k =a2*sin(Lamata1*x)+a3*kesai*Lamata1*(cos((kesai-Lamata1)*x)/2/(kesai-
Lamata1)
+cos((kesai+Lamata1)*x)/2/(kesai+Lamata1))+a4*kesai*Lamata1*(sin((kesai-
Lamata1)*x)/2/(kesai-Lamata1) + sin((kesai+Lamata1)*x)/2/(kesai+Lamata1));
B2k =a2*cos(Lamata1*x)+a3*kesai*Lamata1*(sin((kesai-Lamata1)*x)/2/(kesai-
Lamata1) -sin((kesai+Lamata1)*x)/2/(kesai+Lamata1))+a4*kesai*Lamata1*(-
cos((kesai-Lamata1)*x)/2/(kesai-Lamata1) +
cos((kesai+Lamata1)*x)/2/(kesai+Lamata1));
B3k=a2*sinh(Lamata2*x)a3*kesai*Lamata2/(Lamata2^2+kesai^2)*(Lamata2*sin(ke
sai*x)*sinh(Lamata2*x)-kesai*cos(kesai*x)*cosh(Lamata2*x))+a4*kesai*Lamata2
/(Lamata2^2+kesai^2)*(Lamata2*cos(kesai*x)*sinh(Lamata2*x)+kesai*sin(kesai*x)
*cosh(Lamata2*x));
B4k=a2*cosh(Lamata2*x)-a3*kesai*Lamata2/(Lamata2^2+kesai^2)
*(Lamata2*sin(kesai*x)*cosh(Lamata2*x)-kesai*cos(kesai*x)*sinh(Lamata2*x))
+a4*kesai*Lamata2/(Lamata2^2+
kesai^2)*(Lamata2*cos(kesai*x)*cosh(Lamata2*x)+
kesai*sin(kesai*x)*sinh(Lamata2*x));
B5k = (a3^2+a4^2)/2*kesai^2*x + a2*a3*cos(kesai*x)+a2*a4*sin(kesai*x) - (a3^2-
a4^2)/4*kesai*sin(2*kesai*x) + a3*a4/2*kesai*cos(2*kesai*x);
```

function CharacteristicofAdyn_buckle(w1, w2, Beam, C, P_cr, b,n)

```
EI = Beam.EI;
pA = Beam.rho;
Length_dim = Beam.Length;
i = 0;  m = 0;   w0= [];     zero_frequency = [];
step = (w2-w1)/n;
[A, kesai, Lamata1, Lamata2,wk, a]=A_dynamic(w1,Beam, C, P_cr, b);
s1 = sign(det(A));
s2 = 0;
for wn = w1 : w2
   i = i + 1;
   [A, kesai, Lamata1, Lamata2,wk, a]=A_dynamic(wn,Beam, C, P_cr, b);
   w(i) = wn;
   detA(i) = det(A);
   detB(i) = detAdynamic(wn,Beam, C, P_cr, b);
   s2 = sign(detA(i));
   if s1 ~= s2
      m = m + 1;
      w0(m) = wn;
      s1 = s2;
   end
```

```
end
freq = w .* sqrt(EI(2)/pA(2))/Length_dim(4)^2/(2*pi);
freq = freq/1e+003;
zero_frequency = w0 .* sqrt(EI(2)/pA(2))/Length_dim(4)^2/(2*pi);
zero_frequency = zero_frequency / 1e+003;
plot(freq, detA, freq, detB)
grid on
xlabel('frequency kHz')
ylabel('Value of the Characteristic Equation')
```

function CharacteristicofAdyn_flat(w1, w2, Beam)

```
i = 0;
for wn = w1 : w2
   i = i + 1;
   [ A, Lamata1, Lamata2 ] = Adyn_flat(wn,Beam);
   w(i) = wn;
   detA(i) = det(A);
end
plot(w, detA, 'linewidth',3)
grid on
xlabel('Angular Speed {\omega}')
ylabel('Value of the Characteristic Equation')
```

function [Beam] = Choose_beam (Beam_Name, wafer_No, Apply_V)

```
if Beam_Name == 1
  fprintf('PZT Resonator, Wafer Number = %g \n\n', wafer_No)
  [ Beam ] =  PZT_beam ( wafer_No, Apply_V );
else if Beam_Name == 2
     fprintf('AlGaAs Resonator, Wafer Number = %g \n\n', wafer_No)
     [ Beam ] =  AlGaAs_beam (wafer_No, Apply_V);
  end
end
```

function compare_w_exp_200(Ampl, frequency)

```
CC1 =1.0e+006 * [1.88495559215388;1.89123877746106;1.89752196276823;
  1.90380514807541;1.91008833338259;1.91637151868977;1.92265470399695;
  1.92893788930413;1.93522107461131;1.94150425991849;1.94778744522567;
  1.95407063053285;1.96035381584003;1.96663700114721;1.97292018645439;
  1.97920337176157;1.98548655706875;1.99176974237593;1.99805292768311;
  2.00433611299029;2.01061929829747;2.01690248360465;2.02318566891183;
  2.02946885421901;2.03009717274972;2.03072549128044;2.03135380981116;
  2.03198212834188;2.03261044687260;2.03323876540331;2.03386708393403;
  2.03449540246475;2.03512372099547;2.03575203952619;2.03638035805690;
  2.03700867658762;2.03763699511834;2.03826531364906;2.03889363217978;
  2.03952195071049;2.04015026924121;2.04077858777193;2.04140690630265;
  2.04203522483337;2.04831841014055;2.05460159544772;2.06088478075490;
```

```
  2.06716796606208;2.07345115136926];
DD1 = 1.0e-006 * [0.01386378928688;0.01503269022391;0.01643032903585;
  0.01801816564693;0.02011544386515;0.02293260361173;0.02601847135848;
  0.03035042858619;0.03677498355694;0.04598802134789;0.06113522429240;
  0.08444283679584;0.11618059858010;0.15242066994150;0.18722056677019;
  0.22028384578511;0.24930794625231;0.27661067821285;0.30308614489284;
  0.32684550803011;0.34889377870104;0.37021854641074;0.39100952056369;
  0.41025669908810;0.41317234562073;0.41504659147304;0.41630583600001;
  0.41903296328561;0.41998513452375;0.42150690235431;0.42411682769243;
  0.42488985268825;0.01440927917347;0.01440649037811;0.01405802051281;
  0.01430837102674;0.01405905905035;0.01379978620778;0.01371003307713;
  0.01359266733680;0.01364805974871;0.01327660954420;0.01337221936481;
  0.01328984276486;0.01208608386966;0.01129549976976;0.01065318232845;
  0.00983348151575;0.00944146231109];
CC2 = 1.0e+006 * [2.07345115136926;2.06716796606208;2.06088478075490;
  2.05460159544772;2.04831841014055;2.04203522483337;2.03575203952619;
  2.02946885421901;2.02318566891183;2.01690248360465;2.01061929829747;
  2.00433611299029;1.99805292768311;1.99176974237593;1.98548655706875;
  1.98485823853803;1.98422992000731;1.98360160147660;1.98297328294588;
  1.98234496441516;1.98171664588444;1.98108832735372;1.98046000882301;
  1.97983169029229;1.97920337176157;1.97857505323085;1.97794673470013;
  1.97731841616942;1.97669009763870;1.97606177910798;1.97543346057726;
  1.97480514204654;1.97417682351583;1.97354850498511;1.97292018645439;
  1.96663700114721;1.96035381584003;1.95407063053285;1.94778744522567;
  1.94150425991849;1.93522107461131;1.92893788930413;1.92265470399695;
  1.91637151868977;1.91008833338259;1.90380514807541;1.89752196276823;
  1.89123877746106;1.88495559215388];
DD2 = 1.0e-006 * [0.00945342675922;0.00989366738567;0.01054458179475;
  0.01193315965282;0.01216285708183;0.01332508054152;0.01461026837421;
  0.01595514228059;0.01764198026891;0.02010935640405;0.02302519014775;
  0.02594851570952;0.03124827757358;0.03859170279310;0.05189985220328;
  0.05369125776467;0.05602618848994;0.05774024493379;0.06108241638724;
  0.06319807356950;0.06613654671667;0.07021489212735;0.07453958919010;
  0.07998430961482;0.08575661890701;0.21554380394747;0.21221128738419;
  0.20996236732973;0.20557934851050;0.20260378473822;0.19989902061808;
  0.19663862226473;0.19289768827929;0.19033570598905;0.18623167767482;
  0.15117113234691;0.11523876880656;0.08332547819206;0.06035197820465;
  0.04501888394590;0.03666928882568;0.02877496660235;0.02535897976970;
  0.02113992121200;0.01828435396265;0.01771579210585;0.01557206689685;
  0.01464322407468;0.01396149576732];
beam_length = 2.0000e-004;
VA = 0.3980;
figure;
set(gcf,'Color',[1,1,1]);
plot(CC1/(2000*pi),DD1*1e9,'*',CC2/(2000*pi),DD2*1e9,'o', ...
```

```
   frequency(:,1),Ampl, frequency(:,3), Ampl)%, frequency(1:90,2),Ampl(1:90),
frequency(90:609,2), Ampl(90:609),'linewidth',3);
title(['Frequency-Response Curve of ',num2str(beam_length*1e6),' \mum PZT
Resonator at ',num2str(VA),' VAC']);
xlabel('Excitation Frequency, kHz');
ylabel('Response Amplitude, nm');
legend('Increasing Frequency','Decreasing Frequency',2);

function determinantA = detA1(lamata2, EI, x)
[determinantA, A] = A_static(lamata2, EI, x);

function y=detAdyn(wn,BeamProperties, C, P_cr, b)
EI = BeamProperties(:,1);
EA = BeamProperties(:,2);
Lngth = BeamProperties(:,3);
P = BeamProperties(:,4);
L(1) = Lngth(1);
L(2) = Lngth(1) + Lngth(2);
Lamata1=zeros(1,3);
Lamata2=zeros(1,3);
lamata1 = sqrt(P_cr(1));
lamata2 = sqrt(P_cr(2));
lamata3 = sqrt(P_cr(3));
for j = 1 : length(P)
  Lamata1(j)=(1/2*( P(j)+(P(j).^2+4*wn.^2).^0.5)).^0.5;    %wn is the frequency of
nth mode, that's what we want to know
  Lamata2(j)=(1/2*(-P(j)+(P(j).^2+4*wn.^2).^0.5)).^0.5;
end
%############### THE PARAMETER OF C1--C5##################
C11=C(2)*sin(Lamata1(1)*0)+(1-(lamata1/Lamata1(1)).^2).^(-1)*(-
C(3)*(sin(lamata1*0)*sin(Lamata1(1)*0)*lamata1+(lamata1.^2/Lamata1(1))*cos(la
mata1*0)*cos(Lamata1(1)*0))+C(4)*(cos(lamata1*0)*sin(Lamata1(1)*0)*lamata1-
(lamata1.^2/Lamata1(1))*sin(lamata1*0)*cos(Lamata1(1)*0)));
C12=C(2)*sin(Lamata1(1)*L(1))+(1-(lamata1/Lamata1(1)).^2).^(-1)*(-
C(3)*(sin(lamata1*L(1))*sin(Lamata1(1)*L(1))*lamata1+(lamata1.^2/Lamata1(1))*c
os(lamata1*L(1))*cos(Lamata1(1)*L(1)))+C(4)*(cos(lamata1*L(1))*sin(Lamata1(1)
*L(1))*lamata1-(lamata1.^2/Lamata1(1))*sin(lamata1*L(1))*cos(Lamata1(1)*L(1))));
C13=C(6)*sin(Lamata1(2)*L(1))+(1-(lamata2/Lamata1(2)).^2).^(-1)*(-
C(7)*(sin(lamata2*L(1))*sin(Lamata1(2)*L(1))*lamata2+(lamata2.^2/Lamata1(2))*c
os(lamata2*L(1))*cos(Lamata1(2)*L(1)))+C(8)*(cos(lamata2*L(1))*sin(Lamata1(2)
*L(1))*lamata2-(lamata2.^2/Lamata1(2))*sin(lamata2*L(1))*cos(Lamata1(2)*L(1))));
C14=C(6)*sin(Lamata1(2)*L(2))+(1-(lamata2/Lamata1(2)).^2).^(-1)*(-
C(7)*(sin(lamata2*L(2))*sin(Lamata1(2)*L(2))*lamata2+(lamata2.^2/Lamata1(2))*c
os(lamata2*L(2))*cos(Lamata1(2)*L(2)))+C(8)*(cos(lamata2*L(2))*sin(Lamata1(2)
*L(2))*lamata2-(lamata2.^2/Lamata1(2))*sin(lamata2*L(2))*cos(Lamata1(2)*L(2))));
```

```
C15=C(10)*sin(Lamata1(3)*L(2))+(1-(lamata3/Lamata1(3)).^2).^(-1)*(-
C(11)*(sin(lamata3*L(2))*sin(Lamata1(3)*L(2))*lamata3+(lamata3.^2/Lamata1(3))*
cos(lamata3*L(2))*cos(Lamata1(3)*L(2)))+C(12)*(cos(lamata3*L(2))*sin(Lamata1(
3)*L(2))*lamata3-
(lamata3.^2/Lamata1(3))*sin(lamata3*L(2))*cos(Lamata1(3)*L(2))));
C16=C(10)*sin(Lamata1(3)*1)+(1-(lamata3/Lamata1(3)).^2).^(-1)*(-
C(11)*(sin(lamata3*1)*sin(Lamata1(3)*1)*lamata3+(lamata3.^2/Lamata1(3))*cos(la
mata3*1)*cos(Lamata1(3)*1))+C(12)*(cos(lamata3*1)*sin(Lamata1(3)*1)*lamata3-
(lamata3.^2/Lamata1(3))*sin(lamata3*1)*cos(Lamata1(3)*1)));
C1=(C12-C11)+(C14-C13)+(C16-C15);
C21=C(2)*cos(Lamata1(1)*0)+(1-(lamata1/Lamata1(1)).^2).^(-1)*(C(3)*(-
sin(lamata1*0)*cos(Lamata1(1)*0)*lamata1+(lamata1.^2/Lamata1(1))*cos(lamata1*
0)*sin(Lamata1(1)*0))-C(4)*(-cos(lamata1*0)*cos(Lamata1(1)*0)*lamata1-
(lamata1.^2/Lamata1(1))*sin(lamata1*0)*sin(Lamata1(1)*0)));
C22=C(2)*cos(Lamata1(1)*L(1))+(1-(lamata1/Lamata1(1)).^2).^(-1)*(C(3)*(-
sin(lamata1*L(1))*cos(Lamata1(1)*L(1))*lamata1+(lamata1.^2/Lamata1(1))*cos(la
mata1*L(1))*sin(Lamata1(1)*L(1)))-C(4)*(-
cos(lamata1*L(1))*cos(Lamata1(1)*L(1))*lamata1-
(lamata1.^2/Lamata1(1))*sin(lamata1*L(1))*sin(Lamata1(1)*L(1))));
C23=C(6)*cos(Lamata1(2)*L(1))+(1-(lamata2/Lamata1(2)).^2).^(-1)*(C(7)*(-
sin(lamata2*L(1))*cos(Lamata1(2)*L(1))*lamata2+(lamata2.^2/Lamata1(2))*cos(la
mata2*L(1))*sin(Lamata1(2)*L(1)))-C(8)*(-
cos(lamata2*L(1))*cos(Lamata1(2)*L(1))*lamata2-
(lamata2.^2/Lamata1(2))*sin(lamata2*L(1))*sin(Lamata1(2)*L(1))));
C24=C(6)*cos(Lamata1(2)*L(2))+(1-(lamata2/Lamata1(2)).^2).^(-1)*(C(7)*(-
sin(lamata2*L(2))*cos(Lamata1(2)*L(2))*lamata2+(lamata2.^2/Lamata1(2))*cos(la
mata2*L(2))*sin(Lamata1(2)*L(2)))-C(8)*(-
cos(lamata2*L(2))*cos(Lamata1(2)*L(2))*lamata2-
(lamata2.^2/Lamata1(2))*sin(lamata2*L(2))*sin(Lamata1(2)*L(2))));
C25=C(10)*cos(Lamata1(3)*L(2))+(1-(lamata3/Lamata1(3)).^2).^(-1)*(C(11)*(-
sin(lamata3*L(2))*cos(Lamata1(3)*L(2))*lamata3+(lamata3.^2/Lamata1(3))*cos(la
mata3*L(2))*sin(Lamata1(3)*L(2)))-C(12)*(-
cos(lamata3*L(2))*cos(Lamata1(3)*L(2))*lamata3-
(lamata3.^2/Lamata1(3))*sin(lamata3*L(2))*sin(Lamata1(3)*L(2))));
C26=C(10)*cos(Lamata1(3)*1)+(1-(lamata3/Lamata1(3)).^2).^(-1)*(C(11)*(-
sin(lamata3*1)*cos(Lamata1(3)*1)*lamata3+(lamata3.^2/Lamata1(3))*cos(lamata3*
1)*sin(Lamata1(3)*1))-C(12)*(-cos(lamata3*1)*cos(Lamata1(3)*1)*lamata3-
(lamata3.^2/Lamata1(3))*sin(lamata3*1)*sin(Lamata1(3)*1)));
C2=(C22-C21)+(C24-C23)+(C26-C25);
C31=C(2)*sinh(Lamata2(1)*0)+(1+(lamata1/Lamata2(1)).^2).^(-1)*(-
C(3)*(sin(lamata1*0)*sinh(Lamata2(1)*0)*lamata1-
(lamata1.^2/Lamata2(1))*cos(lamata1*0)*cosh(Lamata2(1)*0))+C(4)*(cos(lamata1*
0)*sinh(Lamata2(1)*0)*lamata1+(lamata1.^2/Lamata2(1))*sin(lamata1*0)*cosh(La
mata2(1)*0)));
C32=C(2)*sinh(Lamata2(1)*L(1))+(1+(lamata1/Lamata2(1)).^2).^(-1)*(-
C(3)*(sin(lamata1*L(1))*sinh(Lamata2(1)*L(1))*lamata1-
```

(lamata1.^2/Lamata2(1))*cos(lamata1*L(1))*cosh(Lamata2(1)*L(1)))+C(4)*(cos(la
mata1*L(1))*sinh(Lamata2(1)*L(1))*lamata1+(lamata1.^2/Lamata2(1))*sin(lamata1
*L(1))*cosh(Lamata2(1)*L(1))));
C33=C(6)*sinh(Lamata2(2)*L(1))+(1+(lamata2/Lamata2(2)).^2).^(-1)*(-
C(7)*(sin(lamata2*L(1))*sinh(Lamata2(2)*L(1))*lamata2-
(lamata2.^2/Lamata2(2))*cos(lamata2*L(1))*cosh(Lamata2(2)*L(1)))+C(8)*(cos(la
mata2*L(1))*sinh(Lamata2(2)*L(1))*lamata2+(lamata2.^2/Lamata2(2))*sin(lamata2
*L(1))*cosh(Lamata2(2)*L(1))));
C34=C(6)*sinh(Lamata2(2)*L(2))+(1+(lamata2/Lamata2(2)).^2).^(-1)*(-
C(7)*(sin(lamata2*L(2))*sinh(Lamata2(2)*L(2))*lamata2-
(lamata2.^2/Lamata2(2))*cos(lamata2*L(2))*cosh(Lamata2(2)*L(2)))+C(8)*(cos(la
mata2*L(2))*sinh(Lamata2(2)*L(2))*lamata2+(lamata2.^2/Lamata2(2))*sin(lamata2
*L(2))*cosh(Lamata2(2)*L(2))));
C35=C(10)*sinh(Lamata2(3)*L(2))+(1+(lamata3/Lamata2(3)).^2).^(-1)*(-
C(11)*(sin(lamata3*L(2))*sinh(Lamata2(3)*L(2))*lamata3-
(lamata3.^2/Lamata2(3))*cos(lamata3*L(2))*cosh(Lamata2(3)*L(2)))+C(12)*(cos(la
mata3*L(2))*sinh(Lamata2(3)*L(2))*lamata3+(lamata3.^2/Lamata2(3))*sin(lamata3
*L(2))*cosh(Lamata2(3)*L(2))));
C36=C(10)*sinh(Lamata2(3)*1)+(1+(lamata3/Lamata2(3)).^2).^(-1)*(-
C(11)*(sin(lamata3*1)*sinh(Lamata2(3)*1)*lamata3-
(lamata3.^2/Lamata2(3))*cos(lamata3*1)*cosh(Lamata2(3)*1))+C(12)*(cos(lamata3
*1)*sinh(Lamata2(3)*1)*lamata3+(lamata3.^2/Lamata2(3))*sin(lamata3*1)*cosh(La
mata2(3)*1)));
C3=(C32-C31)+(C34-C33)+(C36-C35);
C41=C(2)*cosh(Lamata2(1)*0)+(1+(lamata1/Lamata2(1)).^2).^(-1)*(-
C(3)*(sin(lamata1*0)*cosh(Lamata2(1)*0)*lamata1-
(lamata1.^2/Lamata2(1))*cos(lamata1*0)*sinh(Lamata2(1)*0))+C(4)*(cos(lamata1*
0)*cosh(Lamata2(1)*0)*lamata1+(lamata1.^2/Lamata2(1))*sin(lamata1*0)*sinh(La
mata2(1)*0)));
C42=C(2)*cosh(Lamata2(1)*L(1))+(1+(lamata1/Lamata2(1)).^2).^(-1)*(-
C(3)*(sin(lamata1*L(1))*cosh(Lamata2(1)*L(1))*lamata1-
(lamata1.^2/Lamata2(1))*cos(lamata1*L(1))*sinh(Lamata2(1)*L(1)))+C(4)*(cos(lam
ata1*L(1))*cosh(Lamata2(1)*L(1))*lamata1+(lamata1.^2/Lamata2(1))*sin(lamata1*
L(1))*sinh(Lamata2(1)*L(1))));
C43=C(6)*cosh(Lamata2(2)*L(1))+(1+(lamata2/Lamata2(2)).^2).^(-1)*(-
C(7)*(sin(lamata2*L(1))*cosh(Lamata2(2)*L(1))*lamata2-
(lamata2.^2/Lamata2(2))*cos(lamata2*L(1))*sinh(Lamata2(2)*L(1)))+C(8)*(cos(lam
ata2*L(1))*cosh(Lamata2(2)*L(1))*lamata2+(lamata2.^2/Lamata2(2))*sin(lamata2*
L(1))*sinh(Lamata2(2)*L(1))));
C44=C(6)*cosh(Lamata2(2)*L(2))+(1+(lamata2/Lamata2(2)).^2).^(-1)*(-
C(7)*(sin(lamata2*L(2))*cosh(Lamata2(2)*L(2))*lamata2-
(lamata2.^2/Lamata2(2))*cos(lamata2*L(2))*sinh(Lamata2(2)*L(2)))+C(8)*(cos(lam
ata2*L(2))*cosh(Lamata2(2)*L(2))*lamata2+(lamata2.^2/Lamata2(2))*sin(lamata2*
L(2))*sinh(Lamata2(2)*L(2))));
C45=C(10)*cosh(Lamata2(3)*L(2))+(1+(lamata3/Lamata2(3)).^2).^(-1)*(-
C(11)*(sin(lamata3*L(2))*cosh(Lamata2(3)*L(2))*lamata3-

```
(lamata3.^2/Lamata2(3))*cos(lamata3*L(2))*sinh(Lamata2(3)*L(2)))+C(12)*(cos(la
mata3*L(2))*cosh(Lamata2(3)*L(2))*lamata3+(lamata3.^2/Lamata2(3))*sin(lamata3
*L(2))*sinh(Lamata2(3)*L(2))));
C46=C(10)*cosh(Lamata2(3)*1)+(1+(lamata3/Lamata2(3)).^2).^(-1)*(-
C(11)*(sin(lamata3*1)*cosh(Lamata2(3)*1)*lamata3-
(lamata3.^2/Lamata2(3))*cos(lamata3*1)*sinh(Lamata2(3)*1))+C(12)*(cos(lamata3
*1)*cosh(Lamata2(3)*1)*lamata3+(lamata3.^2/Lamata2(3))*sin(lamata3*1)*sinh(La
mata2(3)*1)));
C4=(C42-C41)+(C44-C43)+(C46-C45);
C51=C(2)*C(3)*cos(lamata1*0)+C(2)*C(4)*sin(lamata1*0)+C(3).^2*(lamata1.^2/2*
0-
sin(2*lamata1*0)*lamata1/4)+C(3)*C(4)*lamata1*cos(2*lamata1*0)/2+C(4).^2*(la
mata1.^2/2*0+sin(2*lamata1*0)*lamata1/4);
C52=C(2)*C(3)*cos(lamata1*L(1))+C(2)*C(4)*sin(lamata1*L(1))+C(3).^2*(lamata1
.^2/2*L(1)-sin(2*lamata1*L(1))*lamata1/4)+C(3)*C(4)*lamata1
*cos(2*lamata1*L(1))/2+C(4).^2*(lamata1.^2/2*L(1)+sin(2*lamata1*L(1))*lamata1/
4);
C53=C(6)*C(7)*cos(lamata2*L(1))+C(6)*C(8)*sin(lamata2*L(1))+C(7).^2*(lamata2
.^2/2*L(1)-sin(2*lamata2*L(1))*lamata2/4)+C(7)*C(8)*lamata2*
cos(2*lamata2*L(1))/2+C(8).^2*(lamata2.^2/2*L(1)+sin(2*lamata2*L(1))*lamata2/4
);
C54=C(6)*C(7)*cos(lamata2*L(2))+C(6)*C(8)*sin(lamata2*L(2))+C(7).^2*(lamata2
.^2/2*L(2)-sin(2*lamata2*L(2))*lamata2/4)+C(7)*C(8)*lamata2
*cos(2*lamata2*L(2))/2+C(8).^2*(lamata2.^2/2*L(2)+sin(2*lamata2*L(2))*lamata2/
4);
C55=C(10)*C(11)*cos(lamata3*L(2))+C(10)*C(12)*sin(lamata3*L(2))+C(11).^2*(l
amata3.^2/2*L(2)-sin(2*lamata3*L(2))*lamata3/4)+C(11)*C(12)*lamata3
*cos(2*lamata3*L(2))/2+C(12).^2*(lamata3.^2/2*L(2)+sin(2*lamata3*L(2))*lamata
3/4);
C56=C(10)*C(11)*cos(lamata3*1)+C(10)*C(12)*sin(lamata3*1)+C(11).^2*(lamata3
.^2/2*1-sin(2*lamata3*1)*lamata3/4)+C(11)*C(12)*lamata3*cos(2*lamata3*1)/2
+C(12).^2*(lamata3.^2/2*1+sin(2*lamata3*1)*lamata3/4);
 C5=(C52-C51)+(C54-C53)+(C56-C55);
%############ THE EXPRESSION OF THE PARTICULAR SULUTION
Fip######
%%%% THE EXPRESSION of MATRIX A(ij) FOR THE DYNAMIC
BUCKLING%%%%
Adyn=zeros(15,15);
Adyn(1,1)=sin(Lamata1(1)*x(1));
Adyn(1,2)=cos(Lamata1(1)*x(1));
Adyn(1,3)=sinh(Lamata2(1)*x(1));
Adyn(1,4)=cosh(Lamata2(1)*x(1));
Adyn(1,5)=C(3)*cos(lamata1*x(1))+C(4)*sin(lamata1*x(1));
Adyn(2,1)=Lamata1(1)*cos(Lamata1(1)*x(1));
Adyn(2,2)=-Lamata1(1)*sin(Lamata1(1)*x(1));
Adyn(2,3)=Lamata2(1)*cosh(Lamata1(1)*x(1));
```

```
Adyn(2,4)=Lamata2(1)*sinh(Lamata1(1)*x(1));
Adyn(2,5)=-C(3)*lamata1*sin(lamata1*x(1))+C(4)*lamata1*cos(lamata1*x(1));
Adyn(3,1)= sin(Lamata1(1)*x(2));
Adyn(3,2)= cos(Lamata1(1)*x(2));
Adyn(3,3)= sinh(Lamata2(1)*x(2));
Adyn(3,4)= cosh(Lamata2(1)*x(2));
Adyn(3,5)=C(3)*cos(lamata1*x(2))+C(4)*sin(lamata1*x(2));
Adyn(3,6)=-sin(Lamata1(2)*x(2));
Adyn(3,7)=-cos(Lamata1(2)*x(2));
Adyn(3,8)=-sinh(Lamata2(2)*x(2));
Adyn(3,9)=-cosh(Lamata2(2)*x(2));
Adyn(3,10)=-C(7)*cos(lamata2*x(2))-C(8)*sin(lamata2*x(2));
Adyn(4,1)= Lamata1(1)*cos(Lamata1(1)*x(2));
Adyn(4,2)=-Lamata1(1)*sin(Lamata1(1)*x(2));
Adyn(4,3)= Lamata2(1)*cosh(Lamata2(1)*x(2));
Adyn(4,4)= Lamata2(1)*sinh(Lamata2(1)*x(2));
Adyn(4,5)=-C(3)*lamata1*sin(lamata1*x(2))+C(4)*lamata1*cos(lamata1*x(2));
Adyn(4,6)=-Lamata1(2)*cos(Lamata1(2)*x(2));
Adyn(4,7)= Lamata1(2)*sin(Lamata1(2)*x(2));
Adyn(4,8)=-Lamata2(2)*cosh(Lamata2(2)*x(2));
Adyn(4,9)=-Lamata2(2)*sinh(Lamata2(2)*x(2));
Adyn(4,10)=C(7)*lamata2*sin(lamata2*x(2))-C(8)*lamata2*cos(lamata2*x(2));
Adyn(5,1)=-(Lamata1(1).^2)*sin(Lamata1(1)*x(2));
Adyn(5,2)=-(Lamata1(1).^2)*cos(Lamata1(1)*x(2));
Adyn(5,3)= (Lamata2(1).^2)*sinh(Lamata2(1)*x(2));
Adyn(5,4)= (Lamata2(1).^2)*cosh(Lamata2(1)*x(2));
Adyn(5,5)=(-C(3)*lamata1.^2*cos(lamata1*x(2))-
C(4)*lamata1.^2*sin(lamata1*x(2)));
Adyn(5,6)= (Lamata1(2).^2)*sin(Lamata1(2)*x(2))*EI(2)/EI(1);
Adyn(5,7)= (Lamata1(2).^2)*cos(Lamata1(2)*x(2))*EI(2)/EI(1);
Adyn(5,8)=-(Lamata2(2).^2)*sinh(Lamata2(2)*x(2))*EI(2)/EI(1);
Adyn(5,9)=-(Lamata2(2).^2)*cosh(Lamata2(2)*x(2))*EI(2)/EI(1);
Adyn(5,10)=(C(7)*lamata2.^2*cos(lamata2*x(2))+C(8)*lamata2.^2*sin(lamata2*x(2
))*EI(2)/EI(1);
Adyn(6,1)=-(Lamata1(1).^3)*cos(Lamata1(1)*x(2));
Adyn(6,2)= (Lamata1(1).^3)*sin(Lamata1(1)*x(2));
Adyn(6,3)= (Lamata2(1).^3)*cosh(Lamata2(1)*x(2));
Adyn(6,4)= (Lamata2(1).^3)*sinh(Lamata2(1)*x(2));
Adyn(6,5)= (C(3)*lamata1.^3*sin(lamata1*x(2))-
C(4)*lamata1.^3*cos(lamata1*x(2)));
Adyn(6,6)= (Lamata1(2).^3)*cos(Lamata1(2)*x(2))*EI(2)/EI(1);
Adyn(6,7)=-(Lamata1(2).^3)*sin(Lamata1(2)*x(2))*EI(2)/EI(1);
Adyn(6,8)=-(Lamata2(2).^3)*cosh(Lamata2(2)*x(2))*EI(2)/EI(1);
Adyn(6,9)=-(Lamata2(2).^3)*sinh(Lamata2(2)*x(2))*EI(2)/EI(1);
```

```
Adyn(6,10)=(-
C(7)*lamata2.^3*sin(lamata2*x(2))+C(8)*lamata2.^3*cos(lamata2*x(2)))*EI(2)/EI(1
);
Adyn(7,6)= sin(Lamata1(2)*x(3));
Adyn(7,7)= cos(Lamata1(2)*x(3));
Adyn(7,8)= sinh(Lamata2(2)*x(3));
Adyn(7,9)= cosh(Lamata2(2)*x(3));
Adyn(7,10)=C(7)*cos(lamata2*x(3))+C(8)*sin(lamata2*x(3));
Adyn(7,11)=-sin(Lamata1(3)*x(3));
Adyn(7,12)=-cos(Lamata1(3)*x(3));
Adyn(7,13)=-sinh(Lamata2(3)*x(3));
Adyn(7,14)=-cosh(Lamata2(3)*x(3));
Adyn(7,15)=-C(11)*cos(lamata3*x(3))-C(12)*sin(lamata3*x(3));
Adyn(8,6)= Lamata1(2)*cos(Lamata1(2)*x(3));
Adyn(8,7)=-Lamata1(2)*sin(Lamata1(2)*x(3));
Adyn(8,8)= Lamata2(2)*cosh(Lamata2(2)*x(3));
Adyn(8,9)= Lamata2(2)*sinh(Lamata2(2)*x(3));
Adyn(8,10)=-C(7)*lamata2*sin(lamata2*x(3))+C(8)*lamata2*cos(lamata2*x(3));
Adyn(8,11)=-Lamata1(3)*cos(Lamata1(3)*x(3));
Adyn(8,12)= Lamata1(3)*sin(Lamata1(3)*x(3));
Adyn(8,13)=-Lamata2(3)*cosh(Lamata2(3)*x(3));
Adyn(8,14)=-Lamata2(3)*sinh(Lamata2(3)*x(3));
Adyn(8,15)= C(11)*lamata3*sin(lamata3*x(3))-C(12)*lamata3*cos(lamata3*x(3));
Adyn(9,6)=-(Lamata1(2).^2)*sin(Lamata1(2)*x(3))*EI(2)/EI(3);
Adyn(9,7)=-(Lamata1(2).^2)*cos(Lamata1(2)*x(3))*EI(2)/EI(3);
Adyn(9,8)= (Lamata2(2).^2)*sinh(Lamata2(2)*x(3))*EI(2)/EI(3);
Adyn(9,9)= (Lamata2(2).^2)*cosh(Lamata2(2)*x(3))*EI(2)/EI(3);
Adyn(9,10)=(-C(7)*lamata2.^2*cos(lamata2*x(3))-
C(8)*lamata2.^2*sin(lamata2*x(3)))*EI(2)/EI(3);
Adyn(9,11)= (Lamata1(3).^2)*sin(Lamata1(3)*x(3));
Adyn(9,12)= (Lamata1(3).^2)*cos(Lamata1(3)*x(3));
Adyn(9,13)=-(Lamata2(3).^2)*sinh(Lamata2(3)*x(3));
Adyn(9,14)=-(Lamata2(3).^2)*cosh(Lamata2(3)*x(3));
Adyn(9,15)=(C(11)*lamata3.^2*cos(lamata3*x(3))+C(12)*lamata3.^2*sin(lamata3*
x(3)));
Adyn(10,6)= -(Lamata1(2).^3)*cos(  Lamata1(2)*x(3))*EI(2)/EI(3);
Adyn(10,7)=  (Lamata1(2).^3)*sin(  Lamata1(2)*x(3))*EI(2)/EI(3);
Adyn(10,8)=  (Lamata2(2).^3)*cosh( Lamata2(2)*x(3))*EI(2)/EI(3);
Adyn(10,9)=  (Lamata2(2).^3)*sinh( Lamata2(2)*x(3))*EI(2)/EI(3);
Adyn(10,10)=(C(7)*lamata2.^3*sin(lamata2*x(3))-
C(8)*lamata2.^3*cos(lamata2*x(3))) *EI(2)/EI(3);
Adyn(10,11)= (Lamata1(3).^3)*cos( Lamata1(3)*x(3));
Adyn(10,12)=-(Lamata1(3).^3)*sin( Lamata1(3)*x(3));
Adyn(10,13)=-(Lamata2(3).^3)*cosh(Lamata2(3)*x(3));
Adyn(10,14)=-(Lamata2(3).^3)*sinh(Lamata2(3)*x(3));
```

```
Adyn(10,15)=(-
C(11)*lamata3.^3*sin(lamata3*x(3))+C(12)*lamata3.^3*cos(lamata3*x(3)));
Adyn(11,11)= sin(Lamata1(3)*x(4));
Adyn(11,12)=cos(Lamata1(3)*x(4));
Adyn(11,13)=sinh(Lamata2(3)*x(4));
Adyn(11,14)=cosh(Lamata2(3)*x(4));
Adyn(11,15)=C(11)*cos(lamata3*x(4))+C(12)*sin(lamata3*x(4));
Adyn(12,11)= Lamata1(3)*cos(Lamata1(3)*x(4));
Adyn(12,12)=-Lamata1(3)*sin(Lamata1(3)*x(4));
Adyn(12,13)=Lamata2(3)*cosh(Lamata2(3)*x(4));
Adyn(12,14)=Lamata2(3)*sinh(Lamata2(3)*x(4));
Adyn(12,15)=-C(11)*lamata3*sin(lamata3*x(4))+C(12)*lamata3*cos(lamata3*x(4));
Adyn(13,1)=C1;
Adyn(13,2)=C2;
Adyn(13,3)=C3;
Adyn(13,4)=C4;
Adyn(13,5)=C5-wn.^2/parameter1*lamata1.^2;
Adyn(14,6)=C1;
Adyn(14,7)=C2;
Adyn(14,8)=C3;
Adyn(14,9)=C4;
Adyn(14,10)=C5-wn.^2/parameter1*lamata2.^2;
Adyn(15,11)=C1;
Adyn(15,12)=C2;
Adyn(15,13)=C3;
Adyn(15,14)=C4;
Adyn(15,15)=C5-wn.^2/parameter1*lamata3.^2;
%%%%%% EXPRESSION Adyn ENDED%%%%%
y=det(Adyn);
```

function y = detAdyn1(wn,Beam)

```
 [Adyn, Lamata1, Lamata2]  = Adyn_flat(wn,Beam);
y = det(Adyn);
```

function y=detAdynamic(wn,Beam, C, P_cr, b)

```
 [Adyn, kesai, Lamata1, Lamata2,wk, a]=A_dynamic(wn,Beam, C, b);
 y = det(Adyn);
```

function y = dfdx(f,x)

```
% this function is to give df/dx
% f is a n x 1 (or 1 x n) vector, represent n values of f(x)
% x is the x-axis span

n = length(f)-1;
dx = x/n;
for i = 1 : n;
```

```
   df = f(i+1)-f(i);
   y(i) = df/dx;
end
y(n+1) = 2*y(n)-y(n-1); % linearize the curve to calculate the last element
```

function [Wbk,wn, Beam]=dynamicdeflc(Beam, Mode_No, BucklingFactor, resolution, static_eigVector)

```
options = optimset;%( 'Display', 'final', 'TolX', 1.0E-17 );
%------------------  Calculate wn    -------------------------------------
if BucklingFactor ~= 0
   wn = 1E003; i = 1;    w0(1) = 1E-002;
   walksteps = 1E-002;%(wn - w0(1))/1000;
   s1 = sign(detAdynamic(w0(1), Beam, static_eigVector, BucklingFactor));
   for w = w0(1) : walksteps : wn  %looking for 0 point by looking for sign change
      if i <= max(Mode_No)
         s = sign((detAdynamic(w, Beam, static_eigVector, BucklingFactor)));
         if s1 ~= s             %if change sign
            i = i+1;
            w0(i) = w;
            s1 = s;
         end
      end

   end
%---------------------------------------------------------------------
   Mode_min = min(Mode_No);
   Mode_max = max(Mode_No);
   Mode_now = Mode_min;
   for j = 1: ( Mode_max-Mode_min+1 )
      wn(j)  =fzero('detAdynamic',[w0(Mode_now),w0(Mode_now+1)],options,  Beam,
static_eigVector,  BucklingFactor);
      wn1 =fzero('detAdynamic',[w0(Mode_now +1),w0(Mode_now)],options, Beam,
static_eigVector,  BucklingFactor);
      if wn(j) ~= wn1
         'Calculation needs refining, the region includes more than 2 zero values'
      else
      [Adynamic, kesai, Lamata1, Lamata2, wn(j), a, Beam] =
A_dynamic(wn(j),Beam, static_eigVector,  BucklingFactor);
      a1 = a(:,1);
      a2 = a(:,2);
      a3 = a(:,3);
      a4 = a(:,4);
      Mode_now = Mode_now + 1;
      end
   end
end
```

```
[V,D]=eig(Adynamic);                    %D is the eigenvector and V is the eigenvalue

%-------------------     DRAW THE MODE SHAPE      ------------------------
clmnumber=length(V);    % clmnumber is the max colume nunber of the matrix,
                        % 12 is the homogenious case and 15 is the nonhomogenious case
%--- CHOOSE THE SMALLEST EIGENVALUE, AND THE CORRESPONDING
EIGENVECTOR ---
DD = diag(D);
[Dmin clm]=min(abs(DD));   %the eigenvector closest to 0
%fprintf('at dynamicdeflc.m line 93, eigenvalue = %g\n\n', DD(clm))
% CONSTRUCT THE MODE SHAPE%
mm=0;
kk=resolution;
Length = Beam.NondimSection;
xx = Beam.Node;
%############################
if BucklingFactor==0
if clmnumber==12
   C1 = V(1:4:12,clm);             %the  corresponding eigenvector V(:,clm)
   C2 = V(2:4:12,clm);
   C3 = V(3:4:12,clm);
   C4 = V(4:4:12,clm);
 for x = xx(1) : 1/kk : xx(2)
    mm=mm+1;
    Wbk(mm) = C1(1) * sin(Lamata1(1)*x)...
            +C2(1) * cos(Lamata1(1)*x)...
            +C3(1) * sinh(Lamata2(1)*x)...
            +C4(1) * cosh(Lamata2(1)*x);
 end
 for x = xx(2)+1/kk : 1/kk : xx(3)
    mm=mm+1;
    %y=x-1/2;
    y=x;
    Wbk(mm) = C1(2) * sin(Lamata1(2)*y)...
            +C2(2) * cos(Lamata1(2)*y)...
            +C3(2) * sinh(Lamata2(2)*y)...
            +C4(2) * cosh(Lamata2(2)*y);
 end
 for x = xx(3)+1/kk : 1/kk : xx(4)+1/kk
    mm=mm+1;
    %z=x-1;
    z=x;
    Wbk(mm) = C1(3) * sin(Lamata1(3)*z)...
            +C2(3)* cos(Lamata1(3)*z)...
            +C3(3)*sinh(Lamata2(3)*z)...
            +C4(3)*cosh(Lamata2(3)*z);
```

```
  end
  [Wbk ampl] = normalization(Wbk, 1);
  C1 = C1/ampl;
  C2 = C2/ampl;
  C3 = C3/ampl;
  C4 = C4/ampl;
end
end
%############################
if BucklingFactor~=0
if clmnumber==15
    C1 = V(1:5:15,clm);          %the  corresponding eigenvector V(:,clm)
    C2 = V(2:5:15,clm);
    C3 = V(3:5:15,clm);
    C4 = V(4:5:15,clm);
    C5 = V(5:5:15,clm);
    for x = xx(1) : 1/kk : xx(2)
     mm=mm+1;
     Wbk(mm) = C1(1) * sin(Lamata1(1)*x)...
            +C2(1) * cos(Lamata1(1)*x)...
            +C3(1) * sinh(Lamata2(1)*x)...
            +C4(1) * cosh(Lamata2(1)*x)...
            +C5(1) * (a3(1)*cos(kesai(1)*x)+a4(1)*sin(kesai(1)*x));
  end
  for x = xx(2)+1/kk : 1/kk : xx(3)
     mm=mm+1;
     %y=x-1/2;
     y=x;
     Wbk(mm) = C1(2) * sin(Lamata1(2)*y)...
            +C2(2) * cos(Lamata1(2)*y)...
            +C3(2) * sinh(Lamata2(2)*y)...
            +C4(2) * cosh(Lamata2(2)*y)...
            +C5(2)* (a3(2)*cos(kesai(2)*x)+a4(2)*sin(kesai(2)*x));
  end
  for x = xx(3)+1/kk : 1/kk : xx(4)
     mm=mm+1;
     %z=x-1;
     z=x;
     Wbk(mm) = C1(3) * sin(Lamata1(3)*z)...
            +C2(3) * cos(Lamata1(3)*z)...
            +C3(3) * sinh(Lamata2(3)*z)...
            +C4(3) * cosh(Lamata2(3)*z)...
            +C5(3) * (a3(3)*cos(kesai(3)*x)+a4(3)*sin(kesai(3)*x));
  end
  [Wbk ampl] = normalization(Wbk, 1);
  C1 = C1/ampl;
```

```
  C2 = C2/ampl;
  C3 = C3/ampl;
  C4 = C4/ampl;
  C5 = C5/ampl;
end
end
```

function Free_Vib_Loop

```
%-------------------------------------------------------------------------
%-- Calculate the Free Vibration Mode Shape  upon PostBuckling Position ---
%-------------------------------------------------------------------------
   %###########THE DYNAMIC BUCKLED MODE SHAPE#############
   % clmnumber=12: FOR THE HOMOGENOUS EQUATION############
   % clmnumber=15: FOR THE NONHOMUGENOUS EQUATION ########
   [ W1_dy, wk, Beam] = dynamicdeflc( Beam, Dynamic_Mode_No, BucklingFactor,
Image_Resol, static_eigVector ) ;
   freq = wk*sqrt(EI(2)/pA(2))/Length_dim(4)^2/(2*pi)/1E3;%wk is dimensionless
angular frequency
   ampl = 1e-003;
   Wdispl1 = BucklingFactor*W_st + ampl*W1_dy;
   Wdispl2 = BucklingFactor*W_st - ampl*W1_dy;
```

function freq_vs_b_general

```
clc;clear all;  close all;  ti = cputime;
Beam_name  = 1;        %PZT=1,  AlGaAs=2
Wafer_name = 6;
Image_Resol = 1000;
%------------------------------
StaticBucklingLock = 1;
FreeVibrationLock  = 1;
ForceVibrationLock = 0;
%------------------------------
m = 0;
b1 = 1E-3;    %BucklingFactor start value
b2 = 20E-3;      %BucklingFactor ends value
Dynamic_Mode_No = [1, 4];     %# of dynamic mode calculated
Static_Mode_No = 1;
n = 10;        %Resolution
steps = (b2 - b1)/n;
%-------------------------------------------------------------------------
%----                    Data Preparation                    --------
%-------------------------------------------------------------------------
%------------------     Beam Data  ------------------------------------
```

```
fprintf('*********   Resonator Geometry/Material/Stress Information
**********\n\n')
[Beam] = beam_structure ( Beam_name, Wafer_name, Apply_V );
P0_dim = Beam.AxF_dim;
EI = Beam.EI;
EA = Beam.EA;
pA = Beam.rho;
Length_dim = Beam.Length;
for i = 1 : Image_Resol+1        % every point in X-axis
   x_cord(i) = (i-1)/Image_Resol;
end
%--------------------     Non-Dimensionalize Data     ---------------------
P0 = P0_dim * Length_dim(4)^2 ./ EI;        %non-dim form of axial force
Lngth = Length_dim(1:3) / Length_dim(4);   %length of each section
Beam.AxF_nondim = P0;
Beam.Node = [0; Lngth(1); sum(Lngth(1:2)); sum(Lngth)]; % non-dim x position of
each node
Beam.NondimSection = Beam.Length(1:3)/Beam.Length(4);    %Non-dim Section
Length
fprintf('Length of the Resonator:       %g [um]\n\n',Length_dim(4)'*1e6)
fprintf('Density/UnitLength :          %e      %e      %e [kg/m]\n\n',pA')
fprintf('Bending Stiffness:            %e      %e      %e [Nm^2]\n\n',EI')
fprintf('Axial   Stiffness :           %e      %e      %e [N]\n\n',EA')
fprintf('Axial Stress:                 %e      %e      %e [N]\n\n\n\n',P0_dim')

%-------------------------------------------------------------------------
%----      Calculate the Static Critical Buckling Mode Shape       --------
%-------------------------------------------------------------------------
% To calculate the static critical buckling modeshape of a E-U beam
if StaticBucklingLock == 1
   fprintf( '         ---S T A T I C   B U C K L I N G ---\n\n')
   [P_cr W_st, static_eigVector] =Staticbuckleshape(Beam, Static_Mode_No,
Image_Resol);
   Beam.Pcr_nondim = P_cr;
   Beam.Pcr_dim = P_cr.*EI/Length_dim(4)^2;     %dim form of P_critical [N]
   fprintf('The %gth/nd/st Static Bcukling Equlibrium Position\n\n', Static_Mode_No);
   fprintf('     Kesai = %g    %g    %g  \nPcr_nondim = %g    %g    %g      \n\n\n\n',...
         sqrt(P_cr),P_cr);
end

%-------------------------------------------------------------------------
%-- Calculate the Free Vibration Mode Shape  upon PostBuckling Position ---
%-------------------------------------------------------------------------
fprintf( '   ---  Dynamic Mode Shape  upon PostBuckling Position  ---\n\n');
m = 0;
for BucklingFactor = b1 : steps : b2
```

```
   m = m + 1;
   fprintf('Calculation Cycle Number = %g \n', m)
   Free_Vib_Loop;
   b(m) = BucklingFactor;
   Frquency(:,m) = freq;
End
plot(b,Frquency,'linewidth',3)%,b,Frquency2*1e3,'*')%,b,Frquency3*1e3,'*')
grid on
xlabel('b','fontsize',16)
ylabel('Natural Frequencies (kHz)','fontsize',16)
title('Free Vibration of 400{\it{\mu}m} Around The 1st Static Buckling
Mode','fontsize',16)
```

function [sigma] = Frequency_Response(Beam, W_st, W_dy, gx, F, a, mu, wn,b)

```
q  = Beam.q;
EI = Beam.EI;
m  = Beam.rho;
n  = length(Beam.r);
L  = Beam.Length(n+1);
x  = Beam.Node;
w_dim = sqrt(EI(2)/m(2))/L^2*wn;
mu_dim= sqrt(EI(2)*m(2))/L^2*mu;
N = round((length(W_st)-1)*x + 1);        % the node number at the end of each
section
dW_st = dfdx(W_st,1);
ddW_st= dfdx(dW_st,1);
%Force = F*b*dW_st(N)-b*qk*F*ddW_st;
nom1 = 0;
nom2 = 0;
nom3 = 0;
dnom = 0;nom = 0;
for k = 1 : n
   Force( N(k):N(k+1) ) = b*q(k)*F*ddW_st( N(k):N(k+1) ); % double check with
this expression
end
for k = 1 : n
   nom1 = nom1 + innerproduct(W_dy, Force,x(k),
x(k+1),1);%***************!!!!!!!!!!!!!!!!!!!!!!
   nom2 = nom2 + innerproduct(W_dy, W_dy, x(k), x(k+1),1)*L^4/EI(k);
   nom3 = nom3 + innerproduct(W_dy, gx,   x(k), x(k+1),1);
   dnom = dnom + innerproduct(W_dy, W_dy, x(k), x(k+1),1)*L^4*m(k)/EI(k);
end
f = nom1/dnom;
C = nom2/dnom;
alpha = 1/(8*w_dim)*nom3/dnom;
```

```
sigma(1) = -alpha*a^2 - sqrt( f^2/4/w_dim^2/a^2-C^2*mu_dim^2 ); % curve of the
left
sigma(2) = -alpha*a^2;                                  % curve of the center
sigma(3) = -alpha*a^2 + sqrt( f^2/4/w_dim^2/a^2-C^2*mu_dim^2 ); % curve of the
right
```

function F = get_Axial_F(resid_stress, thick, Width, EA, Length)

```
% this function is to get the averaged axial force using a linear method
% without changing the dimensions
residual_F = ( resid_stress' * thick * Width)';
K1 = EA(1)/Length(1);
K2 = EA(2)/Length(2);
K3 = EA(3)/Length(3);
K  = [  -1     K1                    0
          -1      -K2       K2
       -1      0       -K3  ];
U  = - K^-1 * residual_F;  %U = { P_average, U1, U2}' = { [N]    [m]     [m] }'
F = U(1);
```

function [e, K] = get_e_K(E, density, thickness, width, D31,appl_V)

```
% this function is to calculate the {strain , curvature} vector of a composite f-f
BEAM, using Euller-Bernoulli assumption
%E                              is the Young's Modulus matrix
%density                is the density matrix
%thickness              is the thickness of different layer
%width                          is the width of the beam
%D31                            is the d31 vector of each layer
%h                                      is the coordinates of different layers in the
composite beam
%appl_V                         is the voltages applied for each layer
%v=[0.27 0.35 0.3 0.35];
%E=E.*((1-2*v)./((1-v.^2).*(1-v).^2))
nlayer = length( density( : , 1 ) );
mclm = length( density( 1 , : ) );
h = zeros( nlayer+1 , mclm);
lamata = ((D31) .* appl_V) ./ thickness;
for j = 1 : nlayer
  h(j+1 , :) = h(j , :) + thickness(j , :);
end
EA = zeros(1 , mclm);          ES = zeros(1 , mclm);          EI = zeros(1 , mclm);
F = zeros(1 , mclm);                   M = zeros(1 , mclm);
for j = 1 : nlayer
  EA = EA + E(j) * ( h(j+1 , :)    - h(j , :) ) * width;
  ES = ES + E(j) * ( h(j+1 , :).^2 - h(j , :).^2)/2 * width;
  EI = EI + E(j) * ( h(j+1 , :).^3 - h(j , :).^3)/3 * width;
end
```

```
h_NeuturalAxis = ES / EA;
h = h - h_NeuturalAxis;
EA = zeros(1 , mclm);          ES = zeros(1 , mclm);          EI = zeros(1 , mclm);
for j = 1 : nlayer
  EA = EA + E(j) * ( h(j+1 , :)    - h(j , :) ) * width;
  ES = ES + E(j) * ( h(j+1 , :).^2 - h(j , :).^2)/2 * width;
  EI = EI + E(j) * ( h(j+1 , :).^3 - h(j , :).^3)/3 * width;
  F  = F  + E(j) * lamata(j) * ( h(j+1 , :) - h(j , :) ) * width;
  M  = M  - E(j) * lamata(j) * ( h(j+1 , :).^2 - h(j , :).^2)/2 * width;
end
Result = [ EA  -ES;  -ES  EI ]^-1 * [ F ; M ];
e = Result( 1 );
K = Result( 2 );
```

function y=get_EA(E,thick,b)

```
% To get the aixal stifness information of the beam structure
% E                 Young's modulus of each layer, a vector
% thick             thickness information of each layer
%                       the structure of E and thick should be 1 to 1
% width             width of the beam, a scaleer
for No_of_column = 1 : length(thick(1,:));
    EA(No_of_column)=E'*thick(:,No_of_column)*b;
end
y=EA;
```

function [y,x]=getEI(E,d,t,width)

```
%E          is the Young's Modulus matrix
%d          is the density matrix
%t          is the thickness of different layer
%width      is the width of the beam
%h                  is the coordinates of different layers in the composite beam
v=[0.27 0.35 0.3 0.35];
%E=E.*((1-2*v)./((1-v.^2).*(1-v).^2))
nlayer=length(t(:,1));
mclm=length(t(1,:));
h=zeros(nlayer+1,mclm);
for j=1:nlayer
  h(j+1,:)=h(j,:) + t(j,:);
end
pA=zeros(1,mclm);
A11=zeros(1,mclm);                  B11=zeros(1,mclm);
        D11=zeros(1,mclm);
for j=1:nlayer
  A11= A11 + E(j) * (h(j+1,:)-h(j,:))*width;
  B11= B11 + E(j) * (h(j+1,:).^2-h(j,:).^2)/2 * width;
  D11= D11 + E(j) * (h(j+1,:).^3-h(j,:).^3)/3 * width;
```

```
   pA = pA + d(j) * t(j,:)* width;
end
y=D11-(B11.^2)./A11;
y=y;
x=pA;
```

function g = gx(Beam, W_st, W_dy, b, Fi1, Fi2)

```
% W_st  the static post buckling modeshape, 1 x n vector
% W_dy  the dynamic modeshape, 1 x n vector
dFi1 = dfdx(Fi1,1);
dFi2 = dfdx(Fi2,1);
dW_st = dfdx(W_st, 1);
dW_dy = dfdx(W_dy,1);
ddFi1 = dfdx(dFi1,1);
ddFi2 = dfdx(dFi2,1);
ddW_st = dfdx(dW_st, 1);
ddW_dy = dfdx(dW_dy, 1);
n = length(Beam.r); % number of sections in the beam
x = Beam.Node;      % coordinate of the ends of each section
r = Beam.r;         % slenderness ratio of each section
Aik = Beam.Aik;
cmpnt1 = innerproduct(dW_st, dW_dy, x(1), x(n+1), 1);
cmpnt2 = innerproduct(dW_st, dFi1,  x(1), x(n+1), 1);
cmpnt3 = innerproduct(dW_st, dFi2,  x(1), x(n+1), 1);
cmpnt4 = innerproduct(dW_dy, dFi1,  x(1), x(n+1), 1);
cmpnt5 = innerproduct(dW_dy, dFi2,  x(1), x(n+1), 1);
cmpnt6 = innerproduct(dW_dy, dW_dy, x(1), x(n+1), 1);
g = 0;
N = round((length(W_st)-1)*x +1);  % the element# corresponding to x(k)
for k = 1 : n
   gg = zeros(1,N(k+1)-N(k)+1);
   gg = gg + ( 2*ddFi1(N(k):N(k+1)) *cmpnt1 ...
            +  ddFi2(N(k):N(k+1)) *cmpnt1 ...
            +2*ddW_dy(N(k):N(k+1))*cmpnt2 ...
            +  ddW_dy(N(k):N(k+1))*cmpnt3 ...
            +2*ddW_st(N(k):N(k+1))*cmpnt4 ...
            +  ddW_st(N(k):N(k+1))*cmpnt5 ...
            +1.5/b^2*ddW_dy(N(k):N(k+1))*cmpnt6);
   g(N(k):N(k+1)) = gg * 2*b^2*Aik(k)/r(k)^2;
end
```

function ampl = innerproduct(X1, X2, x1,x2,L)

```
% This function does innerproduct calculation in the given x span, vector
% X1 and X2 are values of function f1 and f2 in the full span x = [a, b],
% the caluculated span is given as x = [x1, x2], the program identifies the
% coressponding element of X1 and X2 first, then do inner product within
```

```
% this given area;
%X      the vector with full length
%x1,x2  the span of the inner prodcut intergration, dimensional or non-dim form
%L      over all length of the whole span, for non-dim case, L = 1
%ampl   the amplitude of X
%non-dim span
x1 = x1/L;
x2 = x2/L;
N = length(X1)-1;       % N is the number of sections between [x1, x2]
N1= round(N*x1)+1;      % N1 is the element# corresponding to x1
N2= round(N*x2)+1;      % N2 is the element# corresponding to x2
dx = L/N;
ampl = 0;
for i = N1 : N2
   ampl = ampl + X1(i)*X2(i)*dx;        % inner product <X1,X2> @[x1~x2]
end
```

function [Y, ampl] = normalization (X, L)

```
%X      the vector to be normalized
%L      the length of the inner prodcut intergration, for nondim case, L = 1
%Y      the vector being normalized
%ampl   the amplitude of X
N = length(X);
dx = L/N;
ampl = 0;
for i = 1 : N
   ampl = ampl + X(i)^2*dx;        % inner product <X,X> @[0~L]
end
ampl = sqrt(ampl);
Y = X/ampl;
```

function [Beam]= PZT_beam (wafer_No, appV)

```
% This function is to give the basic material properties and dimensions of the PZT
beam
%**************          Material Properties          ******************
E(4,:)=160e9;   d(4,:)=18762;   %Pt
E(3,:)=25e9;    d(3,:)=8800;    %PZT
E(2,:)=160e9;   d(2,:)=17839;   % Pt
E(1,:)=100e9;   d(1,:)=2200;    % SiO2
d31=[0 0 -50e-12 0]';           % d31 is the piezoelectric coefficient of PZT, for a thin
film of 0.5um, d31=190~250 pC/N
applied_V = [0 appV 0 0]';
v=[0.27 0.35 0.3 0.35]';
nu = 0.3;
%**************          Geometry Properties          ******************
%-----------------------------------------------------
```

```
% Thickness of each layer   [m]
thickness(4,:)=[200e-9, 190e-9, 168e-9, 166e-9, 92e-9, 90e-9, 90e-9, 90e-9];
thickness(3,:)=[0.53e-6, 1.04e-6, 0.55e-6, 1.06e-6, 0.52e-6, 1.09e-6, 0.52e-6, 1.01e-6];
thickness(2,:)=[135e-9, 135e-9, 170e-9, 170e-9, 85e-9, 85e-9, 85e-9, 85e-9];
thickness(1,:)=[1.06e-6, 1.08e-6, 2.13e-6, 2.12e-6, 1.03e-6, 1.03e-6, 1.97e-6,1.99e-6];

%Thickness information of Section I, II, and III
thicknessI = thickness;
thicknessII = thickness;
thicknessII(4,:)=thickness(4,:)*0;
thicknessIII = thickness;
%-----------------------------------------------------
%Stress information        Pa=[N/m^2]
stress = [55, -13.5, 0.5, 1.1, 31.9, 24.1, -52.9 , 21
          1677, 1682, 1733, 1803, 2590, 2520, 2572, 3350
          184, 153, 139, 158, 318, 260, 325, 224
          24, 26, 66, 28, 178, 126, 29, 100]*1e6;
% Dimension information     [m]
width = 20e-6;                                    % the width of the beam, [m]
L = 200e-6;                                       % overall length
Electr_posit = 0.25;                              % position of the electrode / Length
L1 = L * Electr_posit;                            % Length of the 1st section
L3 = L * Electr_posit;                            % Length of the 3rd section
L2 = L - L1 - L3;                % Length of the 2nd section
if wafer_No <= size(thickness,2)       % if the wafer we choose is a valid wafer
  resid_stress = stress( :,wafer_No ).*(1-v); % Pa
  thick = [ thicknessI(:,wafer_No)     thicknessII(:,wafer_No)
        thicknessIII(:,wafer_No)];
  Length = [L1; L2; L3; L];
  Width = width;
  density = d;                                    % density of each layer
else disp ('!!!!!!!!!!!!!!   Wafer Number Exceeds the Number Fabricated, check the
DAtabase in "PZT_beam.m"   !!!!!!!!!!!!!!!')
end
Beam.ResidualStress = resid_stress;
Beam.d31    = d31;
Beam.E = E;
Beam.Thickness = thick;
Beam.Width = Width;
Beam.LayerRho = density;
Beam.Length = Length;

function S = Sm(W_static, W_dyn, wm, Beam, m);
% this function is to calculate the constant parameter of Sm appears in the
% 3rd order dynamic deflection
%=====================================================
```

```
% wm is non-dimensional angular frequency of mode 1 -- m
% W_dyn is the dynamic mode shape from mode 1 -- m
EA = Beam.EA;
rho= Beam.rho;
Aik= Beam.Aik;
EA_avg = Beam.EA_avg;
W_dy  = W_dyn(1,:);
W_st  = W_static;
dW_st = dfdx(W_st, 1);
dW_dy = dfdx(W_dy,1);
ddW_st = dfdx(dW_st, 1);
ddW_dy = dfdx(dW_dy, 1);
x = Beam.Node;            % record the position of the end of each section
n = length(rho);
L = Beam.Length(n+1);
S =0;
wm_dim = sqrt(EA(2)/rho(2)/L^4)*wm;     % dimensional angular frequency
element1 = innerproduct(dW_st,dW_dy,x(1),x(n+1),1);
element2 = innerproduct(dW_dy,dW_dy,x(1),x(n+1),1);
element3 = innerproduct(W_dyn(m,:), W_dyn(m,:), x(1),x(n+1),1);
S_m = 0;
for k = 1 : n
   increament1 = innerproduct(ddW_dy, W_dyn(m,:), x(k),x(k+1),1);
   increament1 = EA_avg/rho(k)*increament1;
   increament2 = innerproduct(ddW_st, W_dyn(m,:), x(k),x(k+1),1);
   increament2 = EA_avg/(2*rho(k))*increament2;
   S_m = S_m + element1*increament1 + element2*increament2;
end
S_m = S_m/((wm_dim(m)^2-4*wm_dim(1)^2)*element3*L^2);
```

function [P, W, C]=Staticbuckleshape(Beam, Mode_No, steps)

```
EI = Beam.EI;
EA = Beam.EA;
pA = Beam.rho;
Length = Beam.NondimSection;
x = Beam.Node;
%EI(2)=EI(1); EA(2)=EA(1); pA(2)= pA(1);
%------------------  Estimate Frequency Range    --------------------------
PickupData = [5 10 14 18 23 26 29 32 36];  % Data for PickupPoint
if Mode_No <= length(PickupData)
      PickupPoint = PickupData(Mode_No); %for c-c critical buckling uniform beam,
lamata = n*pi
else
      PickupPoint = pi * (Mode_No+1);
      fprintf('  Please  Manually  Choose  Pickup  Range  at  Staticbucklesahp.m
\n\n')
```

```
end
%-------------------------------------------------------------------------
option = optimset;
zeropoint =fzero('detA1', PickupPoint, option, EI, x);
[ determinA, A ] = A_static(zeropoint, EI, x);
clmnumber1=length(A);
lamata2=zeropoint;
lamata1=lamata2 * sqrt(EI(2)/EI(1));
lamata3=lamata2 * sqrt(EI(2)/EI(3));
P=[lamata1^2 lamata2^2 lamata3^2]';   %Pi is used to calculate the Lamatas in the
dynamic model. It's also the Non_dim critical buckling force

%%%%%%%%%%%%%%%%%%%%%%%%%%%%%
[V1,D1]=eig(A);                %V is the eigenvector and D is the eigenvalue
%------   Choose the eigenvector corresponding to the 0 eigenvalue  -------
eigenvalue=max(diag(D1));        % reference eigenvalue, the largest one.
clm=0;
for counter = 1 : clmnumber1    %Choose the smallest eigenvalue (0 in this case)
   if abs(real(eigenvalue)) > abs(real(D1(counter, counter)))
     if abs(imag(eigenvalue))>=abs(imag(D1(counter,counter)))
          eigenvalue=D1(counter, counter);
          clm=counter;
     end
   end
end

C = V1(:,clm);                  % The eigenvector of 0 eigenvalue
%--------------     Calculate the ModeShape        ------------------------
xx = Beam.Node;                 %[0 .25 .75 1]
mm=0;   kk=steps;
 for x = xx(1) : 1/kk : xx(2)
    mm=mm+1;
    W(mm)=C(1) + C(2)*x + C(3)*cos(lamata1*x) + C(4)*sin(lamata1*x);
 end
 for x = xx(2)+1/kk : 1/kk : xx(3)
    mm=mm+1;
    W(mm)=C(5) + C(6)*x + C(7)*cos(lamata2*x) + C(8)*sin(lamata2*x);
 end
 for x = xx(3)+1/kk : 1/kk : xx(4)
    mm=mm+1;
    W(mm)=C(9) + C(10)*x + C(11)*cos(lamata3*x) + C(12)*sin(lamata3*x);
 end
 %--------------   normalize static bcukling mode shape W   --------------
 [W, ampl] = normalization(W, 1); %normalize the static buckling modeshape
 C = C/ampl;                 %modify the corresponding parameters of the modeshape
 Pdms = 1;
```

```
function S = Tm(W_static, W_dyn, wm, Beam, m);
EA = Beam.EA;
rho= Beam.rho;
Aik= Beam.Aik;
EA_avg = Beam.EA_avg;
W_dy  = W_dyn(1,:);
W_st  = W_static;
dW_st = dfdx(W_st, 1);
dW_dy = dfdx(W_dy,1);
ddW_st = dfdx(dW_st, 1);
ddW_dy = dfdx(dW_dy, 1);
x = Beam.Node;            % record the position of the end of each section
n = length(EA);
L = Beam.Length(n+1);
S =0;
wm_dim = sqrt(EA(2)/rho(2)/L^4)*wm;     % dimensional angular frequency
element1 = innerproduct(dW_st,dW_dy,x(1),x(n+1),1);
element2 = innerproduct(dW_dy,dW_dy,x(1),x(n+1),1);
element3 = innerproduct(W_dyn(m,:), W_dyn(m,:), x(1),x(n+1),1);
T_m = 0;
for k = 1 : n
   increament1 = innerproduct(ddW_dy, W_dyn(m,:), x(k),x(k+1),1);
   increament1 = EA_avg/rho(k)*increament1;
   increament2 = innerproduct(ddW_st, W_dyn(m,:), x(k),x(k+1),1);
   increament2 = EA_avg/(2*rho(k))*increament2;
   T_m = T_m + element1*increament1 + element2*increament2;
end
T_m = T_m/((wm_dim(m)^2-4*wm_dim(1)^2)*element3*L^2);

function P = V_F( max_strain, EA, Length)
% this function is to get the averaged axial force generated by tha applied voltage
K1 = EA(1)/Length(1);
K2 = EA(2)/Length(2);
K3 = EA(3)/Length(3);
K  = [1+K2/K3                  K2
         1                      -K1];
F  = [0 EA(1)*max_strain]';
PP = K^-1 * F; P  = PP(1);
```

Bibliography

[1] R. T. Howe and R.S. Muller, "Integrated Resonant-microbridge Vapor Sensor," *IEEE International Electronic Devices Meeting*, San Francisco, California, December 10-12, 1984, pp. 213-216.

[2] C. T.-C. Nguyen, "High-Q Micromechanical Oscillators and Filters for Communications," *Proceedings of the IEEE International Symposium on Circuits and Systems*, 1997, pp. 2825-2828.

[3] K. Wang and C. T.-C. Nguyen, "High-order Micromechanical Electronic Filters," *Proceedings of the 1997 IEEE International MEMS Workshop*, 1997, pp. 25-30.

[4] K. Wang, A.-C. Wong and C. T.-C. Nguyen, "VHF Free-Free Beam High-Q Micromechanical Resonators," *Journal of Microelectromechanical Systems*, Vol.9, No.3, Sept. 2000, pp. 347-359.

[5] T. Roessig, R. T. Howe and A. P. Pisano, "Surface Micromachined Resonant Accelerometer," *Proceedings of Transducers* '97, Vol. 2, 1997, pp. 859-862.

[6] C. T.-C. Nguyen and R. T. Howe, "An Integrated CMOS Micromechanical Resonator High-Q Oscillator," *IEEE Journal of Solid-State Circuits*, Vol. 34, No.4, 1999, pp. 440-455.

[7] L. Lin, R. T. Howe and A. P. Pisano, "Microelectromechanical Filters for Signal Processing," *Journal of Microelectromechanical Systems*, Vol. 7, No. 3. Sept. 1998, pp. 286-294.

[8] C. T.-C. Nguyen, "Micromechanical Filters for Miniaturized Low-power Communications," *Proceedings of SPIE: Smart Structures and Materials (Smart Electronics and MEMS)*, Newport Beach, Ca. Mar. 1-5, 1999.

[9] S. Lee and C. T.-C. Nguyen, "Mechanically-coupled Micromechanical Arrays for Improved Phase Noise," *Proceedings*, IEEE Int. Ultrasonics, Ferroelectrics, and Frequency Control 50th Anniv. Joint Conf., Montreal, Canada, Aug. 2004, pp. 280-286.

[10] J. Wang, Z. Ren and C. T.-C. Nguyen, "Self-aligned 1.14-GHz Vibrating Radialmode Disk Resonators," *The 12th International Conference on Solid State Sensors, Actuators and Microsystems*, Boston, June 8-12, 2003, pp. 947-950.

[11] L. Weisbord, "Single Beam Force Transducer with Integral Mounting Isolation," US Patent #3470400, 1969.

[12] C. J. V. Mullem F. R. Blom, J. Fluitman and M. Elwenspoek, "Piezoelectrically Driven Silicon Beam Frce Sensor," *Sensors and Actuators* A: Physical, Vol. 26, 1991, pp. 279-283.

[13] T. Fabula, H.-J. Wagner and B. Schmidt, "Triple-beam Resonant Silicon Force Sensor Based on Piezoelectric Thin Films," *Sensors and Actuators* A: Physical, Vol. 42, 1994, pp. 257-280.

[14] K. Funk, T. Fabula, G. Flik and F. Larmer, “Piezoelectrical Driven Resonant Force Sensor: Fabrication and Cross Talk,” *Journal of Micromechanics and Microengineering*, Vol. 5, 1995, pp. 143-146.

[15] A. Prak, M. Elwenspoek and J. Fluitman, “Selective Mode Excitation and Detection of Micromachined Resonators,” *Journal of Microelectromechanical Systems*, Vol.1, No.4, Dec. 1992, pp. 170-178.

[16] M. M. Abdalla, C. K. Reddy, W. F. Faris and Z. Gürdal, “Optimal Design of an Electrostatically Actuated Microbeam for Maximum Pull-in Voltage,” *Computers and Structures*, Vol. 83, 2005, pp. 1320-1329.

[17] K. L. Turner, S. A. Miller, P. G. Hartwell, N.C. Macdonald, S. H. Strogartz and S. G. Adams, “Five Parametric Resonances in a Microelectromechanical System,” *Nature*, Vol. 396, 1998, pp. 149-152.

[18] K. L. Turner and W. Zhang, “Design and Analysis of a Dynamic MEMS Chemical Sensor,” in: *Proceedings of the 2001 American Control Conference*, Arlington, VA, USA, 25-27 June 2001, pp. 1214-1218.

[19] J. P. Raskin, A. R. Brown, B. Khuri-Yakub and G. M. Rebeiz, “A Novel Parametric-effect MEMS Amplifier,” *Journal of Microelectromechnical Systems*, Vol, 9, No. 4, Dec. 2000, pp. 528-537.

[20] D. L. DeVoe, *Thin Film Zinc Oxide Microsensors and Microactuators*, Ph.D. Thesis, Department of Mechanical Engineering, U.C. Berkeley, 1997.

[21] D. L. DeVoe, “Piezoelectric Thin Film Micromechanical Beam Resonators,” *Sensors and Actuators* A: Physical, Vol. 88, 2001, pp. 263-272.

[22] P. Kumar, L. Li, Li. Calhoun, P. Boudreaux and D. DeVoe, “Fabrication of Piezoelectric Al0.3Ga0.7As Microstructures,” *Sensors and Actuators* A: Physical, Vol. 115, 2004, pp. 96-103.

[23] B. Piekarski, D. DeVoe, M. Dubey, R. Kaul, J. Conrad and R. Zeto, “Surface Micromachined Piezoelectric Resonant Beam Filters,” *Sensors and actuators* A: Physical, Vol. 91, 2001, pp. 313-320.

[24] A. Husain, J. Hone, H. W. C. Postma, X. M. H. Huang, T. Drake, M. Barbic, A. Scherer, and M. L. Roukes, “Nanowire-based Very-high-frequency Electromechanical Resonator,” *Applied Physics Letters*, Vol. 83, Issue 6, 2003, pp. 1240-1242.

[25] O. Paul and H. Baltes, “Mechanical Behavior and Sound Generation Efficiency of Prestressed, Elastically Clamped and Thermomechanically Driven Thin Film Sandwiches,” *Journal of Micromechanics and Microengineering*, Vol.9, 1999, pp. 19-29.

[26] L. Currano, *Experimental and Finite Element Analysis of Piezoelectrically Driven MEMS Actuators*, M.S. Thesis, Department of Mechanical Engineering, University of Maryland, College Park, 2002.

[27] H. Li and B. Balachandran, “Nonlinear Oscillations of Micromechanical Oscillators,” *Proceedings of the ASME International Design Engineering Technical Conferences*, Chicago, 2003, Paper No. DETC2003/VIB-48520.

[28] S. W. Shaw, K. L. Turner, J. F. Rhoads and R. Baskaran, "Parametrically Excited MEMS-Based Filters," *Proceedings of the IUTAM Symposium on Chaotic Dynamics and Control of Systems and Processes in Mechanics*, Rome, Italy, 2003.

[29] W. Zhang, R. Baskaran and K. L. Turner, “Effect of Cubic Nonlinearity on Auto-Parametrically Excited MEMS Mass Sensor,” *Sensors and Actuators* A: Physical, Vol. 102, 2002, pp. 139–150.

[30] M. Vangob, “Analytical Analysis of a Compressed Bistable Buckled Beam,” *Sensors and Actuators* A: physical, Vol. 69, No.3, 1998, pp.212-216.

[31] Y. Yang and C. J. Kim, “Testing and Characterization of a Bistable Snapping Microactuator Based on Thermo-mechanical Analysis," *Proceedings of Solid-State Sensors Actuators*, 1995, pp. 337-340.

[32] B. Wagner, H. Quenzer, S. Hoerschelmann, T. Lisec and M. Juerss, "Bistable Microvalve with Pneumaticaly Coupled Membranes," in: *Proceedings of IEEE MEMS 1996 Conference*, 1996, pp.384-338.

[33] H. W. Ch. Postma, I. Kozinsky, A. Husain and M. L. Roukes, “Dynamic Range of Nanotube- and Nanowire-based Electromechanical Systems,” *Applied Physics Letters*, Vol. 86, Issue 22, No.223105, 2005.

[34] T. Anderson, A. H. Nayfeh and B. Balachandran, “Experimental Verification of the Importance of the Nonlinear Curvature in the Response of a Cantilever Beam,” *Journal of Vibration and Acoustics*, Vol.118, 1996, pp. 21-27.

[35] J. A. Thornton and D. W. Hoffman, “Stress-related Effects in Thin Film,” *Thin Solid Films*, Vol. 171, 1989, pp.5-31.

[36] J. Qiu, J. H. Lang and A. H. Slocum, “A Curved-Beam Bistable Mechanism,” *Journal of Microelectromechanical Systems*, Vol. 13, No.2, Apr. 2004, pp.137-146.

[37] W. Fang and J. A. Wickert, “Post-Buckling of Micromachined Beams,” *Journal of Micromechanics and Microengineering*, Vol. 4, 1994, pp. 116-122.

[38] W. Fang and J. A. Wickert, “Comments on Measuring Thin-film Stresses Using Bi-layer Micromachined Beams”, *Journal of Micromechanics and Microengineering*, Vol. 5, 1995, pp. 276-281.

[39] M. Chiao and L. Lin, “Self-Buckling of Micromachined Beams under Resistive Heating,” *Journal of Microelectromechanical Systems*, Vol. 9, No. 1, Mar. 2000, pp. 146-151.

[40] O. Brand, M. Hornung, H. Baltes and C. Hafner, “Ultrasound Barrier Microsystem for Object Detection Based on Micromachined Transducer Elements,” *Journal of Microelectromechanical Systems*, Vol. 6, No. 2, 1997, pp.151-160.

[41] H. Li and B. Balachandran, "Buckling Induced Nonlinear Phenomenon in a Micro-electromechancial Resonator," *Proceedings of the ASME International Mechanical Engineering Congress and Exposition*, New Orleans, 2002, Paper No. IMECE2002-39010.

[42] S. Preidikman, H. Li and B. Balachandran, "Forced Oscillations of Microelectromechanical Resonators," *Proceedings of Symposium on Nonlinear Dynamics and Stochastic Mechanics: 2003 ASME International Mechanics Engineering Congress and R&D Expo*, Washington, D.C., November 15-21, 2003, Paper No. IMECE2003-44552.

[43] M. Chiao and L. Lin, "Self-Buckling of Micromachined Beams Under Resistive Heating," *Journal of Microelectromechanical Sytems*, Vol. 9, No. 1, 2000, pp. 146-151.

[44] U. Lindberg and J. Soderkvist, T. Lammerink and M. Elwenspoek, "Quasi-buckling of Micromachined Beams," *Journal of Micromechics and Microengineering*, Vol. 3, 1998, pp. 183-186.

[45] W. Fang and J. A. Wickert, "Post-Buckling of Micromachined Beams," *Micro Electro Mechanical Systems, 1994, MEMS '94, Proceedings, IEEE Workshop*, 25-28 Jan. 1994, pp. 182-187.

[46] M. T. A. Saif, "On a Tunable Bistable MEMS – Theory and Experiment," *Journal of Microelectromechanical Systems*, Vol. 9, No. 2, 2000, pp. 157-170.

[47] A. H. Nayfeh, W. Kreider and T. J. Anderson, “Investigation of Natural Frequencies and Mode Shapes of Buckled Beams,” AIAA Journal, Vol. 33, No.6, 1995, pp. 1121-1126.

[48] A. H. Nayfeh and W. Lacarbonara, “On the Discretization of Spatially Continuous Systems with Quadratic and Cubic Nonlinearities,” *JSME International Journal*, Series C, Vol. 41, No. 3, 1998, pp. 510-531.

[49] L. R. Calcote, *The Analysis of Laminated Composite Structures*, New York, Van Nostrand Reinhold Co., 1969, pp120-123.

[50] A. H. Nayfeh and D. T. Mook, *Nonlinear Oscillations*, Wiley, New York, 1979, pp. 447-453.

[51] Y. R. Talpaert, *Tensor Analysis and Continuum Mechanics*, Kluwer Academic Publishers, 2002, pp. 199-209.

[52] E. F. Crawley and K. B. Lazarus, “Induced Strain Actuation of Isotropic and Anisotropic Plates,” AIAA Journal, Vol. 29, No. 6, 1991, pp. 944-951.

[53] R. Seshadri, *Active Vibration Control of Beams Using Piezoelectric Actuators*, M.S. Scholarly Paper, Department of Mechanical Engineering, University of Maryland, College Park, 1994.

[54] J. A. Murdock, *Perturbations: Theory and Methods*, Wiley, New York, 1991, pp. 227-274.

[55] A. H. Nayfeh, *Introduction to Perturbation Techniques*, John Wiley & Sons, Inc., 1981, pp. 388-471.

[56] W. Lacarbonara and A. H. Nayfeh, "Experimental Validations of Reduction Methods for Nonlinear Vibrations of Distributed-Parameter Systems: Analysis of a Buckled Beam," *Nonlinear Dynamics*, Vol. 17, 1998, pp.95-117, 1998.

[57] P. L. Kapitza, *Collected Papers of P. L. Kapitza*, edited by D. Ter Haar, Pergamon Press 1965, Vol. 2, pp. 714 – 725.